

## **PREFACE**

The present PhD dissertation “Gene Transfer of Signals Critical for Allograft Healing Using the Adeno-associated Viral Vector“ is based on experimental work performed in the laboratories of Edward M. Schwarz, The Center for Musculoskeletal Research, University of Rochester, Rochester, NY, USA and Professor Thomas G. Jensen, Department of Human Genetics, Aarhus University, Denmark.

### **Supervisors:**

Kjeld Søballe, Professor, MD, DMSc, Department of Orthopaedics, Aarhus University Hospital, Århus, Denmark.

Michael Ulrich-Vinther, Associate professor, MD, PhD, DMSc, Department of Orthopaedics, Aarhus University Hospital, Århus, Denmark.

Thomas G. Jensen, Professor, MD, DMSc, Department of Human Genetics, Aarhus University, Aarhus, Denmark.

### **This thesis is based on the following papers:**

Ito H., Koefoed M., Tiyyapatanaputi P., Gromov K., Goater J.J., Carmouche J., Zhang X., Rubery P.T., Rabinowitz J., Samulski R.J., Nakamura T., Soballe K., O’Keefe R.J., Boyce B.F., Schwarz E.M. Remodeling of cortical bone allografts mediated by adherent rAAV-RANKL and VEGF gene therapy. *Nat Med.* 2005 Mar;11(3):291-7.

Koefoed M., Ito H., Gromov K., Reynolds D.G., Awad H.A., Rubery P.T., Ulrich-Vinther M., Soballe K., Guldborg R.E., Lin A.S.P., O’Keefe R.J., Zhang X., Schwarz E.M. Biological Effects of rAAV-caAlk2 Coating on Structural Allograft Healing. *Mol Ther.* 2005 Aug;12(2):212-8.

Koefoed M., Pedersen A.G., Foldager C.B., Hansen K., Pedersen M., Cucchiari M., Schwarz E.M., Soballe K., Jensen T.G., Ulrich-Vinther M. Manuscript ready for submission.

## ACKNOWLEDGEMENTS

I would like to thank my supervisors Professor Kjeld søballe, Associate-professor Michael Ulrich-Vinther and Professor Thomas G Jensen for enthusiastic support, guidance and encouragement when needed. I am also thankful to Professor Edward Schwarz for introducing me to science and for being a very enthusiastic and dedicated advisor.

I would also like to thank Michael Pedersen for his help and guidance in my attempt to get to know “the world of imaging”. Further, Kasper Nielsen and Casper Foldager have been of great help with data analysis and improving my understanding of micro-CT. In addition, Jane Pauli and Anette Baatrup have been of great assistance (and great patience) with the histology.

Finally, my friends and colleagues at the Department of Human Genetics have made my work more fun and less troublesome.

The studies were supported by grants from “Fonden til Lægevidenskabens Fremme”, “Danish Medical Research Council, and “University of Aarhus Research Foundation.”

## TABLE OF CONTENTS

<b>PREFACE</b> .....	<b>1</b>
<b>ACKNOWLEDGEMENTS</b> .....	<b>2</b>
<b>TABLE OF CONTENTS</b> .....	<b>3</b>
<b>ABBREVIATIONS</b> .....	<b>5</b>
<b>SUMMARY (English)</b> .....	<b>6</b>
<b>SUMMARY (Danish)</b> .....	<b>8</b>
<b>INTRODUCTION</b> .....	<b>10</b>
<b>Biological aspects of bone grafts</b> .....	<b>11</b>
<i>Autograft</i> .....	11
<i>Allograft</i> .....	12
<i>Synthetic matrix</i> .....	13
<b>Repair and incorporation of bone grafts</b> .....	<b>13</b>
<i>Fracture healing</i> .....	13
<i>Graft repair</i> .....	14
<i>Animal models of structural bone defects</i> .....	15
<i>Murine femoral allograft model</i> .....	15
<b>Critical factors and osteoinductive cells</b> .....	<b>18</b>
<i>Demineralized bone matrix</i> .....	18
<i>Recombinant proteins</i> .....	19
<i>Osteoprogenitor cells</i> .....	19
<b>Gene transfer</b> .....	<b>20</b>
<b>Vector systems</b> .....	<b>21</b>
<i>Adenoviral vectors</i> .....	22
<i>Retroviral and Lentiviral vectors</i> .....	22
<i>Recombinant Adeno-associated viral vectors</i> .....	23
<i>Non-viral vectors</i> .....	24
<i>Controlled expression of growth factors and cytokines</i> .....	26
<b>Factors used to induce allograft repair</b> .....	<b>27</b>
<i>Bone Morphogenetic Proteins</i> .....	27
<i>Vascular Endothelial Growth Factor</i> .....	28
<i>Fibroblast Growth Factor-2</i> .....	29
<i>RANKL – Receptor activator of nuclear factor-<math>\kappa</math>B (NF-<math>\kappa</math>B) ligand</i> .....	29
<b>HYPOTHESIS &amp; AIMS</b> .....	<b>31</b>
<b>METHODS</b> .....	<b>33</b>
- A short description of most important methods used in this thesis .....	33
<b>RESULTS SUMMARY</b> .....	<b>35</b>
<b>Localized transduction mediated by freeze-dried rAAV</b> .....	<b>35</b>
<b>STUDY I. Revitalization of rAAV-RANKL and rAAV-VEGF coated allografts</b> .....	<b>35</b>
<b>STUDY II. Biological effects of BMP signaling on structural allograft healing</b> .....	<b>36</b>
<b>STUDY III. Increased bone formation and remodeling of bone allografts mediated by rAAV-VEGF gene transfer</b> .....	<b>37</b>
<b>DISCUSSION</b> .....	<b>38</b>
<b>Local gene expression</b> .....	<b>38</b>
<b>Revitalization of structural allografts</b> .....	<b>38</b>

<b>Limitations .....</b>	<b>41</b>
<b>CONCLUSION.....</b>	<b>43</b>
<b>PERSPECTIVE .....</b>	<b>44</b>
<b>REFERENCES.....</b>	<b>45</b>
<b>APPENDIX.....</b>	<b>55</b>
<b>PAPER I .....</b>	<b>55</b>
<b>PAPER II.....</b>	<b>63</b>
<b>PAPER III .....</b>	<b>71</b>

## ABBREVIATIONS

AAV	Adeno-associated virus	PDGF	platelet derived growth factor
AAV-2	Adeno-associated virus, serotype 2	PTH	Parathyroid hormone
Alk2	Activin receptor-like kinase-2	RANK	Receptor activator of nuclear factor $\kappa$ B
BMP	Bone morphogenetic protein	RANKL	Receptor activator of nuclear factor $\kappa$ B ligand
caAlk2	constitutively active Activin receptor-like kinase-2	rhBMP	recombinant human Bone morphogenetic protein
cDNA	complementary DNA	rAAV	recombinant Adeno-associated virus
DBM	Demineralized bone matrix	scAAV	self-complementary Adeno-associated virus
FGF-2	Fibroblast growth factor 2	SCID	severe combined immuno deficiency
GAM	gene activated matrix	ssAAV	single stranded Adeno-associated virus
GFP	Green fluorescent protein	TGF- $\alpha$	tumore necrosis factor alpha
ITR	Inverted terminal repeat	TGF- $\beta$	tumor necrosis factor beta
kb	kilobases	TRAP	Tartrate resistant acid phosphatase
Luc	Luciferase	VEGF	vascular endothelial growth factor
micro-CT	micro-computed tomography	RT-PCR	Reverse transcriptase-polymerase chain reaction
M-CSF	microphage colony stimulating factor		
MSCs	Mesenchymal stem cells		
OP-1	Ostegenic protein-1		
OPG	Osteoprotegrin		

## SUMMARY (English)

Bone grafting is commonly used in reconstructive orthopaedic surgeries such as spinal fusion, revision of failed total joint arthroplasty, or repair of skeletal defects following trauma or the removal of tumor. Both experimental and clinical studies have shown that fresh autogenous grafts are vastly superior to allograft bone in graft repair and remodeling. In the case of autografts, both graft and host bones contribute to the osteogenesis by delivering living cells that can produce early new bone, growth factors and bone inducing substances. Following union autografts continue to remodel and are sustained through normal bone homeostasis. In contrast, since processed allograft does not contain any living cells, healing relies upon invasion of the graft by host cells and tissues. The consequent bone formation is delayed and insufficient and causes a 20 - 25 % failure rate due to nonunion and fracture. Therefore, it is important to elucidate the factors involved in autograft healing and to devise a method to transfer these factors to processed allografts giving these grafts similar favorable healing properties.

We have studied whether critical factors on the surface of allografts would lead to autograft-like healing using local gene transfer mediated by freeze-dried Adeno-associated viral vectors (rAAV). In order to improve allograft healing we focused on affecting osteogenesis, angiogenesis and remodeling.

Collectively, the three studies demonstrate the efficiency of lyophilized rAAV to confer bone-healing capacities, which are normally missing in processed allografts. Several key factors in bone formation can be used to stimulate allograft repair. We find that RANKL and VEGF are necessary for autograft healing and can be transferred using rAAV to revitalize structural allografts. In addition, the introduction of Bone morphogenetic protein signals on the cortical surface of allografts leads to the formation of a new bone cortex and remodeling that does not normally occur. Finally, we find that VEGF is able to induce a significant increase in newly formed bone and remodeling. In conclusion our results indicate that allografts coated with rAAV mediating gene transfer of key

factors have the potential to improve allograft incorporation and repair. Further, the method of freeze-drying AAV can be used on several kinds of biomaterials and therefore is of general interest.

## SUMMARY (Danish)

Knogletransplantation bruges ofte i ortopædkirurgi til spinal fusion, revision af total hofte alloplastik eller udbedring af segmentære knogledefekter efter tumor resektion eller traume. Både kliniske og eksperimentielle studier har vist, at autolog knoglegrafts (autograft) evne til remodellering og integration med værtsknoglen er langt bedre end donor knoglegrafts (allograft). Ved brug af friske autografter bidrager celler og osteoinduktive faktorer fra både graft og vært til knoglehelingen. Efter den tidlige knogledannelse fortsætter autograften med at remodellere, og på den måde vedligeholdes autograften som del af den naturlige knogleomsætning. En allograft har været frosset ned og indeholder derfor ingen levende celler, og heling kan udelukkende ske vha. værtsceller, som invaderer graften. Derved bliver knogledannelsen forsinket og ofte utilstrækkelig. Der opstår ophobning af mikrofrakturer, som inden for få år er årsag til, at 20 - 25 % af allografterne svigter, og der bliver behov for reoperation. Derfor er det vigtigt at identificere de faktorer, som er nødvendige for knogledannelse, revaskularisering og remodellering af knogler, samt at udvikle en metode til at overføre disse faktorer til allografter for derved at opnå en bedre heling.

Vi har undersøgt, om tilførslen af vigtige faktorer til overfladen af allografter vil føre til forbedret knogledannelse og indvækst efter transplantation. Vi benyttede frysetørrede Adeno-associerede virale vektorer til at udtrykke faktorer med indflydelse på knogledannelse, kardannelse og remodellering.

De 3 studier viser, at det er muligt at benytte frysetørret AAV til at tilføre allografter en forbedret knogledannelse og helingsevne. Flere forskellige faktorer centrale for knogledannelse kan benyttes til at stimulere denne knogleheling. Vi har vist, at Vascular endothelial growth factor (VEGF) og Receptor activator of nuclear factor- $\kappa$ B ligand (RANKL) er nødvendige for autografter heling og at disse faktorer, som stimulerer karnydannelse og remodellering, kan overføres til overfladen af allografter vha. AAV. Derved opnås forøget knogledannelse og resorption af autograften. Derudover kan tilførslen af signaler for knogledannelse (Bone morphogenetic proteins), til knogleoverfladen af allografter, stimulere dannelsen af en ny knoglecortex, som omgiver autograften og desuden remodellering. Endelig viser vi, at VEGF

alene kan inducere en signifikant forøget mængde nydannet knogle og øget antal aktive osteoclaster på knogleoverfladen. Sammenfattende viser vores resultater, at allografter coated med AAV, som udtrykker nøgle-faktorer for knogleheling, kan forbedre allografters knogledannelse og integration. Frysetørret AAV kan også bruges i forbindelse med andre syntetiske materialer og er derfor af generel interesse.

## INTRODUCTION

Bone grafting is commonly used in reconstructive orthopedic surgery such as revision of failed total hip arthroplasty, spinal fusion, or repair of segmental skeletal defects after trauma or removal of tumors (6, 7). Fractures exceeding a certain “critical size” do not heal spontaneously (8). The lack of healing is named “non-union”. This can lead to significant pain and impaired physical function, and consequently a decline in the patient’s quality of life. The rate of fracture non-union has been reported to range from 4 % to 10 % (9, 10). Factors contributing to delayed healing and non-union include open fractures, inadequate blood supply, crushed or splintered bone, association with tumor or infection, smoking and underlying chronic illness (11, 12). Experimental and clinical studies have shown that fresh autologous bone grafts are superior to devitalized allograft donor bone in graft repair and remodeling (13). However, due to the limited size of available autologous bone, and associated donor site morbidity, allograft bone is widely used for large segmental defects. Autografts contain living cells, which can contribute to the healing response with both proliferation and production of critical factors. In contrast to this, allografts have been processed and do not contain living cells. In this case the healing response rely on invasion of the allograft by host cells. This invasion leads to a delayed and insufficient healing response causing a 20-25 % failure rate due to non-union and fracture (14). Therefore, it is important to elucidate the factors involved in autograft healing and to devise a method to transfer these factors to processed allografts giving these grafts similar favorable healing properties.

Two approaches have been studied in order to confer properties of bone regeneration to allografts. The first is to transplant mesenchymal stem cells (MSCs) to promote bone formation from the graft followed by subsequent vascularization and remodeling (15). For clinical applications this approach is complicated due to questions such as cell source, manufacturing costs and reproducibility. The second approach is to deliver the critical factors directly to the surface of the allograft. For example the use of recombinant human bone morphogenetic proteins (rhBMPs) to enhance bone formation is approved for

certain orthopedic surgeries (16). This approach is restricted for large segmental defects due to the need of high dose and fast degradation and diffusion of the proteins *in vivo* (17). Localized gene transfer is an attractive alternative procedure allowing sustained expression of specific factors stimulating bone regeneration and repair from cells adjacent to the fracture site.

In this thesis we have studied whether addition of critical factors to the surface of allografts will lead to autograft-like healing. We have focused on local gene transfer mediated by Adeno-associated viral vectors to deliver these signals efficiently.

## **Biological aspects of bone grafts**

### ***Autograft***

In severe fractures it is possible to induce bone formation at the fracture site in order to assist healing. The use of autogenous iliac crest bone is considered the current best practice because it possesses the three properties required for bone formation. It is (1) osteogenic, (2) osteoinductive and (3) osteoconductive (tbl. 1). Since the graft is harvested from the patient it is histocompatible and non-immunogenic. However, there are several disadvantages to the use of autografts. They can only be harvested in limited amounts. Furthermore, they require a second surgical site, which increases the operation time and blood loss. Finally, morbidity at the donor site is commonly reported. The primary reasons are pain at the donor site and problematic scars. The frequency of donor site pain varies with 18-31 % of the patients still experiencing pain after 24 months (18, 19). Complications to the harvesting procedure include superficial and deep infection, vessel damage and nerve injury leading to an altered sensation (20, 21).

---



---

The three elements required for bone regeneration

---

Osteogenic cells	Cells which possess the potential to differentiate and facilitate bone formation.
Osteoinductive factors	Agents that stimulate the recruitment of progenitor cells and induce differentiation into the bone forming cell-lineage.
Osteoconductive matrix	Framework or surface which bone grows on.

---

**Table 1**

***Allograft***

In large segmental bone defects it is often necessary to use large pieces of bone from a donor (allograft) instead of autogenous bone. An allograft has osteoconductive properties but only limited osteoinductive and no osteogenic progenitor cells for biological incorporation (3). Still this type of graft is commonly used for large structural defects in long bones providing structure due to its innate load-bearing strength. The allograft has been processed by freezing or by freeze-drying. As a result all living cells are destroyed to avoid immunological reactions due to histocompatibility mismatch. Instead the allograft bone often induces a reaction comparable to a foreign body reaction with the bone being enclosed in fibrous tissue. Furthermore, the processing of the bone leads to mechanical changes associated with micro-cracks along the collagen fibers, which makes it prone to failure (22). The clinical consequences of these limiting factors are a 20-25 % failure rate of the bone allografts due to infection, nonunion and fracture within 3 years (14) and up to 60 % within 10 years (7, 23). The limitations also implies that if the defect is associated with infection or damaged soft tissue at the grafting site, the allograft has to be combined with other graft substitutes which provide growth factors and osteoprogenitor cells. Finally, there is a small risk of transmission of disease such as hepatitis and HIV. Strict control to avoid this include donor screening and repeated testing for infectious diseases.

***Synthetic matrix***

Different kinds of synthetic matrices are used for bone grafting. The most widely used clinically are ceramics composed of hydroxyapatite, tricalcium phosphate or a combination. But also collagen and synthetic polymers based on e.g. polylactic acid are used. They are all exclusively osteoconductive and they possess little mechanical stability making them unsuited for applications requiring significant impact or stress (3).

Properties of bone-graft alternatives

Graft material	Osteogenic	Osteo-inductive	Osteo-conductive	Immuno-genic	Donor-site morbidity	Strength
Autograft	+++	++	++++	-	+	-
Allograft	-	+/-	+	+/-	-	++
Ceramics	-	-	+	-	-	+/-
Demineralized bone matrix	-	++	+	-	-	-

**Table 2** Adapted from Gazdag A.R. et al (3).**Repair and incorporation of bone grafts*****Fracture healing***

The repair and incorporation of bone grafts is a regulated process very similar to fracture healing. It consists of 4 phases: 1. Inflammation and hematoma. 2. Cartilage formation. 3. Primary bone formation. 4. Remodeling (24). The initial inflammatory response is triggered by the injury forming a fracture hematoma. The dominant cell type in the hematoma is platelets. These cells initiate the fracture repair by releasing numerous cytokines such as platelet derived growth factor (PDGF) and transforming growth factor beta (TGF- $\beta$ ) (25). These proteins elicit the inflammatory response leading to accumulation of inflammatory cells. Thereafter these cells release chemotactic molecules in a spatial pattern

initiating the proliferation and differentiation of mesenchymal progenitor cells from the periosteum, bone marrow and surrounding soft tissue into osteoblasts and chondroblasts. Within the first days the repair stage begins leading to intramembranous bone formation and endochondral ossification (26). Intramembranous bone formation is a process where osteoblasts produce unmineralized bone matrix – osteoid - on the surface of necrotic bone, which in turn is resorped by osteoclasts. Intramembranous bone formation is limited in rodents. In these animals healing predominantly occur through endochondral bone formation (24). This starts with a cartilage scaffold giving rise to the soft callus. During the later phases the soft callus is calcified and the chondrocytes become hypertrophic and apoptic. Thereafter osteoclasts, which have been downregulated in the early stages of fracture healing, are activated through the elevation of systemic levels of parathyroid hormone (PTH) and tumor necrosis factor alpha (TNF- $\alpha$ ). The osteoclasts then begin to resorp bone, turning the callus into mature lamellar bone (24, 27). This process is known as remodeling leading to restored anatomy and function of the broken bone.

### ***Graft repair***

The successful healing of autologous bone is characterized by the contribution of cells from both host and graft bone in the healing response. This results in complete incorporation and remodeling of the autograft. In allograft bone the situation is different. Since these grafts do not contain any living cells, the healing relies upon invasion of the graft by host cells from the graft host boundaries. This leads to bone formation restricted to the ends of the graft leaving the mid part unaffected (fig. 1). Furthermore, neovascularization is similarly limited to the host-graft junction. Typically this type of allograft bone is not completely replaced by new bone leaving a necrotic segment of the mid graft prone to necrosis and fracture (28).

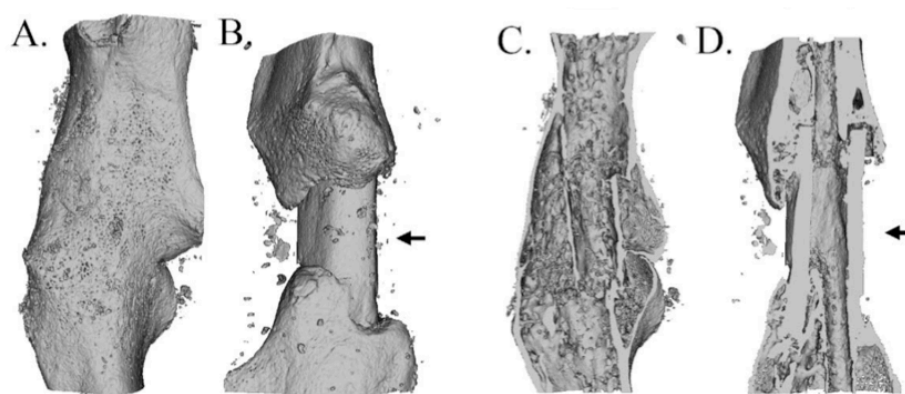


**Figure 1** Micro-CT pictures of autograft (A and C) and allograft (B and D) healing after 6 weeks. The allograft shows an impaired callus formation and poor integration with reduced remodeling (arrows), compared to the autograft (1).

### ***Animal models of structural bone defects***

Several animal models have been used to study the healing response during fracture healing. Both rodent but also large animal models have been used (29, 30). The biology and anatomical differences between animals should be taken into consideration when selecting animal model and interpreting the results. Small rodents have a more simple bone structure without haversian canals, which are seen in human bone. They heal primarily by endochondral bone formation followed by remodeling at the fracture site by the osteoclastic formation of resorption pits on the periosteal surface. In turn osteoblasts fill up the pits with new bone. This is similar to full haversian remodeling but without the formation of secondary haversian systems (30). There is little knowledge of the implications of this anatomical difference. This is a problem with the use of rodents for fracture research but there are several advantages. These include the lower cost of rodent studies making it possible to use larger study groups, a more widespread screening of possible therapeutic interventions and the possibility of using transgenic mouse models.

### ***Murine femoral allograft model***

For the animal studies in this thesis a murine femoral allograft model was used (5). This model demonstrates the biological differences between autograft and allograft healing.

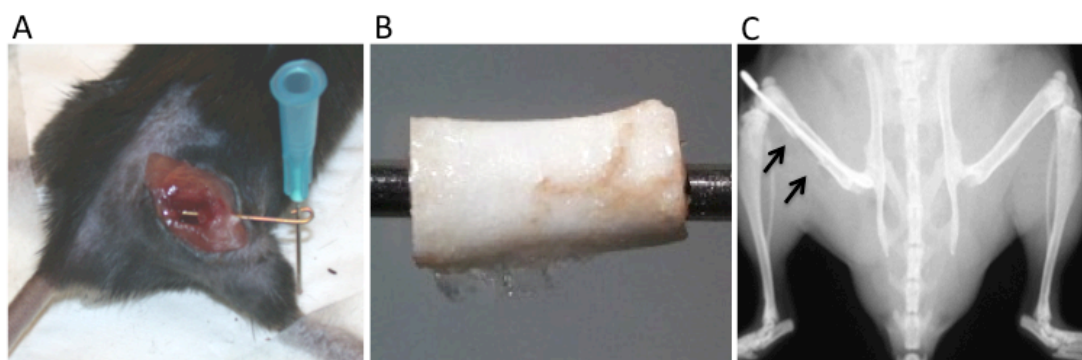


**Figure 2** A metal pin was inserted through the marrow cavity of the femur to illustrate the created 4 mm defect (A). Then a piece of allograft bone (B) was inserted into the defect followed by fixation and post-operative x-ray (C).

We used 8 – 12 weeks old, male C57Bl/6 mice. To create a critical sized defect a 4 mm segment of the mid shaft of the femur was removed by an electrical saw and a freeze thawed graft from an allogenic strain of mice (allograft) was immediately inserted and fixed with a metal pin through the marrow canal to ensure a fairly rigid fixation (fig. 2). Mechanical stability has been demonstrated to be one of the most important factors of cortex-cortex bone healing facilitating the ingrowth of blood vessels and host bone (31, 32). The used stabilization method is adapted from a widely used model of fracture healing (33).

Using this model Tiyyapatanaputi et al. (5) have shown that autograft repair exhibits coordinated endochondral bone formation at the host-graft junction. At the cortical surface of the graft the periosteum gives rise to intramembranous bone formation after 2 weeks. All autografts were healed after 4 weeks. This is similar to what have been shown in other animal models and in clinical studies (7, 34). In contrast the allografts (and frozen isografts as well) show no evidence of intramembranous bone formation. In fact the mid part of the graft was enclosed in fibrous tissue. The formation of new bone was completely dependent on the host at the host-graft boundary (5). By 5 weeks only 85% of the allografts were healed at the host-graft junction. Furthermore, numerous osteoclasts were present on the surface of autografts after 4 weeks initiating the remodeling process. However, only few osteoclasts were observed on the allograft surface indicating the allograft was not integrated into the renewal and turnover of bone. There was no difference between allografts and frozen isografts in regard to new

bone formation and resorption of the grafts, suggesting that an immunogenic response does not affect the graft healing in this model (fig. 3). This is consistent with recent clinical data (35). In addition, it has been demonstrated that the formation of new blood vessels in allograft repair is restricted to the host-graft junction. This was shown after injection of a contrast agent followed by micro-computed tomography (micro-CT) scans (36). This result suggests that the requirement for a functional vascular network is very important to give access for vital progenitor cells to the devitalized graft. More over, Zhang et al. (36) showed that the lack of a live periosteum is a major shortcoming of the processed allografts. Isografts from ROSA 26A mice expressing beta-galactosidase constitutively were inserted into wild type control mice. X-gal staining after 10 days revealed that 70 % of the newly formed bone could be attributed to the proliferation and differentiation of donor progenitor cells on the surface of inserted live bone grafts. Subsequently, the donor-derived cells

were substituted by host cells and at day 28 only few donor-derived cells were present in the sections. Furthermore, the donor cells contributed to neoangiogenesis demonstrated by x-gal staining of endothelial cells within the newly formed bone (36). Off note is also that the removal of the periosteum from the isograft led to allograft like healing. This resulted in bone formation at the graft ends being largely dependent on the host and the formation of fibrotic tissue at the graft surface. In contrast, the removal of bone marrow cells from the isograft did not alter the healing process, underlining the importance of the periosteum for healing in this

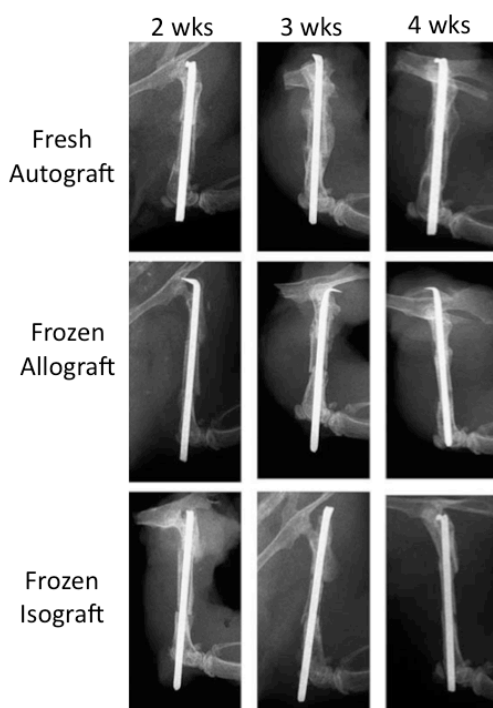


**Figure 3** Radiographic healing of autografts, isografts, and allografts in the murine model. Bone healing was monitored by x-rays taken at 2,3 and 4 weeks post-grafting. A decrease in bone callus was observed surrounding isografts and allografts compared to autografts (5).

model. Finally, the biomechanical performance of the grafts was evaluated. The autografts are superior to allografts at 6 weeks after implantation both with regards to torsional stiffness and ultimate torque. The biomechanical properties of allografts were equivalent to autografts at 9 weeks but decreased significantly at 12 and 18 weeks. The biological and biomechanical properties of auto- and allograft healing demonstrated in this model resemble what has been shown in both other animal models and clinical studies (6, 37-39).

### **Critical factors and osteoinductive cells**

Attempts to overcome the limitations of bone graft repair include strategies focusing on the two shortcomings of allografts: (i) the need for critical factors and (ii) the need for osteoprogenitor cells at the fracture site.

#### ***Demineralized bone matrix***

Osteoinductive properties can be introduced through the use of demineralized bone matrix (DBM). This material possesses minor osteoconductive properties as well but no structural strength. DBM is produced by acid extraction of bone derived from human banked allograft bone. It consists of noncollagenous proteins, bone growth factors and collagen. Among others it contains Bone morphogenetic protein (BMP) -2, -4 and -7 in different amounts dependent on the donor bone it originates from and the sterilization process used. Thus the efficacy and osteoinductive properties between samples differ. Furthermore, the amount of BMP-2 and BMP-7 is limited and lower than what is needed for rhBMP clinical studies (40). DBM can promote bone repair and have been widely used as a graft substitute for smaller defects or a bone graft extender in clinical studies (41-43).

***Recombinant proteins***

The introduction of critical factors through the use of recombinant proteins added to the fracture site has been successful both in preclinical animal studies and in clinical trials (44, 45). The most abundantly used proteins are BMP-2 and BMP-7 (also known as osteogenic protein-1 (OP-1)). The cloning of the human BMP-2 gene made it possible to produce recombinant protein in large quantities. rhBMP are now approved for a limited number of orthopedic surgeries. These proteins are sold in combination with a carrier leading to slow release of the rhBMP after insertion into the fracture site. In spite of several promising in vivo large animal studies, the effect of rhBMP in clinical studies has been limited. One reason is difficulties in maintaining sufficient levels of protein at the fracture site required to achieve bone repair in humans due to fast protein degradation (17). Another reason is that humans seem to be less responsive to rhBMP than animals maybe due to differences in receptor affinity. This has made it necessary to use supraphysiological doses of rhBMP. Finally, there have been reports of adverse effects in relation to the use of rhBMP. Recently, heterotopic bone formation has been reported even at low dose-BMP levels as well as acute airway obstruction caused by soft tissue swelling induced by an inflammatory response 4-7 days after cervical spine fusion (46, 47). Thus there is a continuous uncertainty about the potential of the use of rhBMP. However, rhBMP can be used for some clinical applications although there is a need for further controlled clinical trials to establish the benefits and indications for use (16, 48).

***Osteoprogenitor cells***

Mesenchymal stem cells (MSCs) are derived from different tissues including bone marrow, adipose tissue, skeletal muscle and umbilical cord blood (49-52). These cells possess the ability to proliferate and differentiate into different lineages including bone, cartilage and adipocyte cells (50). For the repair of large bone defects the MSCs have been combined with scaffolds or matrixes to provide an osteoconductive scaffold containing cells able to (i) proliferate and differentiate into bone or cartilage forming cells and (ii) to produce osteoinductive factors which recruit and activate osteoprogenitor cells from the host thereby increasing the reparative response. Zhang et al. have shown that

MSCs were not on their own efficient for the induction of solid bridging and integration when using the previously described murine allograft model (36). Several groups have studied the use of MSCs combined with polymer-carriers (53-55). Some of the problems with this type of tissue engineering approach include poor vascularization of large scaffolds leading to a limited life span of the seeded cells due to insufficient nutrition and hypoxia (56-58). Furthermore, the tissue engineering constructs tested so far have not been able to carry heavy loads making them less useful for the repair of large load-bearing defects (58).

## Gene transfer

To overcome the limitations associated with in vivo use of recombinant proteins and MSCs alternative strategies are being explored. Several groups have studied approaches based on localized gene transfer. In this way it should be possible to

achieve controlled delivery of factors either alone or in combination with cells for bone formation (59-62).

Gene therapy involves the transfer of genetic information to patient cells and the consequent synthesis of RNA or protein in target cells for therapeutic purposes. Gene therapy has been tested for treatment of inherited disorders such as Cystic Fibrosis and Hemophilia (63, 64). Furthermore it is tested clinically for other diseases including various cancers (65), arthritis (66),

Indications	Gene Therapy Clinical Trials	
	Number	%
Cancer diseases	1060	64,5
Cardiovascular diseases	143	8.7
Gene marking	50	3
Healthy volunteers	38	2.3
Infectious diseases	131	8
Monogenic diseases	134	8.2
Neurological diseases	30	1.8
Ocular diseases	18	1.1
Others	40	2.4
Total	1644	

**Table 3** Diseases addressed by ongoing or completed clinical trials worldwide in 2010 (2).

Parkinson disease (67) and congenital eye disease (68). More than 1600 protocols of gene therapy clinical trials have been approved worldwide up till 2010 (tbl. 3) (2).

In the context of bone healing the research still occur at the preclinical level. For bone tissue repair the aim is to deliver genes for osteogenic factors to the fracture site allowing local transcription, translation and expression of the osteogenic protein. Continuous gene expression at low levels are less likely than the bolus application needed for recombinant protein therapy to elicit systemic spread, ectopic bone formation and it may reduce the risk of eliciting an inflammatory or immune response (69). The key questions of gene therapy for bone fracture repair are where to deliver the genes, how to deliver them and what genes to deliver. Moreover safety is of utmost importance since fracture is not a life-threatening disease. Given that fracture repair naturally occurs locally most research has focused on the delivery of the therapeutic gene directly to cells localized in near proximity to the fracture (70-72). This allows a more efficient local gene transfer, less side effects and hopefully increased safety.

### **Vector systems**

On its own DNA is very insufficient in crossing both the cell and nuclear membranes because of its high polarity. As a result, various carrier systems have been developed facilitating the delivery and expression of transgenes in the cell nucleus. These vector systems can be divided into viral and nonviral vectors. The disadvantages associated with viral vectors include difficulties in the production, but most of all the concern for safety. The viral vectors are associated with a risk of immune responses towards the vector, integration into the genome to disrupt normal gene function and recombination (73). In spite of these concerns they are still used for the majority of clinical trials (almost 70 %) due to a much higher efficiency compared to the nonviral vectors in general (2). Viral vectors are derived from wildtype viruses having most viral genes removed except genes

required for the vector to transfer and express the gene of interest. Consequently, most of the pathogenicity and the ability to replicate and produce new infectious viral particles have been eliminated. Viral vectors most often used for bone healing studies are adenovirus, retrovirus including lentivirus and adeno-associated virus (29, 74). Each of these viral systems has advantages and limitations.

### ***Adenoviral vectors***

Adenovirus is a double stranded DNA virus. Adenoviral vectors can transduce many different kinds of cells with high efficiency including both dividing and non-dividing cells. These vectors only integrate into the host genome at low frequency most often leading to transient gene expression. However, there is a concern that 2 – 3 weeks of protein production may not induce an adequate bone repair *in vivo* (37). The natural (wildtype) adenovirus frequently cause infections of the upper respiratory tract, gastrointestinal and conjunctivitis (75). As a consequence most people have neutralizing antibodies. Therefore, the administration of the vector can elicit a severe innate immune response, which can be fatal (76). In 1999 this led to a pause in the use of the adenoviral vector in human gene therapy trials but still it has been widely used for preclinical studies of fracture repair.

### ***Retroviral and Lentiviral vectors***

The retroviruses including the lentiviruses are RNA viruses. After infection of the cell, the viral RNA is reverse transcribed into DNA followed by insertion into the host cell genome. Thereafter the introduced genetic material is replicated as part of the host genome and passed on to the next generation of cells allowing for long-term gene expression. This can be beneficial for monogenic diseases like hemophilia where life long treatment is necessary. The integration process causes the risk of insertional mutagenesis. This has led to the development of leukemia in children treated for severe combined immuno deficiency (SCID) (77). Another limitation of retroviral vectors is that host cell division is necessary for successful transduction (78). This has led to widespread use of

lentiviral vectors since these possess the ability to transduce postmitotic cells like neurons, skeletal muscle and retinal cells (73). Lentiviral vectors have been modified to reduce the risk of integration (79) but since the most used lentiviral vectors are derived from HIV it will be problematic to achieve permission for a clinical trial with non life-threatening diseases.

### ***Recombinant Adeno-associated viral vectors***

Vectors based on adeno-associated virus (AAV) are commonly regarded as safe. This virus is a non-pathogenic parvovirus and it has not been associated with human disease. It is dependent on co-infection with a helper virus (most often adeno- or herpes virus) for productive infection. If a helper virus is lacking the AAV latently infects the cell. The natural (wildtype) AAV tends to integrate into the host genome in a site-specific manner in chromosome 19 (80). Recombinant AAV (rAAV) rarely integrates and the majority persists as nuclear concatemers formed by head to tail recombination leading to a higher safety profile (81). The AAV has a linear single stranded DNA genome (ssAAV) that is 4.7 kb, but only 145 bp at each end – the inverted terminal repeats (ITR) – are required for packaging of the therapeutic transgene into viral particles and internalization of the virus. In the recombinant viral vector the remainder of the genome is deleted including the viral proteins (82). This leaves only the viral capsid and the transgene as possible antigens to the host reducing the likelihood of an immunogenic response. The most commonly used AAV vector is the serotype 2 (AAV-2). Most people have antibodies against AAV-2 and 32 % have neutralizing antibodies (83), which reduces the transduction efficiency and makes readministration problematic. To avoid this problem several other serotypes have been investigated, and some of these have a lower seroprevalence in humans. Furthermore, the different serotypes target different tissues and cells allowing targeted transgene delivery. For example serotype 6 targets skeletal muscle and serotype 8 show specific tropism for liver cells (84, 85). The rAAV transduces both dividing and non-dividing cells. But these vectors depend on the host cell replication to generate a double stranded DNA template needed for mRNA transcription. In postmitotic cells this characteristic can delay the onset of

transgene expression. In order to circumvent this self-complementary AAV (scAAV) were constructed. These vectors have a pseudo-double stranded genome attained by a small deletion in one of the ITRs resulting in a dimeric genome linked by a mutant ITR, which can serve as template for transcription immediately after transduction. These vectors are more efficient but they have a limited packaging capacity (2.15 kb) (86). Increased efficiency allows the use of a reduced amount of viral vector particles and thereby less risk of an immune response. Recently, further progress has been made to increase the transduction efficiency. It has been demonstrated that the exchange of single amino acids in the capsid made the vectors less prone to ubiquitination and degradation before entry into the nucleus leading to a 100-fold increase in efficiency (87, 88). Because of the efficiency, possibility of targeted delivery, low immune response and the mainly episomal nuclear form the rAAV are promising for gene transfer in the musculoskeletal system. Recently two clinical trials of rheumatoid arthritis were reported with rAAV-2 carrying cDNA encoding a TNFR:Fc fusion protein inhibiting the function of TNF- $\alpha$ . The vector was injected intraarticularly (89). However, limitations to the use of rAAV are the restricted size of the transgene (4.5 kb), which is insufficient for some applications but efficient for most of the growth factors used for bone repair. Furthermore, the production of the viral vector is generally constrained by the difficulties of producing high titer vector (90).

### ***Non-viral vectors***

The main advantage of the nonviral vectors compared to viral vectors is their safety. In addition, they are flexible with regards to the size of the transgene to deliver, and manufacturing is simplified. Furthermore they possess less immunogenicity, even though they may elicit an inflammatory response as reported by Ruiz et al. after airway administration of lipid-DNA complexes to cystic fibrosis patients (91, 92). The major drawback of the nonviral vectors is their generally low efficiency *in vivo* and it has been difficult to demonstrate efficient gene transfer for bone healing *in vivo*. However, some studies did demonstrate some effect on bone formation. (59, 93, 94). Barriers to nonviral

gene delivery result in degradation of the DNA during the extra and intracellular trafficking from administration to nuclear transcription. The degradation can be caused by for example toxicity of the nonviral delivery system and degradation of the DNA by extracellular nucleases or lysosomes in the cytosol (95). Nonviral methods can be as simple as the delivery of plasmid DNA, chemical approaches and physical approaches.

Plasmid DNA has a very limited lifespan in the extracellular environment and is inefficient for gene delivery. Nevertheless Osawa et al. have recently demonstrated that repeated injections of a plasmid expressing BMP-2 was able to induce the formation of ectopic mature bone with bone marrow in skeletal muscle after 2 – 8 repeated intramuscular injections (96). Several groups have tried to combine plasmid DNA with polymer scaffolds or bioactive matrices to protect the DNA from degradation and control the release to avoid an initial burst of plasmid and instead obtain a slow, sustained release pattern. One example of this is the use of gene-activated matrices (GAMs). Here the plasmids are incorporated into the matrix, and when the matrix is degraded the plasmids are slowly released leading to transfection of surrounding cells. This technology was used to promote the formation of new bone in segmental bone defects (59, 93, 97). Bonadio et al. delivered a plasmid containing the cDNA of a secreted peptide fragment of human PTH in a GAM inserted in a critical size bone defect in dogs. The gene transfer led to new bone formation not achieved when inserting the matrix or the plasmid alone (59). Furthermore, Vascular endothelial growth factor (VEGF) gene-activated matrix inserted in a rabbit large critical size defect in the radius resulted in increased angiogenesis and osteogenesis (93). Several research groups have investigated polymer scaffolds allowing ingrowth of MSCs, genetically engineered cells or host cells to promote healing. Gazit et al. demonstrated the ability of engrafted MSCs expressing BMP-2 to differentiate and stimulate bone growth in a model of segmental defect repair (98). A shortcoming of this method was fluctuation in the amount of growth factor produced dependent on cell survival during implantation. Furthermore, scaffolds can serve as means for gene delivery. Chemical modification of scaffolds with

cationic polymers or calcium phosphate promotes bone formation through complex formation with the plasmid. These methods protect the DNA from degradation and create a positively charged particle to facilitate internalization and intracellular trafficking (94, 99). Moreover, scaffolds can combine the transfer of cells and plasmids integrating the two primary components needed for bone healing – critical factors and cells. The efficacy of this approach was demonstrated by delivering osteogenic cells and plasmid DNA complexed with calcium phosphate in an injectable hydrogel into the fracture site (100). Finally, physical approaches like electroporation and sonoporation have been developed to enhance the delivery of plasmid DNA to cells. Both methods have been used to promote ectopic bone formation in vivo (96, 101). Recently, electroporation of an osteogenic gene in a non-union bone defect in mice led to induction of bone bridging the gap (101).

#### ***Controlled expression of growth factors and cytokines***

Regenerative bone tissue involves complex, temporal and coordinated expression of several growth factors and cytokines (24, 102). Several groups have tried to control parts of these mechanisms. The efficacy of combining angiogenic and osteogenic factors to improve repair of critical sized defects have been demonstrated in various animal studies (103-105). Recently, the release of selected growth factors at different rates during bone repair has been accomplished using scaffolds consisting of a combination of polymers with different degradation rates (106, 107). Finally, exogenous control of transgene expression has been obtained with a dual-construct vector based on rAAV-BMP-2 regulated by the tetracycline sensitive promotor (TetOn) (108) and through chemical control of an unstable fusion protein (109). Both constructs led to improved bone healing when combined with MSCs.

## Factors used to induce allograft repair

### *Bone Morphogenetic Proteins*

Bone Morphogenetic Proteins (BMPs) are a part of the TGF- $\beta$  family. They affect the development of several kinds of tissues. They are able to induce ectopic bone formation and they can induce osteogenic differentiation of non-bone cells (110). The continuous osteogenesis required for bone growth, remodeling and repair is regulated by the availability of a minor group of BMPs including BMP-2, -4, -7, and -9 (111). These factors act as both chemotactic agents and growth and differentiation factors. As chemotactic agents the BMPs stimulate progenitor cell migration to the site of injury. As growth factors BMPs stimulate angiogenesis and stem cell proliferation, and as differentiation factors they induce the differentiation of stem cells into chondrocytes, osteoblasts and osteocytes (112). Thus the BMPs are able to induce the entire process of new bone formation. These proteins have been demonstrated to promote bone healing in several animal models and they are used clinically.

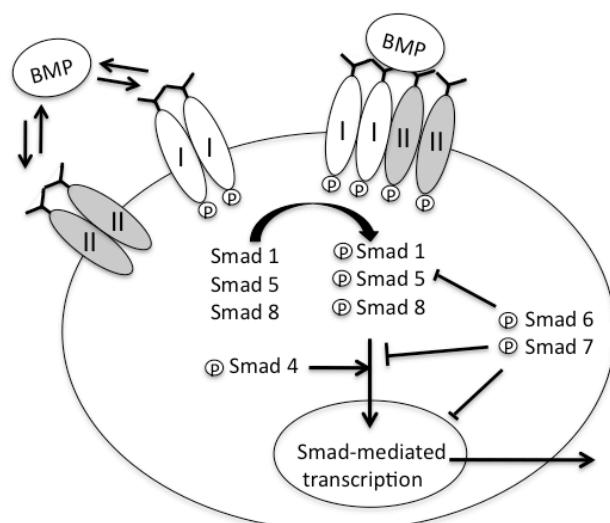


**Figure 4** Schematic drawing showing cellular mechanisms of BMP-induced osteoinduction. Adapted from Samartzis et al (4).

The BMPs send their signals to the cell nucleus through different receptors. The signaling by BMP requires two types of transmembrane serine/threonine receptors. Both receptors of type-I and type-II exist independently in the cell membrane. Complexes of type-I and type-II receptors have high affinity for BMP.

Activation by BMP leads to phosphorylation of the type-I receptor by the type-II receptor, which is auto-phosphorylated. This leads to phosphorylation of the intracellular receptor-Smad proteins 1, 5 and 8 into active forms followed by association with the cofactor Smad4. The activated Smad-complex translocates to the nucleus leading to specific gene transcription (113). Inhibitory Smad proteins are phosphorylated as well and they antagonize the phosphorylation of the receptor-Smads, compete for the binding of Smad4 and down regulate transcription. However, the control of the feedback system is not fully known (4).

For one of the studies in this thesis the activin receptor-like kinase-2 (Alk2) was used (also known as ActR-I). This receptor binds both activins and BMPs and its signaling specificity is like a BMP receptor type-I (114, 115). Alk2 is activated by BMP-2, 4 and 7 - all very potent stimulators of osteoinduction and osteoblast differentiation (116). Alk2 was mutated into a constitutively active form (caAlk2). Accordingly, binding of a type-II receptor or ligand is not required for signal transduction (117). Further, caAlk2 signals cannot be blocked by the endogenous BMP antagonists noggin and chordin.

### ***Vascular Endothelial Growth Factor***

The blood supply at the fracture site has been identified as one of the most important parameters of successful fracture healing (118). VEGF is an essential regulator of angiogenesis (24, 119). During endochondral ossification hypertrophic chondrocytes express VEGF. This protein promotes the invasion of the cartilage by new blood vessels, chondrocyte apoptosis, cartilage remodeling and ossification. In this way the avascular cartilaginous tissue is transformed into vascular new bone. VEGF binds to the tyrosine kinase receptors VEGFR1 and VEGFR2 expressed on the surface of endothelial cells. This binding leads to proliferation, angiogenesis and endothelial cell survival (120). The role of angiogenesis during fracture repair has been demonstrated by the administration of a soluble, neutralizing VEGF receptor in animal models of fracture healing (60, 120). The consequent inhibition of VEGF signaling led to an almost completely suppressed angiogenesis, an extended area of hypertrophic

chondrocytes and prevention of fracture healing. In two studies discontinuation of the inhibition was followed by resumption of vessel formation and bone growth (60, 120-122). Moreover, Mori et al. demonstrated that an anti-angiogenic compound disrupted ectopic bone formation induced by recombinant BMP-2 (122). Finally, adding VEGF when treating critical sized defects promoted the mineralization of the bone and increased bone density (93).

### ***Fibroblast Growth Factor-2***

Fibroblast growth factor-2 (FGF-2) is known to stimulate bone formation (123, 124). FGF-2 is produced by cells from the osteoblast lineage and modulates bone formation through the regulation of fibroblast and osteoblast proliferation (125). In contrast to the bone stimulatory effect, high doses of FGF-2 have been shown to stimulate bone resorption. Evidence suggests that the mechanism involves an indirect effect of FGF-2 on osteoclast precursors through induction of cyclooxygenase 2. This leads to expression of Receptor activator of NF- $\kappa$ B ligand (RANKL) in osteoblasts resulting in differentiation of osteoclast precursors (126). FGF-2 is also known to have an angiogenic potential further improving bone formation. FGF-2 stimulates the production of VEGF in endothelial cells, increases the expression of VEGF receptors and endothelial cell migration (127). FGF-2 and VEGF have been reported to promote increased angiogenesis and formation of more mature blood vessels (128). The combination of the two growth factors has additionally been shown to promote increased vessel and bone formation in a model of vascularized allografts (103).

### ***RANKL – Receptor activator of nuclear factor- $\kappa$ B (NF- $\kappa$ B) ligand***

Receptor activator of NF- $\kappa$ B (RANK), RANKL and osteoprotegerin (OPG) are the main regulators of osteoclast activation and bone resorption. Osteoclasts are the cells responsible for bone resorption. They are multinucleated cells derived from the monocyte/macrophage family. Marrow stromal cells and osteoblasts express macrophage colony stimulating factor (M-CSF) and RANKL, which are essential and sufficient to promote osteoclastogenesis (129). RANKL is a surface-residing molecule. It binds to the receptor RANK on the surface of osteoclast progenitors

thereby inducing the formation of osteoclasts and concomitant bone resorption. OPG inhibits the action of RANKL (130). OPG is a decoy receptor competing with RANK for RANKL. The balance between the stimulator RANK and the inhibitor OPG expressed during fracture healing controls the resorption of the mineralized cartilage in the callus and the later restoration of the bone structure during remodeling (102).

## HYPOTHESIS & AIMS

Allograft healing is limited compared to autograft healing due to 1. Reduced bone formation at the surface of the allograft, 2. Impaired formation of new blood vessels and 3. Lack of osteoclastic remodeling of the allograft bone. In order to improve structural allograft healing it is necessary to identify key factors facilitating these central processes and to develop a method to transfer these factors to processed allografts to obtain similar healing properties as seen in autograft healing.

Main hypothesis in this thesis: Targeted delivery of critical factors to the surface of bone allografts leads to autograft-like healing.

The three papers included in this thesis each had specific hypothesis and aims:

- I. "Remodeling of cortical bone allografts mediated by adherent rAAV-RANKL and VEGF gene therapy."

Hypothesis and aims:

We aimed at defining factors present in autograft healing and absent in allograft healing using RT-PCR. Further, we tested the transduction efficiency of a new delivery system of freeze-dried rAAV. Finally, we tested if the addition of the absent factors (VEGF and RANKL) mediated by freeze-dried rAAV could stimulate allograft vascularization and remodeling assessed by histomorphometry and histology.

- II. "Biological effects of rAAV-caAlk2 coating on structural allograft healing."

Hypothesis and aims:

We aimed to evaluate the transduction efficiency of immobilized rAAV in vivo. Further, the effect of BMP signaling on allograft healing was evaluated by coating allografts with rAAV expressing a constitutively active Alk2 receptor. Bone formation was measured by histomorphometry and micro-CT analysis. The characteristics of allograft healing were evaluated on OrangeG/alcian blue, x-gal and tartrate resistant acid phosphatase (TRAP) stained sections. BMP is a strong

osteogenic promotor and we expected an increase in newly formed bone to improve allograft healing.

- III. "AAV2 mediated VEGF gene transfer leads to increased bone formation and remodeling of bone allografts."

Hypothesis and aims:

To alleviate the restricted angiogenesis in allograft healing and stimulate bone formation we used rAAV immobilized to the surface of bone allografts to obtain local and sustained expression of VEGF and FGF-2. New bone formation was evaluated by histology and micro-CT analysis. We hypothesized that bone healing would be improved as a result of combined stimulation of bone and vessel formation.

## METHODS

### - A short description of most important methods used in this thesis

**Preparation of rAAV vectors.** The rAAV-LacZ, rAAV-GFP and rAAV-Luc vectors (serotype 2/2) with gene expression under the control of the CMV promotor, were obtained directly from the Gene Therapy Center of the University of North Carolina, Chapel Hill, North Carolina, USA. Plasmids containing cDNA for VEGF (131), RANKL (132), Flt1 (104) and caAlk2 (117) were used for subcloning into the pAAV-BGHA transfer vector. After ligation and transformation positive clones were confirmed by restriction digest and DNA sequencing. The resulting plasmids were used for viral vector production through a helper plasmid-free method at the Gene Therapy Center of the University of North Carolina (90). The functional activity of the vectors was determined (117, 133-135).

The cDNA for FGF-2 was inserted into rAAV-LacZ and the rAAV were packaged, purified and titrated (136).

**Preparation of coated allografts.** Allografts harvested from Balb/C mice were washed with 70 % ethanol, rinsed in saline to remove residual ethanol, and then frozen at -80°C for at least 24 hours prior to use (5). For the addition of viral vectors the allograft is placed on dry ice and the rAAV particles in a 50 µL 1 % sorbitol-PBS solution are pipetted onto the cortical surface. Then they were lyophilized and stored at -80°C until transplantation.

**Murine segmental allograft model.** A 4 mm middiaphysial segment was removed from the right femur using an electrical saw. The segment was replaced by an auto- or allograft. When the graft was placed in the femoral defect, and it was secured by a 22-gauge steel pin inserted through the marrow canal (5).

**X-ray.** 2 dimensional x-ray images are used to evaluate successful positioning of the fracture after operation and fracture repair. They are of low resolution and can only be used for qualitative assessment of bone formation and not for quantitative analysis (137).

**Micro computed tomography (micro-CT).** An x-ray based technology, which can create cross sections of an object for production of high-resolution 3D reconstructions (6  $\mu\text{m}$ ). Analysis of these data can provide quantitative outcome measures based on x-ray attenuations of e.g. bone volume and mineral density (138). Advanced micro-CT scanners that allow for in vivo imaging exist. But most often the data are acquired ex vivo and do not allow for longitudinal studies.

**Histology and histomorphometry.** To evaluate cellular and tissue structures of bone healing the tissue must be processed for histological sections (139-141). Histomorphometry is a quantitative method for measuring the volume of a 3D structure from 2-dimensional sections (5). Well known limitations are associated with chosen field of view and the evaluation of irregular structures with high variability in the treatment group.

**Bioluminescence imaging and bioluminescence tomography.** It is an in vivo, quantitative and non-invasive imaging technique based on light emission in living organisms. We have used it with the firefly luciferase, which requires the injection of the substrate D-luciferin to the subject prior to imaging. Temporal and spatial in vivo gene expression can be recorded (142, 143).

## RESULTS SUMMARY

### Localized transduction mediated by freeze-dried rAAV.

We developed a new method to express proteins involved in bone healing from the graft surface mediated by freeze-dried rAAV (fig. 5). In vitro analyses of freeze-dried AAV vectors applied to a monolayer of 293 human embryonic kidney cells revealed no decrease in the transduction efficiency of the vector after freeze-drying and storage at  $-80^{\circ}\text{C}$  determined by  $\beta$ -galactosidase activity. The staining was dispersed throughout the culture disk indicating that the virus readily rehydrates and diffuses in the culture medium.



**Figure 5** Murine femoral allograft with rAAV-LacZ lyophilized onto the surface.

In vivo transduction efficiency of rAAV-LacZ immobilized on the surface of allografts was determined after insertion in mice femurs. X-gal staining of histological section showed the transduction of fibroblasts (~ 1-5 %) in the fibrous tissue in close proximity of the graft, as well as stromal cells in the fracture callus (fig. 6).

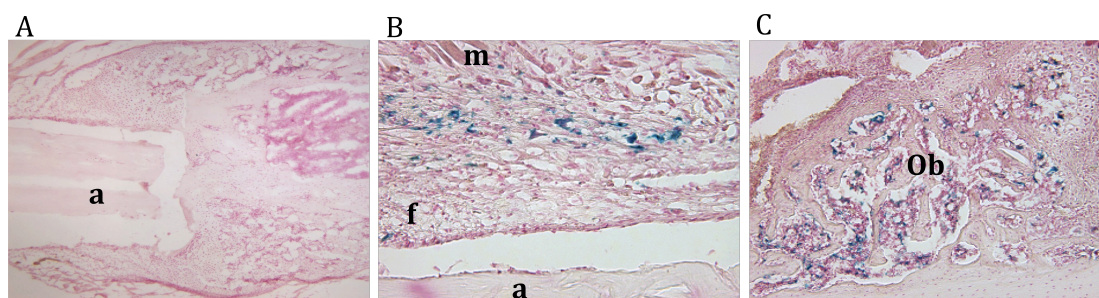


**Figure 6** In vivo transduction efficiency of rAAV-LacZ coated allografts after 14 days. Representative histology of control (A) and rAAV-LacZ coated allografts (B and C). The blue staining indicates transduction of the fibroblast (f) and osteoblasts (Ob) between the allograft (a) or host bone (h) and muscle (m).

### STUDY I. Revitalization of rAAV-RANKL and rAAV-VEGF coated allografts

We show that allografts are deficient of VEGF and RANKL during the healing response compared to autografts. There fore we treated allograft with rAAV mediated gene transfer of RANKL and VEGF individually or in combination. The allografts were inserted in a murine femoral defect model. Histology of the combination group after 4 weeks showed a marked new bone formation on the periosteal surface of the allografts. The live new bone was deposited in regions of previous resorption of the allograft bone (fig. 7). Tartrate resistant acid phosphatase staining indicated active osteoclastic bone resorption of the dead graft and remodeling of the newly formed bone simultaneously. There was

also evidence of neovascularization of the marrow cavity along the length of the graft. In contrast, none of these features were found in the individual treatment groups or the controls.



**Figure 7** Revitalization of processed allografts via rAAV mediated-RANKL and VEGF gene transfer. Representative histology of rAAV\_LacZ (A) and rAAV-RANKL + rAAV-VEGF (B) coated allografts on day 28. The marked amount of new bone on the rAAV-RANKL + rAAV-VEGF coated allograft is highlighted by a reversal line (arrows). In some regions, up to 50 % of the cortical thickness was resorped compared to the rAAV-LacZ coated allograft. The new bone that formed on the allografts was quantified by histomorphometry (C) and the data are presented as the area of new bone formation on the graft  $\pm$  SD. (\* $P < 0.05$  vs. LacZ control).

## STUDY II. Biological effects of BMP signaling on structural allograft healing

To determine the effect of BMP signaling on allograft healing we coated allografts with rAAV-Alk2 and inserted them in a mouse femoral defect. At day 14 there was evidence of endochondral bone formation directly at the surface of the allograft. At day 28 there were signs of remodeling of the mineralized callus and active osteoclasts on the graft surface in the rAAV-Alk2 treated grafts only. Micro-CT analysis after 42 days revealed a significant increase in new bone formation and complete bridging of bone along the entire length of the graft (fig. 8).

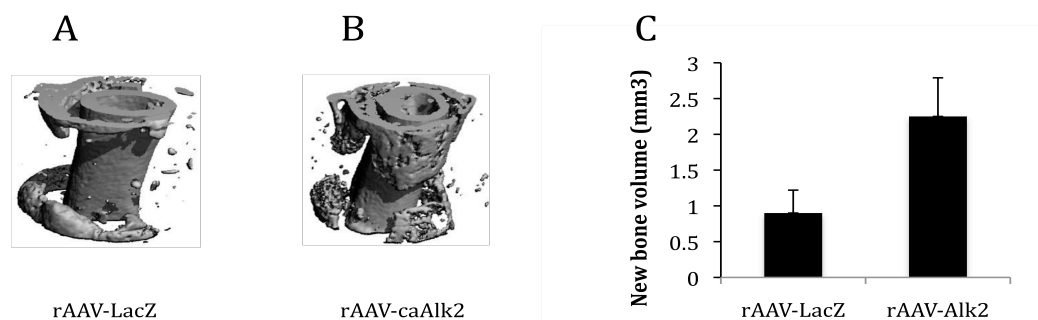


**Figure 8** Micro-CT analysis of rAAV-caAlk2 mediated allograft healing. The 3D reconstructions (A and B) show a marked increase in the amount of new bone formed around the rAAV-caAlk2 coated allograft compared to rAAV-LacZ control (C).

### STUDY III. Increased bone formation and remodeling of bone allografts mediated by rAAV-VEGF gene transfer

We studied the potential effects of stimulating both neovascularisation and new bone formation using AAV2 mediated gene transfer of VEGF and FGF-2. While there was no effect on bone formation in the combination group or the FGF-2 group compared to controls the VEGF coated allografts led to an almost two fold increase in new bone volume (VEGF: 31.7 +/- 11.6 mm<sup>3</sup>, GFP: 16.4 +/- 8.6 mm<sup>3</sup>, p < 0.05). Furthermore, both histology and 3D reconstructions of the micro-CT data showed the formation of new bone covering the entire surface of the VEGF treated allografts (fig. 9). Finally, the VEGF group showed clear signs of remodeling both at the ends and along the side of the graft.

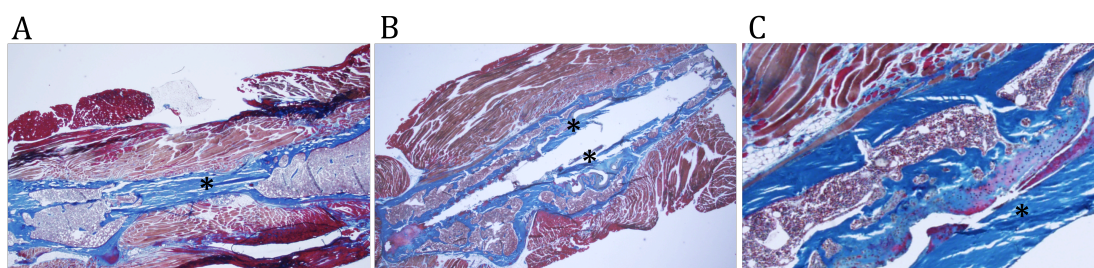


**Figure 9** Increased bone formation in de-vitalized allografts by rAAV-mediated gene transfer of VEGF. Representative Goldner Trichrome stained section of mice in the control (A) and VEGF group (B and C). Allograft is marked by asterixs. The VEGF group is characterized by new bone formation along the entire length of the graft (B) and the presence of calcified cartilage (light blue) and osteoid (red) at the mid part of the graft after 10 weeks.

## DISCUSSION

Allografts are used clinically for the repair of segmental bone defects due to their osteoconductive and biomechanical properties. However, due to the lack of osteogenic and osteoinductive properties the long-term clinical results need to be improved. We have studied whether critical signals to the cortical surface of bone allograft would lead to autograft-like healing by freeze-drying rAAV onto the cortical surface of devitalized allografts. In order to improve allograft healing we focused on affecting osteogenesis, angiogenesis and remodeling.

### **Local gene expression**

Initially, we studied the localization of gene expression. Using LacZ as marker gene we demonstrate that approximately 100 % of the transduction efficiency was maintained after freeze-drying and storage. For in vivo evaluation rAAV-LacZ coated allografts were inserted in a murine femoral allograft model. We observed transduction of cells in the immediate proximity of the graft as well as stromal cells in the fracture callus (1~ 5 % of the cells). Localized gene expression was confirmed by bioluminescence imaging. This method revealed low luciferase expression in the skin in close proximity to the site of insertion of the graft in the split muscle.

### **Revitalization of structural allografts**

Based on the finding that reduced amounts of VEGF and RANKL are expressed during allograft repair compared to autograft, we introduced rAAV-RANKL and VEGF to allografts in vivo. This led to the formation of new bone at the graft surface in areas of already resorped bone and new blood vessels in the marrow cavity of the graft. The observed changes were explained by a central role of VEGF in angiogenesis leading to recruitment of progenitor cells to the fracture site. Further, VEGF is known to be essential for callus formation and mineralization during endochondral osteogenesis (60, 120). In addition, RANKL is the central activator of osteoclast activity leading to induction of extensive

remodeling (129). There was no effect of the two factors alone, supporting the paradigm that VEGF and RANKL work closely together (24).

In order to form a homogenous bone collar surrounding the allograft similar to the one seen in autograft healing, we conferred BMP-2 signals to the surface of the allograft. Histology and micro-CT scans revealed an increase in newly formed bone. Endochondral bone formation was seen directly on the surface of the graft, extending its entire length. Furthermore, there was active osteoclasts on the graft surface and, finally, there was a live, vascularized bone marrow in the treated allografts. It has previously been shown that the Alk2 receptor exerts osteogenic effects through the induction of Indian hedgehog signaling in prehypertrophic chondrocytes (117). Additionally, BMP has also been demonstrated to stimulate vascular ingrowth during osteogenesis through the induction of VEGF expression in osteoblasts (144). These factors could explain the effects seen on allograft healing.

One effective treatment to save a failing allograft clinically is to implant a vascular graft in close proximity to the allograft (14). This shows the importance of establishing a functional vascular network for allograft repair. In order to improve angiogenesis and osteogenesis we coated processed allografts with rAAV-VEGF and FGF-2. We demonstrated increased new bone formation covering the entire length of the graft and evidence of remodeling in the VEGF treated group. We also used VEGF in study I but here we found no effect on bone formation. In the two studies we used VEGF in different amounts ( $5 \times 10^7$  versus  $1 \times 10^9$  transducing units) underlining the importance of making dose-response studies to evaluate the most effective dose. Similar results were found using the BMP-2 gene. Allografts coated with scAAV2.5-BMP-2 in low dose ( $1 \times 10^7$ , -  $10^8$ , -  $10^9$ ) led to unaltered biomechanics of the allografts. However, high dose ( $1 \times 10^{10}$ ) resulted in biomechanics equal to autografts after 6 weeks (145). We could not detect an additive effect on bone formation using the combination of VEGF and FGF-2. This is in contrast to other studies (103). The explanation may be that high levels of FGF-2 have been shown to inhibit bone formation (146). The FGF-2 treated group showed induction of remodeling and increased resorption of the

allograft leading to a significantly reduced graft volume after 10 weeks. This effect may be explained by the effect of FGF-2 on osteoclast differentiation (126).

Several findings in the three studies indicate that the transduction of an active transgene to cells close to the allograft initiates a healing response, which triggers further steps in the repair process elicited by the host. Firstly, there was no formation of fibrous tissue surrounding the allografts contrary to what is normally seen. This may be explained by the transduction of the neighboring cells leading to an altered perception of the graft from being a foreign body to become part of the host. As a result the ingrowth of vessels and osteoclastic resorption are allowed. This may be followed by a host remodeling response converting nonvital bone into live bone including a live bone marrow, even though the genes in the coating does not have access to the marrow cavity. Furthermore, osteoclasts were only observed in areas of previous formation of new bone close to the graft surface suggesting that bone formation on the surface is required to initiate remodeling.

We observed a tendency of uncoordinated bone formation. In the group treated with VEGF and RANKL the resorption and subsequent bone formation did not occur in a coordinated fashion. In some of the grafts resorption was observed initially at the time of sacrifice after 4 weeks. In the VEGF treated group (study III) the presence of new cartilage and osteoid formation at 10 weeks likewise indicate that the osteogenesis response did not occur uniformly. This may be due to variation in the level of transgene expression. This could be caused by variation in local tissue damage eliciting second strand synthesis necessary for successful transduction of rAAV. Recently, Yazici et al. (145) compared the efficacy of ssAAV2.0-BMP-2 and scAAV2.5-BMP-2. They were able to obtain allograft healing superior to autograft healing using a scAAV2.5-BMP-2 coating. Furthermore, they did not detect any new cartilage in the histological sections after 6 weeks indicating that the effect of scAAV-BMP-2 was exerted through enhanced bone formation followed by remodeling rather than exaggerated and

ongoing endochondral ossification. This could be explained by the use of scAAV for a more consistent gene transfer.

### **Limitations**

Although, our results show the potential of allografts coated with rAAV to improve allograft integration and repair, further studies have to be performed to prove the efficacy of this approach. The connectivity of the formed bone has to be improved. This could be obtained from a more uniform coating procedure and perhaps by using scAAV to increase transduction efficiency and get a more uniform response. Further, the biomechanical properties of the formed bone have to be evaluated. This can be done both mechanically and using micro-CT based methods (70, 147). It is also important to evaluate the efficacy of the approach in large animal models with bone structure and weight bearing more similar to humans. Large animals would also allow long-term follow-up so that allograft remodeling could be evaluated. For example the presence of live bone marrow in the caAlk2 group may make the bone less prone to microfractures.

In addition, the safety of the vector system has to be carefully evaluated. AAV is a replication deficient, non-integrating vector derived from a nonpathogenic virus, but the potential for integration and cellular transformation cannot be entirely eliminated. Moreover, we observed sustained luciferase expression for more than 6 months in vivo. Allografts coated with AAV-luciferase have been shown to decay after 3-4 weeks after insertion into the femoral muscle of mice (142). The difference may be due to the insertion into muscle being less traumatic, creating less inflammation, which can induce the necessary second strand synthesis of the AAV. The control of transgene expression could be obtained using an inducible system. Such an approach was used to regulate angiogenesis and bone regeneration mediated by rAAV-based BMP-2 gene delivery to MSCs in a calvarial defect model (108). In addition, it is important to determine the maximum effect elicited by a specific amount of transgene expressed in order to increase safety and avoid side effects induced by overdosing. Overdosing side effects were observed clinically using supraphysiological doses of rhBMP (46,

47). Most importantly, this underlines that the kinetics of gene expression and the distribution of the vector have to be evaluated carefully.

We demonstrate the efficacy of various growth factors for improvement of allograft repair. Further, we demonstrate the potential of a simple cell-free method, creating a “pseudo periosteum”, which can easily be applied in clinical medicine as an of-the-shelf product. The method we described has already been used by other scientists on several biomaterials and also on freeze-dried tendons (143, 148) showing that the technology has broad implications throughout transplantation medicine.

## CONCLUSION

We have shown the ability of immobilized AAV gene transfer to confer osteogenic, angiogenic and remodeling capabilities most often absent in devitalized allograft healing. Several key factors can be used to improve allograft repair. We found that RANKL and VEGF are necessary for autograft healing and can be transferred using rAAV to revitalize structural allografts. Furthermore introduction of BMP signals on to the cortical surface of allografts mediated by rAAV lead to a new bone cortex and remodeling. Finally, we found that VEGF can induce significant bone formation and remodeling. In conclusion our results show that allografts coated with rAAV expressing key factors have the potential to improve the performance of structural allografts.

## PERSPECTIVE

Several issues must be addressed to improve the efficacy of revitalizing allografts adding critical signals mediated by rAAV. Careful evaluation of the kinetics of the transgene expression and the biodistribution of the vector has to be performed. Further, to extend the understanding of the revitalization of the allografts the biomechanics has to be evaluated to ensure proper function of the formed bone. In addition, the method should be established in a large animal model with external fixation similar to what is needed for clinical use. Finally, visualization of bone formation and neovascularization in *in vivo* large animal models may provide further insight into the mechanisms of allograft incorporation and repair.

---

## REFERENCES

1. Koefoed M, Ito H, Gromov K, Reynolds DG, Awad HA, Rubery PT, Ulrich-Vinther M, Soballe K, Guldberg RE, Lin AS, O'Keefe RJ, Zhang X, Schwarz EM. 2005. Biological effects of rAAV-caAlk2 coating on structural allograft healing. *Mol Ther* 12: 212-8
2. 2010. Gene Therapy Clinical Trials Worldwide. *Journal of Gene Medicine* [www.abedia.com/wiley/years.php](http://www.abedia.com/wiley/years.php)
3. Gazdag AR, Lane JM, Glaser D, Forster RA. 1995. Alternatives to Autogenous Bone Graft: Efficacy and Indications. *J Am Acad Orthop Surg* 3: 1-8
4. Samartzis D, Khanna N, Shen FH, An HS. 2005. Update on bone morphogenetic proteins and their application in spine surgery. *J Am Coll Surg* 200: 236-48
5. Tiyyapattanaputi P, Rubery PT, Carmouche J, Schwarz EM, O'Keefe R J, Zhang X. 2004. A novel murine segmental femoral graft model. *J Orthop Res* 22: 1254-60
6. Stevenson S, Li XQ, Davy DT, Klein L, Goldberg VM. 1997. Critical biological determinants of incorporation of non-vascularized cortical bone grafts. Quantification of a complex process and structure. *J Bone Joint Surg Am* 79: 1-16
7. Enneking WF, Campanacci DA. 2001. Retrieved human allografts : a clinicopathological study. *J Bone Joint Surg Am* 83-A: 971-86
8. McKee MD. 2006. Management of segmental bony defects: the role of osteoconductive orthobiologics. *J Am Acad Orthop Surg* 14: S163-7
9. Friedlaender GE, Perry CR, Cole JD, Cook SD, Cierny G, Muschler GF, Zych GA, Calhoun JH, LaForte AJ, Yin S. 2001. Osteogenic protein-1 (bone morphogenetic protein-7) in the treatment of tibial nonunions. *J Bone Joint Surg Am* 83-A Suppl 1: S151-8
10. Littenberg B, Weinstein LP, McCarren M, Mead T, Swiontkowski MF, Rudicel SA, Heck D. 1998. Closed fractures of the tibial shaft. A meta-analysis of three methods of treatment. *J Bone Joint Surg Am* 80: 174-83
11. Gandhi A, Liporace F, Azad V, Mattie J, Lin SS. 2006. Diabetic fracture healing. *Foot Ankle Clin* 11: 805-24
12. Kwiatkowski TC, Hanley EN, Jr., Ramp WK. 1996. Cigarette smoking and its orthopedic consequences. *Am J Orthop (Belle Mead NJ)* 25: 590-7
13. Stevenson S. 1999. Biology of bone grafts. *Orthop Clin North Am* 30: 543-52
14. Eward WC, Kontogeorgakos V, Levin LS, Brigman BE. 2010. Free vascularized fibular graft reconstruction of large skeletal defects after tumor resection. *Clin Orthop Relat Res* 468: 590-8
15. Gafni Y, Turgeman G, Liebergal M, Pelled G, Gazit Z, Gazit D. 2004. Stem cells as vehicles for orthopedic gene therapy. *Gene Ther* 11: 417-26
16. Garrison KR, Shemilt I, Donell S, Ryder JJ, Mugford M, Harvey I, Song F, Alt V. 2010. Bone morphogenetic protein (BMP) for fracture healing in adults. *Cochrane Database of Systematic Reviews*: -
17. Seeherman H, Wozney J, Li R. 2002. Bone morphogenetic protein delivery systems. *Spine (Phila Pa 1976)* 27: S16-23

18. Goulet JA, Senunas LE, DeSilva GL, Greenfield ML. 1997. Autogenous iliac crest bone graft. Complications and functional assessment. *Clin Orthop Relat Res*: 76-81
19. Sasso RC, LeHuec JC, Shaffrey C. 2005. Iliac crest bone graft donor site pain after anterior lumbar interbody fusion: a prospective patient satisfaction outcome assessment. *J Spinal Disord Tech* 18 Suppl: S77-81
20. Arrington ED, Smith WJ, Chambers HG, Bucknell AL, Davino NA. 1996. Complications of iliac crest bone graft harvesting. *Clin Orthop Relat Res*: 300-9
21. Banwart JC, Asher MA, Hassanein RS. 1995. Iliac crest bone graft harvest donor site morbidity. A statistical evaluation. *Spine (Phila Pa 1976)* 20: 1055-60
22. Boyce T, Edwards J, Scarborough N. 1999. Allograft bone. The influence of processing on safety and performance. *Orthop Clin North Am* 30: 571-81
23. Wheeler DL, Enneking WF. 2005. Allograft bone decreases in strength in vivo over time. *Clin Orthop Relat Res*: 36-42
24. Gerstenfeld LC, Cullinane DM, Barnes GL, Graves DT, Einhorn TA. 2003. Fracture healing as a post-natal developmental process: molecular, spatial, and temporal aspects of its regulation. *J Cell Biochem* 88: 873-84
25. Probst A, Spiegel HU. 1997. Cellular mechanisms of bone repair. *J Invest Surg* 10: 77-86
26. Komatsu DE, Warden SJ. 2010. The control of fracture healing and its therapeutic targeting: improving upon nature. *J Cell Biochem* 109: 302-11
27. Meller Y, Kestenbaum RS, Mozes M, Mozes G, Yagil R, Shany S. 1984. Mineral and endocrine metabolism during fracture healing in dogs. *Clin Orthop Relat Res*: 289-95
28. Goldberg VM, Stevenson S. 1993. The biology of bone grafts. *Semin Arthroplasty* 4: 58-63
29. Evans CH. 2010. Gene therapy for bone healing. *Expert Rev Mol Med* 12: e18
30. Nunamaker DM. 1998. Experimental models of fracture repair. *Clin Orthop Relat Res*: S56-65
31. Davy DT. 1999. Biomechanical issues in bone transplantation. *Orthop Clin North Am* 30: 553-63
32. Benevenia J, Zimmerman M, Keating J, Cyran F, Blacksin M, Parsons JR. 2000. Mechanical environment affects allograft incorporation. *J Biomed Mater Res* 53: 67-72
33. Bonnarens F, Einhorn TA. 1984. Production of a standard closed fracture in laboratory animal bone. *J Orthop Res* 2: 97-101
34. Stevenson S, Emery SE, Goldberg VM. 1996. Factors affecting bone graft incorporation. *Clin Orthop Relat Res*: 66-74
35. Reikeras O, Reinholt FP, Zinocker S, Shegarfi H, Rolstad B. 2011. Healing of Long-term Frozen Orthotopic Bone Allografts is not Affected by MHC Differences Between Donor and Recipient. *Clin Orthop Relat Res*
36. Zhang X, Xie C, Lin AS, Ito H, Awad H, Lieberman JR, Rubery PT, Schwarz EM, O'Keefe RJ, Goldberg RE. 2005. Periosteal progenitor cell fate in segmental cortical bone graft transplantations: implications for functional tissue engineering. *J Bone Miner Res* 20: 2124-37
37. Virk MS, Conduah A, Park SH, Liu N, Sugiyama O, Cuomo A, Kang C, Lieberman JR. 2008. Influence of short-term adenoviral vector and prolonged lentiviral vector mediated bone morphogenetic protein-2 expression on the quality of bone repair in a rat femoral defect model. *Bone* 42: 921-31

38. Lieberman JR, Daluiski A, Stevenson S, Wu L, McAllister P, Lee YP, Kabo JM, Finerman GA, Berk AJ, Witte ON. 1999. The effect of regional gene therapy with bone morphogenetic protein-2-producing bone-marrow cells on the repair of segmental femoral defects in rats. *J Bone Joint Surg Am* 81: 905-17
39. Brigman BE, Hornicek FJ, Gebhardt MC, Mankin HJ. 2004. Allografts about the Knee in Young Patients with High-Grade Sarcoma. *Clin Orthop Relat Res*: 232-9
40. Bae HW, Zhao L, Kanim LE, Wong P, Delamarter RB, Dawson EG. 2006. Intervariability and intravariability of bone morphogenetic proteins in commercially available demineralized bone matrix products. *Spine (Phila Pa 1976)* 31: 1299-306; discussion 307-8
41. Hierholzer C, Sama D, Toro JB, Peterson M, Helfet DL. 2006. Plate fixation of ununited humeral shaft fractures: effect of type of bone graft on healing. *J Bone Joint Surg Am* 88: 1442-7
42. Cheung S, Westerheide K, Ziran B. 2003. Efficacy of contained metaphyseal and periarticular defects treated with two different demineralized bone matrix allografts. *Int Orthop* 27: 56-9
43. Feng Y, Wang S, Jin D, Sheng J, Chen S, Cheng X, Zhang C. 2009. Free vascularised fibular grafting with OsteoSet((R))2 demineralised bone matrix versus autograft for large osteonecrotic lesions of the femoral head. *Int Orthop*
44. Einhorn TA, Majeska RJ, Mohaideen A, Kagel EM, Boussein ML, Turek TJ, Wozney JM. 2003. A single percutaneous injection of recombinant human bone morphogenetic protein-2 accelerates fracture repair. *J Bone Joint Surg Am* 85-A: 1425-35
45. Cook SD, Wolfe MW, Salkeld SL, Rueger DC. 1995. Effect of recombinant human osteogenic protein-1 on healing of segmental defects in non-human primates. *J Bone Joint Surg Am* 77: 734-50
46. Yaremchuk K, Toma M, Somers M. 2010. Acute Airway Obstruction Associated with the Use of Bone-Morphogenetic Protein in Cervical Spinal Fusion. *Laryngoscope* 120: S140
47. Mannion RJ, Nowitzke AM, Wood MJ. 2010. Promoting fusion in minimally invasive lumbar interbody stabilization with low-dose bone morphogenic protein-2-but what is the cost? *Spine J*
48. Veillette CJ, McKee MD. 2007. Growth factors--BMPs, DBMs, and buffy coat products: are there any proven differences amongst them? *Injury* 38 Suppl 1: S38-48
49. Erices A, Conget P, Minguell JJ. 2000. Mesenchymal progenitor cells in human umbilical cord blood. *Br J Haematol* 109: 235-42
50. Pittenger MF, Mackay AM, Beck SC, Jaiswal RK, Douglas R, Mosca JD, Moorman MA, Simonetti DW, Craig S, Marshak DR. 1999. Multilineage potential of adult human mesenchymal stem cells. *Science* 284: 143-7
51. Williams JT, Southerland SS, Souza J, Calcutt AF, Cartledge RG. 1999. Cells isolated from adult human skeletal muscle capable of differentiating into multiple mesodermal phenotypes. *Am Surg* 65: 22-6
52. Zuk PA, Zhu M, Ashjian P, De Ugarte DA, Huang JI, Mizuno H, Alfonso ZC, Fraser JK, Benhaim P, Hedrick MH. 2002. Human adipose tissue is a source of multipotent stem cells. *Mol Biol Cell* 13: 4279-95
53. Marcacci M, Kon E, Moukhachev V, Lavroukov A, Kutepov S, Quarto R, Mastrogiacomo M, Cancedda R. 2007. Stem cells associated with macroporous

- bioceramics for long bone repair: 6- to 7-year outcome of a pilot clinical study. *Tissue Eng* 13: 947-55
54. Viateau V, Guillemain G, Bousson V, Oudina K, Hannouche D, Sedel L, Logeart-Avramoglou D, Petite H. 2007. Long-bone critical-size defects treated with tissue-engineered grafts: a study on sheep. *J Orthop Res* 25: 741-9
55. Zhou J, Lin H, Fang T, Li X, Dai W, Uemura T, Dong J. 2010. The repair of large segmental bone defects in the rabbit with vascularized tissue engineered bone. *Biomaterials* 31: 1171-9
56. Nakasa T, Ishida O, Sunagawa T, Nakamae A, Yasunaga Y, Agung M, Ochi M. 2005. Prefabrication of vascularized bone graft using a combination of fibroblast growth factor-2 and vascular bundle implantation into a novel interconnected porous calcium hydroxyapatite ceramic. *J Biomed Mater Res A* 75: 350-5
57. Potier E, Ferreira E, Meunier A, Sedel L, Logeart-Avramoglou D, Petite H. 2007. Prolonged hypoxia concomitant with serum deprivation induces massive human mesenchymal stem cell death. *Tissue Eng* 13: 1325-31
58. Cancedda R, Giannoni P, Mastrogiacomo M. 2007. A tissue engineering approach to bone repair in large animal models and in clinical practice. *Biomaterials* 28: 4240-50
59. Bonadio J, Smiley E, Patil P, Goldstein S. 1999. Localized, direct plasmid gene delivery in vivo: prolonged therapy results in reproducible tissue regeneration. *Nat Med* 5: 753-9
60. Street J, Bao M, deGuzman L, Bunting S, Peale FV, Jr., Ferrara N, Steinmetz H, Hoeffel J, Cleland JL, Daugherty A, van Bruggen N, Redmond HP, Carano RA, Filvaroff EH. 2002. Vascular endothelial growth factor stimulates bone repair by promoting angiogenesis and bone turnover. *Proc Natl Acad Sci U S A* 99: 9656-61
61. Viggesswarapu M, Boden SD, Liu Y, Hair GA, Louis-Ugbo J, Murakami H, Kim HS, Mayr MT, Hutton WC, Titus L. 2001. Adenoviral delivery of LIM mineralization protein-1 induces new-bone formation in vitro and in vivo. *J Bone Joint Surg Am* 83-A: 364-76
62. Zhang X, Awad HA, O'Keefe RJ, Guldberg RE, Schwarz EM. 2008. A perspective: engineering periosteum for structural bone graft healing. *Clin Orthop Relat Res* 466: 1777-87
63. Flotte TR, Zeitlin PL, Reynolds TC, Heald AE, Pedersen P, Beck S, Conrad CK, Brass-Ernst L, Humphries M, Sullivan K, Wetzel R, Taylor G, Carter BJ, Guggino WB. 2003. Phase I trial of intranasal and endobronchial administration of a recombinant adeno-associated virus serotype 2 (rAAV2)-CFTR vector in adult cystic fibrosis patients: a two-part clinical study. *Hum Gene Ther* 14: 1079-88
64. Manno CS, Chew AJ, Hutchison S, Larson PJ, Herzog RW, Arruda VR, Tai SJ, Ragni MV, Thompson A, Ozelo M, Couto LB, Leonard DG, Johnson FA, McClelland A, Scallan C, Skarsgard E, Flake AW, Kay MA, High KA, Glader B. 2003. AAV-mediated factor IX gene transfer to skeletal muscle in patients with severe hemophilia B. *Blood* 101: 2963-72
65. Gillet JP, Macadangang B, Fathke RL, Gottesman MM, Kimchi-Sarfaty C. 2009. The development of gene therapy: from monogenic recessive disorders to complex diseases such as cancer. *Methods Mol Biol* 542: 5-54

66. Ghivizzani SC, Gouze E, Gouze JN, Kay JD, Bush ML, Watson RS, Levings PP, Nickerson DM, Colahan PT, Robbins PD, Evans CH. 2008. Perspectives on the use of gene therapy for chronic joint diseases. *Curr Gene Ther* 8: 273-86
67. Fiandaca M, Forsayeth J, Bankiewicz K. 2008. Current status of gene therapy trials for Parkinson's disease. *Exp Neurol* 209: 51-7
68. Stein L, Roy K, Lei L, Kaushal S. 2011. Clinical gene therapy for the treatment of RPE65-associated Leber congenital amaurosis. *Expert Opin Biol Ther* 11: 429-39
69. Hwang CJ, Vaccaro AR, Lawrence JP, Hong J, Schellekens H, Alaoui-Ismaili MH, Falb D. 2009. Immunogenicity of bone morphogenetic proteins. *J Neurosurg Spine* 10: 443-51
70. Xie C, Reynolds D, Awad H, Rubery PT, Pelled G, Gazit D, Guldberg RE, Schwarz EM, O'Keefe RJ, Zhang X. 2007. Structural bone allograft combined with genetically engineered mesenchymal stem cells as a novel platform for bone tissue engineering. *Tissue Eng* 13: 435-45
71. Hu WW, Wang Z, Hollister SJ, Krebsbach PH. 2007. Localized viral vector delivery to enhance in situ regenerative gene therapy. *Gene Ther* 14: 891-901
72. Evans CH, Liu FJ, Glatt V, Hoyland JA, Kirker-Head C, Walsh A, Betz O, Wells JW, Betz V, Porter RM, Saad FA, Gerstenfeld LC, Einhorn TA, Harris MB, Vrahas MS. 2009. Use of genetically modified muscle and fat grafts to repair defects in bone and cartilage. *Eur Cell Mater* 18: 96-111
73. Young LS, Searle PF, Onion D, Mautner V. 2006. Viral gene therapy strategies: from basic science to clinical application. *J Pathol* 208: 299-318
74. Fischer J, Kolk A, Wolfart S, Pautke C, Warnke PH, Plank C, Smeets R. 2011. Future of local bone regeneration - Protein versus gene therapy. *J Craniomaxillofac Surg* 39: 54-64
75. Horwitz MS. 2001. Adenovirus immunoregulatory genes and their cellular targets. *Virology* 279: 1-8
76. Raper SE, Chirmule N, Lee FS, Wivel NA, Bagg A, Gao GP, Wilson JM, Batshaw ML. 2003. Fatal systemic inflammatory response syndrome in a ornithine transcarbamylase deficient patient following adenoviral gene transfer. *Mol Genet Metab* 80: 148-58
77. Hacein-Bey-Abina S, Von Kalle C, Schmidt M, McCormack MP, Wulffraat N, Leboulch P, Lim A, Osborne CS, Pawliuk R, Morillon E, Sorensen R, Forster A, Fraser P, Cohen JI, de Saint Basile G, Alexander I, Wintergerst U, Frebourg T, Aurias A, Stoppa-Lyonnet D, Romana S, Radford-Weiss I, Gross F, Valensi F, Delabesse E, Macintyre E, Sigaux F, Soulier J, Leiva LE, Wissler M, Prinz C, Rabbitts TH, Le Deist F, Fischer A, Cavazzana-Calvo M. 2003. LMO2-associated clonal T cell proliferation in two patients after gene therapy for SCID-X1. *Science* 302: 415-9
78. Kurian KM, Watson CJ, Wyllie AH. 2000. Retroviral vectors. *Mol Pathol* 53: 173-6
79. Sarkis C, Philippe S, Mallet J, Serguera C. 2008. Non-integrating lentiviral vectors. *Curr Gene Ther* 8: 430-7
80. Young SM, Jr., Samulski RJ. 2001. Adeno-associated virus (AAV) site-specific recombination does not require a Rep-dependent origin of replication within the AAV terminal repeat. *Proc Natl Acad Sci U S A* 98: 13525-30

81. Miller DG, Trobridge GD, Petek LM, Jacobs MA, Kaul R, Russell DW. 2005. Large-scale analysis of adeno-associated virus vector integration sites in normal human cells. *J Virol* 79: 11434-42
82. Schwarz EM. 2000. The adeno-associated virus vector for orthopaedic gene therapy. *Clin Orthop Relat Res*: S31-9
83. Sun JY, Anand-Jawa V, Chatterjee S, Wong KK. 2003. Immune responses to adeno-associated virus and its recombinant vectors. *Gene Ther* 10: 964-76
84. Blankinship MJ, Gregorevic P, Allen JM, Harper SQ, Harper H, Halbert CL, Miller AD, Chamberlain JS. 2004. Efficient transduction of skeletal muscle using vectors based on adeno-associated virus serotype 6. *Mol Ther* 10: 671-8
85. Davidoff AM, Gray JT, Ng CY, Zhang Y, Zhou J, Spence Y, Bakar Y, Nathwani AC. 2005. Comparison of the ability of adeno-associated viral vectors pseudotyped with serotype 2, 5, and 8 capsid proteins to mediate efficient transduction of the liver in murine and nonhuman primate models. *Mol Ther* 11: 875-88
86. Choi VW, Asokan A, Haberman RA, Samulski RJ. 2007. Production of recombinant adeno-associated viral vectors for in vitro and in vivo use. *Curr Protoc Mol Biol* Chapter 16: Unit 16 25
87. Petrs-Silva H, Dinculescu A, Li Q, Min SH, Chiodo V, Pang JJ, Zhong L, Zolotukhin S, Srivastava A, Lewin AS, Hauswirth WW. 2009. High-efficiency transduction of the mouse retina by tyrosine-mutant AAV serotype vectors. *Mol Ther* 17: 463-71
88. Zhong L, Li B, Mah CS, Govindasamy L, Agbandje-McKenna M, Cooper M, Herzog RW, Zolotukhin I, Warrington KH, Jr., Weigel-Van Aken KA, Hobbs JA, Zolotukhin S, Muzyczka N, Srivastava A. 2008. Next generation of adeno-associated virus 2 vectors: point mutations in tyrosines lead to high-efficiency transduction at lower doses. *Proc Natl Acad Sci U S A* 105: 7827-32
89. Mease PJ, Hobbs K, Chalmers A, El-Gabalawy H, Bookman A, Keystone E, Furst DE, Anklesaria P, Heald AE. 2009. Local delivery of a recombinant adenoassociated vector containing a tumour necrosis factor alpha antagonist gene in inflammatory arthritis: a phase 1 dose-escalation safety and tolerability study. *Ann Rheum Dis* 68: 1247-54
90. Xiao X, Li J, Samulski RJ. 1998. Production of high-titer recombinant adeno-associated virus vectors in the absence of helper adenovirus. *J Virol* 72: 2224-32
91. Ruiz FE, Clancy JP, Perricone MA, Bebok Z, Hong JS, Cheng SH, Meeker DP, Young KR, Schoumacher RA, Weatherly MR, Wing L, Morris JE, Sindel L, Rosenberg M, van Ginkel FW, McGhee JR, Kelly D, Lyrene RK, Sorscher EJ. 2001. A clinical inflammatory syndrome attributable to aerosolized lipid-DNA administration in cystic fibrosis. *Hum Gene Ther* 12: 751-61
92. Whitmore M, Li S, Huang L. 1999. LPD lipopolyplex initiates a potent cytokine response and inhibits tumor growth. *Gene Ther* 6: 1867-75
93. Geiger F, Bertram H, Berger I, Lorenz H, Wall O, Eckhardt C, Simank HG, Richter W. 2005. Vascular endothelial growth factor gene-activated matrix (VEGF165-GAM) enhances osteogenesis and angiogenesis in large segmental bone defects. *J Bone Miner Res* 20: 2028-35
94. Keeney M, van den Beucken JJ, van der Kraan PM, Jansen JA, Pandit A. 2010. The ability of a collagen/calcium phosphate scaffold to act as its own vector for gene delivery and to promote bone formation via transfection with VEGF(165). *Biomaterials* 31: 2893-902

95. Wiethoff CM, Middaugh CR. 2003. Barriers to nonviral gene delivery. *J Pharm Sci* 92: 203-17
96. Osawa K, Okubo Y, Nakao K, Koyama N, Bessho K. 2010. Osteoinduction by repeat plasmid injection of human bone morphogenetic protein-2. *J Gene Med* 12: 937-44
97. Fang J, Zhu YY, Smiley E, Bonadio J, Rouleau JP, Goldstein SA, McCauley LK, Davidson BL, Roessler BJ. 1996. Stimulation of new bone formation by direct transfer of osteogenic plasmid genes. *Proc Natl Acad Sci U S A* 93: 5753-8
98. Gazit D, Turgeman G, Kelley P, Wang E, Jalenak M, Zilberman Y, Moutsatsos I. 1999. Engineered pluripotent mesenchymal cells integrate and differentiate in regenerating bone: a novel cell-mediated gene therapy. *J Gene Med* 1: 121-33
99. Scherer F, Schillinger U, Putz U, Stemberger A, Plank C. 2002. Nonviral vector loaded collagen sponges for sustained gene delivery in vitro and in vivo. *J Gene Med* 4: 634-43
100. Krebs MD, Salter E, Chen E, Sutter KA, Alsberg E. 2010. Calcium phosphate-DNA nanoparticle gene delivery from alginate hydrogels induces in vivo osteogenesis. *J Biomed Mater Res A* 92: 1131-8
101. Takayama K, Suzuki A, Manaka T, Taguchi S, Hashimoto Y, Imai Y, Wakitani S, Takaoka K. 2009. RNA interference for noggin enhances the biological activity of bone morphogenetic proteins in vivo and in vitro. *J Bone Miner Metab* 27: 402-11
102. Kon T, Cho TJ, Aizawa T, Yamazaki M, Nooh N, Graves D, Gerstenfeld LC, Einhorn TA. 2001. Expression of osteoprotegerin, receptor activator of NF-kappaB ligand (osteoprotegerin ligand) and related proinflammatory cytokines during fracture healing. *J Bone Miner Res* 16: 1004-14
103. Larsen M, Willems WF, Pelzer M, Friedrich PF, Yaszemski MJ, Bishop AT. 2010. Augmentation of surgical angiogenesis in vascularized bone allotransplants with host-derived a/v bundle implantation, fibroblast growth factor-2, and vascular endothelial growth factor administration. *J Orthop Res* 28: 1015-21
104. Peng H, Wright V, Usas A, Gearhart B, Shen HC, Cummins J, Huard J. 2002. Synergistic enhancement of bone formation and healing by stem cell-expressed VEGF and bone morphogenetic protein-4. *J Clin Invest* 110: 751-9
105. Zhang C, Wang KZ, Qiang H, Tang YL, Li Q, Li M, Dang XQ. 2010. Angiopoiesis and bone regeneration via co-expression of the hVEGF and hBMP genes from an adeno-associated viral vector in vitro and in vivo. *Acta Pharmacol Sin* 31: 821-30
106. Ginty PJ, Barry JJ, White LJ, Howdle SM, Shakesheff KM. 2008. Controlling protein release from scaffolds using polymer blends and composites. *Eur J Pharm Biopharm* 68: 82-9
107. Kanczler JM, Ginty PJ, White L, Clarke NM, Howdle SM, Shakesheff KM, Oreffo RO. 2010. The effect of the delivery of vascular endothelial growth factor and bone morphogenetic protein-2 to osteoprogenitor cell populations on bone formation. *Biomaterials* 31: 1242-50
108. Gafni Y, Pelled G, Zilberman Y, Turgeman G, Apparailly F, Yotvat H, Galun E, Gazit Z, Jorgensen C, Gazit D. 2004. Gene therapy platform for bone regeneration using an exogenously regulated, AAV-2-based gene expression system. *Mol Ther* 9: 587-95

109. Kwan MD, Sellmyer MA, Quarto N, Ho AM, Wandless TJ, Longaker MT. 2011. Chemical control of FGF-2 release for promoting calvarial healing with adipose stem cells. *J Biol Chem*
110. Urist MR. 1965. Bone: formation by autoinduction. *Science* 150: 893-9
111. Leboy PS. 2006. Regulating bone growth and development with bone morphogenetic proteins. *Ann N Y Acad Sci* 1068: 14-8
112. Boden SD, Sumner DR. 1995. Biologic factors affecting spinal fusion and bone regeneration. *Spine (Phila Pa 1976)* 20: 102S-12S
113. Zou H, Wieser R, Massague J, Niswander L. 1997. Distinct roles of type I bone morphogenetic protein receptors in the formation and differentiation of cartilage. *Genes Dev* 11: 2191-203
114. Chen YG, Massague J. 1999. Smad1 recognition and activation by the ALK1 group of transforming growth factor-beta family receptors. *J Biol Chem* 274: 3672-7
115. Mishina Y, Crombie R, Bradley A, Behringer RR. 1999. Multiple roles for activin-like kinase-2 signaling during mouse embryogenesis. *Dev Biol* 213: 314-26
116. Azari K, Doll BA, Sfeir C, Mu Y, Hollinger JO. 2001. Therapeutic potential of bone morphogenetic proteins. *Expert Opin Investig Drugs* 10: 1677-86
117. Zhang D, Schwarz EM, Rosier RN, Zuscik MJ, Puzas JE, O'Keefe RJ. 2003. ALK2 functions as a BMP type I receptor and induces Indian hedgehog in chondrocytes during skeletal development. *J Bone Miner Res* 18: 1593-604
118. Axelrad TW, Kakar S, Einhorn TA. 2007. New technologies for the enhancement of skeletal repair. *Injury* 38 Suppl 1: S49-62
119. Tsiroidis E, Upadhyay N, Giannoudis P. 2007. Molecular aspects of fracture healing: which are the important molecules? *Injury* 38 Suppl 1: S11-25
120. Gerber HP, Vu TH, Ryan AM, Kowalski J, Werb Z, Ferrara N. 1999. VEGF couples hypertrophic cartilage remodeling, ossification and angiogenesis during endochondral bone formation. *Nat Med* 5: 623-8
121. Hausman MR, Schaffler MB, Majeska RJ. 2001. Prevention of fracture healing in rats by an inhibitor of angiogenesis. *Bone* 29: 560-4
122. Mori S, Yoshikawa H, Hashimoto J, Ueda T, Funai H, Kato M, Takaoka K. 1998. Antiangiogenic agent (TNP-470) inhibition of ectopic bone formation induced by bone morphogenetic protein-2. *Bone* 22: 99-105
123. Keiichi K, Mitsunobu K, Masafumi S, Yutaka D, Toshiaki S. 2009. Induction of new bone by basic FGF-loaded porous carbonate apatite implants in femur defects in rats. *Clin Oral Implants Res* 20: 560-5
124. Kawaguchi H, Kurokawa T, Hanada K, Hiyama Y, Tamura M, Ogata E, Matsumoto T. 1994. Stimulation of fracture repair by recombinant human basic fibroblast growth factor in normal and streptozotocin-diabetic rats. *Endocrinology* 135: 774-81
125. Radomsky ML, Thompson AY, Spiro RC, Poser JW. 1998. Potential role of fibroblast growth factor in enhancement of fracture healing. *Clin Orthop Relat Res*: S283-93
126. Chikazu D, Katagiri M, Ogasawara T, Ogata N, Shimoaka T, Takato T, Nakamura K, Kawaguchi H. 2001. Regulation of osteoclast differentiation by fibroblast growth factor 2: stimulation of receptor activator of nuclear factor kappaB ligand/osteoclast differentiation factor expression in osteoblasts and

- inhibition of macrophage colony-stimulating factor function in osteoclast precursors. *J Bone Miner Res* 16: 2074-81
127. Presta M, Dell'Era P, Mitola S, Moroni E, Ronca R, Rusnati M. 2005. Fibroblast growth factor/fibroblast growth factor receptor system in angiogenesis. *Cytokine Growth Factor Rev* 16: 159-78
  128. Nillesen ST, Geutjes PJ, Wismans R, Schalkwijk J, Daamen WF, van Kuppevelt TH. 2007. Increased angiogenesis and blood vessel maturation in acellular collagen-heparin scaffolds containing both FGF2 and VEGF. *Biomaterials* 28: 1123-31
  129. Nakagawa N, Kinosaki M, Yamaguchi K, Shima N, Yasuda H, Yano K, Morinaga T, Higashio K. 1998. RANK is the essential signaling receptor for osteoclast differentiation factor in osteoclastogenesis. *Biochem Biophys Res Commun* 253: 395-400
  130. Li J, Sarosi I, Yan XQ, Morony S, Capparelli C, Tan HL, McCabe S, Elliott R, Scully S, Van G, Kaufman S, Juan SC, Sun Y, Tarpley J, Martin L, Christensen K, McCabe J, Kostenuik P, Hsu H, Fletcher F, Dunstan CR, Lacey DL, Boyle WJ. 2000. RANK is the intrinsic hematopoietic cell surface receptor that controls osteoclastogenesis and regulation of bone mass and calcium metabolism. *Proc Natl Acad Sci U S A* 97: 1566-71
  131. Li X, Ionescu AM, Schwarz EM, Zhang X, Drissi H, Puzas JE, Rosier RN, Zuscik MJ, O'Keefe RJ. 2003. Smad6 is induced by BMP-2 and modulates chondrocyte differentiation. *J Orthop Res* 21: 908-13
  132. Lacey DL, Timms E, Tan HL, Kelley MJ, Dunstan CR, Burgess T, Elliott R, Colombero A, Elliott G, Scully S, Hsu H, Sullivan J, Hawkins N, Davy E, Capparelli C, Eli A, Qian YX, Kaufman S, Sarosi I, Shalhoub V, Senaldi G, Guo J, Delaney J, Boyle WJ. 1998. Osteoprotegerin ligand is a cytokine that regulates osteoclast differentiation and activation. *Cell* 93: 165-76
  133. Ulrich-Vinther M, Carmody EE, Goater JJ, K Sb, O'Keefe RJ, Schwarz EM. 2002. Recombinant adeno-associated virus-mediated osteoprotegerin gene therapy inhibits wear debris-induced osteolysis. *J Bone Joint Surg Am* 84-A: 1405-12
  134. Goater J, Muller R, Kollias G, Firestein GS, Sanz I, O'Keefe RJ, Schwarz EM. 2000. Empirical advantages of adeno associated viral vectors in vivo gene therapy for arthritis. *J Rheumatol* 27: 983-9
  135. Deckers M, van der Pluijm G, Dooijewaard S, Kroon M, van Hinsbergh V, Papapoulos S, Lowik C. 2001. Effect of angiogenic and antiangiogenic compounds on the outgrowth of capillary structures from fetal mouse bone explants. *Lab Invest* 81: 5-15
  136. Cucchiaroni M, Madry H, Ma C, Thurn T, Zurakowski D, Menger MD, Kohn D, Trippel SB, Terwilliger EF. 2005. Improved tissue repair in articular cartilage defects in vivo by rAAV-mediated overexpression of human fibroblast growth factor 2. *Mol Ther* 12: 229-38
  137. Zhang X, Schwarz EM, Young DA, Puzas JE, Rosier RN, O'Keefe RJ. 2002. Cyclooxygenase-2 regulates mesenchymal cell differentiation into the osteoblast lineage and is critically involved in bone repair. *J Clin Invest* 109: 1405-15
  138. Gulberg RE, Ballock RT, Boyan BD, Duvall CL, Lin AS, Nagaraja S, Oest M, Phillips J, Porter BD, Robertson G, Taylor WR. 2003. Analyzing bone, blood vessels, and biomaterials with microcomputed tomography. *IEEE Eng Med Biol Mag* 22: 77-83

139. Erben RG. 1997. Embedding of bone samples in methylmethacrylate: an improved method suitable for bone histomorphometry, histochemistry, and immunohistochemistry. *J Histochem Cytochem* 45: 307-13
140. Childs LM, Goater JJ, O'Keefe RJ, Schwarz EM. 2001. Effect of anti-tumor necrosis factor-alpha gene therapy on wear debris-induced osteolysis. *J Bone Joint Surg Am* 83-A: 1789-97
141. Childs LM, Paschalis EP, Xing L, Dougall WC, Anderson D, Boskey AL, Puzas JE, Rosier RN, O'Keefe RJ, Boyce BF, Schwarz EM. 2002. In vivo RANK signaling blockade using the receptor activator of NF-kappaB:Fc effectively prevents and ameliorates wear debris-induced osteolysis via osteoclast depletion without inhibiting osteogenesis. *J Bone Miner Res* 17: 192-9
142. Yazici C, Yanoso L, Xie C, Reynolds DG, Samulski RJ, Samulski J, Yannariello-Brown J, Gertzman AA, Zhang X, Awad HA, Schwarz EM. 2008. The effect of surface demineralization of cortical bone allograft on the properties of recombinant adeno-associated virus coatings. *Biomaterials* 29: 3882-7
143. Basile P, Dadali T, Jacobson J, Hasslund S, Ulrich-Vinther M, Soballe K, Nishio Y, Drissi MH, Langstein HN, Mitten DJ, O'Keefe RJ, Schwarz EM, Awad HA. 2008. Freeze-dried tendon allografts as tissue-engineering scaffolds for Gdf5 gene delivery. *Mol Ther* 16: 466-73
144. Deckers MM, van Bezooijen RL, van der Horst G, Hoogendam J, van Der Bent C, Papapoulos SE, Lowik CW. 2002. Bone morphogenetic proteins stimulate angiogenesis through osteoblast-derived vascular endothelial growth factor A. *Endocrinology* 143: 1545-53
145. Yazici C, Takahata M, Reynolds DG, Xie C, Samulski RJ, Samulski J, Beecham EJ, Gertzman AA, Spilker M, Zhang X, O'Keefe RJ, Awad HA, Schwarz EM. 2011. Self-complementary AAV2.5-BMP2-coated Femoral Allografts Mediated Superior Bone Healing Versus Live Autografts in Mice With Equivalent Biomechanics to Unfractured Femur. *Mol Ther*
146. Nakamura Y, Tensho K, Nakaya H, Nawata M, Okabe T, Wakitani S. 2005. Low dose fibroblast growth factor-2 (FGF-2) enhances bone morphogenetic protein-2 (BMP-2)-induced ectopic bone formation in mice. *Bone* 36: 399-407
147. Reynolds DG, Hock C, Shaikh S, Jacobson J, Zhang X, Rubery PT, Beck CA, O'Keefe R J, Lerner AL, Schwarz EM, Awad HA. 2007. Micro-computed tomography prediction of biomechanical strength in murine structural bone grafts. *J Biomech* 40: 3178-86
148. Nasu T, Ito H, Tsutsumi R, Kitaori T, Takemoto M, Schwarz EM, Nakamura T. 2009. Biological activation of bone-related biomaterials by recombinant adeno-associated virus vector. *J Orthop Res*

## **APPENDIX**

### **PAPER I**

#### **Remodeling of cortical bone allografts mediated by adherent rAAV-RANKL and VEGF gene therapy**

**Ito H. et al. Nat Med. 2005 Mar;11(3):291-7.**

## Remodeling of cortical bone allografts mediated by adherent rAAV-RANKL and VEGF gene therapy

Hiromu Ito<sup>1,2</sup>, Mette Koefoed<sup>1,3</sup>, Prarop Tiyyapanaputi<sup>1</sup>, Kirill Gromov<sup>1,3</sup>, J Jeffrey Goater<sup>1</sup>, Jonathan Carmouche<sup>1</sup>, Xinping Zhang<sup>1</sup>, Paul T Rubery<sup>1</sup>, Joseph Rabinowitz<sup>4</sup>, R Jude Samulski<sup>4,5</sup>, Takashi Nakamura<sup>2</sup>, Kjeld Soballe<sup>3</sup>, Regis J O'Keefe<sup>1</sup>, Brendan F Boyce<sup>1</sup> & Edward M Schwarz<sup>1,6</sup>

**Structural allograft healing is limited because of a lack of vascularization and remodeling. To study this we developed a mouse model that recapitulates the clinical aspects of live autograft and processed allograft healing. Gene expression analyses showed that there is a substantial decrease in the genes encoding RANKL and VEGF during allograft healing. Loss-of-function studies showed that both factors are required for autograft healing. To determine whether addition of these signals could stimulate allograft vascularization and remodeling, we developed a new approach in which rAAV can be freeze-dried onto the cortical surface without losing infectivity. We show that combination rAAV-RANKL- and rAAV-VEGF-coated allografts show marked remodeling and vascularization, which leads to a new bone collar around the graft. In conclusion, we find that RANKL and VEGF are necessary and sufficient for efficient autograft remodeling and can be transferred using rAAV to revitalize structural allografts.**

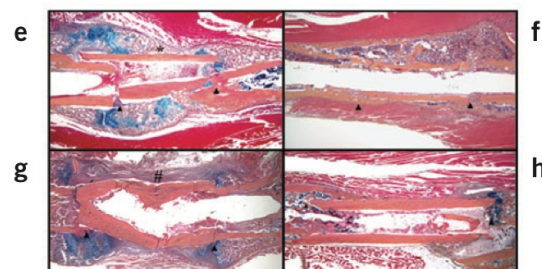
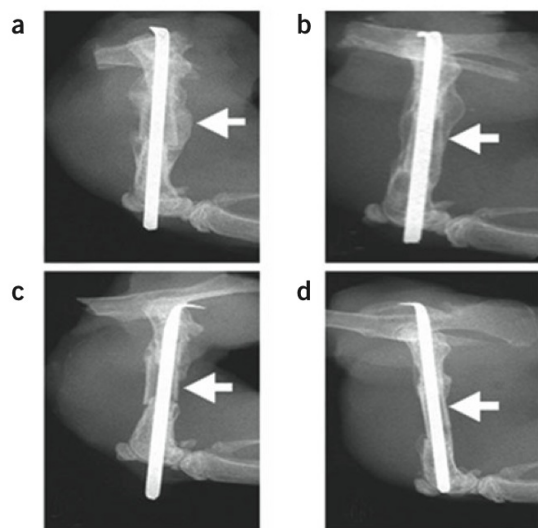
In contrast to soft tissue organ transplantation (*i.e.*, heart, liver, kidney), which must be live from a histocompatible donor, structural musculoskeletal grafts (*i.e.*, bone, ligament) are often derived from allogenic cadavers. Although this convenience makes structural allografts readily available, the utility of these transplants is limited by their lack of viability. This is most evident from experimental and clinical studies showing that fresh vascularized autogenous grafts are vastly superior to allograft in terms of healing and remodeling<sup>1,2</sup>. Structural bone grafts used to heal critical defects and bone fusions undergo a repair and remodeling process that closely resembles fracture healing<sup>3</sup>. In live autograft healing, cells from both the graft and the host contribute to mediate bony union<sup>4,5</sup>. In contrast, healing of a diaphyseal defect that has been allografted can only be accomplished by invasion of the graft by host tissue to obtain a cortex-to-cortex union<sup>6</sup>. Following union, autografts continue to remodel as a result of osteoclastic resorption of necrotic or disused cortical bone that is followed by osteoblastic formation of new woven bone, which is later remodeled into stronger lamellar bone. In this way, autografts are sustained through normal bone homeostasis. In contrast, once creeping callus from the host calcifies on the cortex of an allograft, healing ceases, leaving a large segment of necrotic bone that is unable to respond to normal mechanical loading. Thus, structural allografts have a limited life span because microfractures that occur in them over time cannot be remodeled and repaired, and negative outcomes include a 25–35% failure rate from infection, nonunion and fracture<sup>7,8</sup>.

Two central issues that must be addressed to improve structural allografting are elucidation of the factors that facilitate autograft healing and are absent in allografts and a method to introduce these factors onto allografts. Toward resolving these issues, we have developed a mouse femoral model that faithfully recapitulates the central features of clinical structural bone grafting. Gene expression profiling studies showed that allografts are deficient in several factors known to regulate vascular ingrowth of skeletal elements, osteogenesis, bone resorption and remodeling. The two most notable factors were vascular endothelial growth factor (VEGF) and receptor activator of nuclear factor  $\kappa$ B ligand (RANKL), which are known to dominantly regulate angiogenesis<sup>9</sup> and osteoclastic bone resorption<sup>10</sup>, respectively, during skeletal repair. Specifically, VEGF is expressed by the perichondrium and hypertrophic chondrocytes and recruits endothelial cells to promote blood flow to the avascular tissue<sup>11</sup>. In addition to essential nutrients, this blood supply brings in osteoclast precursors that differentiate in response to RANKL expressed by stromal cells<sup>12</sup>. Based on this information we used *in vivo* blockade and *ex vivo* gene transfer to show that RANKL and VEGF are necessary for complete autograft healing. These findings support the hypothesis that RANKL and VEGF are crucial factors for establishing remodeling of the cortical surface of the autografts and that introduction of these factors onto allografts could result in bone resorption, neovascularization and revitalization of the dead bone. Using a new approach to immobilize recombinant adeno-associated

<sup>1</sup>The Center for Musculoskeletal Research, University of Rochester, 601 Elmwood Avenue, Box 665, Rochester, New York 14642, USA. <sup>2</sup>Department of Orthopaedic Surgery, Graduate School of Medicine, Kyoto University, 54 Kawahara-cho, Shogoin, Sakyo, Kyoto 606-8507, Japan. <sup>3</sup>The Department of Orthopedics, University Hospital of Aarhus, Aarhus Kommunehospital, DK-8000 Aarhus C, Denmark. <sup>4</sup>Gene Therapy Center and <sup>5</sup>Department of Pharmacology, University of North Carolina, 7119 Thurston Building, CB# 7352 Chapel Hill, North Carolina 27599, USA. Correspondence should be addressed to E.M.S. (edward\_schwarz@urmc.rochester.edu).

Published online 13 February 2005; doi:10/nm1190

## ARTICLES

© 2005 Nature Publishing Group <http://www.nature.com/naturemedicine>

**Figure 1** The mouse femoral allograft model. Mice received a femoral autograft or allograft, and were killed at 3 weeks (a,c), 4 weeks (b,d,f,h) or 2 weeks (e,g). Representative radiographs from an autografted (a,b) and an allografted (c,d) mouse are illustrated at 3 and 4 weeks after fracture. The arrows indicate the presence of callus on the cortical surface of the autograft at 3 weeks (a), which is remodeled by 4 weeks (b), and is completely absent in the allograft (c,d). Hematoxylin, eosin, orange G and acian blue-stained sections show the endochondral bone formation at the graft-host junctions (arrow heads) of both auto and allografts at 2 weeks (e,g), which is remodeled to form a bony union at 4 weeks (f,h). Of note is the periosteal intramembranous bone formation (\*), which only occurs in autografts (e), producing a new cortical bone collar with bone marrow at four weeks (f). In contrast, allografts are encased by fibrous tissue (#), heal through creeping callus (g), and are dependent on dead cortical bone for structural integrity after remodeling (h).

virus (rAAV) onto the cortical surface of the allografts we show that RANKL and VEGF signals are sufficient to revitalize processed cortical bone and could be a method to sustain clinical allografts long term.

## RESULTS

## Mouse femoral autograft and allograft healing

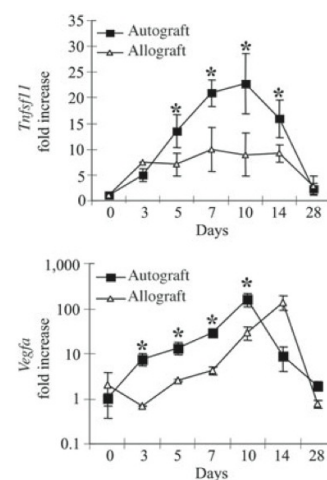
To elucidate the cellular and molecular mechanisms that govern structural bone graft healing, we developed an *in vivo* mouse model in which an ~4-mm osteotomy of the middle of the femoral diaphysis is performed and placed back into the original host as an autograft or 'processed' with fixation in alcohol and freezing and then transplanted as an allograft into an allogenic host<sup>13</sup>. **Figure 1** shows the radiographic and histologic healing of the two grafts. Consistent with current knowledge, the autografts heal through endochondral bone formation at the junctions with concomitant intramembranous bone formation derived from the periosteum of the cortex of the graft. This bone formation results in a new bone collar of cortical bone that partly or completely encircles the graft by 4 weeks. During this time, a new marrow space is created between the new bone collar and the autograft, and accelerated osteoclastic resorption of the graft occurs. In contrast, allografts heal by endochondral bone formation only. At 2 weeks, cartilage derived from the host is observed creeping onto the ends of allografts. Notably, the osteocartilaginous tissue seems to be separated from the periosteum by a fibrous tissue reaction that partly or completely encases the allograft as part of a foreign body reaction to it. By 4 weeks, healing is completed as a new cortical union at the graft-host junctions with a large middle segment of necrotic bone that is completely devoid of osteoclast activity.

## Allografts are deficient in RANKL and VEGF

Over the last few years a wealth of information on the factors that regulate bone repair has been generated from microarray gene expression profiling studies on fracture callus tissue<sup>14</sup>. Based on this information, we performed a screen to identify dysregulated gene expression between

autografts and allografts by RT-PCR. The two factors that showed the most substantial differential gene expression were *Tnfsf11*, which encodes RANKL, and *Vegfa*, which encodes VEGF (**Fig. 2**). The expression of both factors peaked 10 d after autografting, when *Tnfsf11* and *Vegfa* levels were twofold and fivefold higher than those observed in allograft tissue, respectively. Whereas *Tnfsf11* expression was deficient throughout the time course, *Vegfa* expression seemed to be delayed and peaked on day 14 when endochondral ossification is largely completed in stabilized fractures<sup>15</sup>. To follow up these findings, we performed microarray studies using RNA isolated from day 10 autografts and allografts, and found, according to the manufacturer's criteria, that these transcripts were present in the autografts and absent in the allografts.

**Figure 2** Altered *Tnfsf11* and *Vegfa* gene expression during allograft healing. Total RNA was extracted from femoral autografts and allografts at the indicated time and processed for real time RT-PCR. The data are presented as the fold induction  $\pm$  s.d., compared to the day 0 control, after standardization with the internal  $\beta$ -actin control. \* $P < 0.05$  for autograft versus allograft at the same time point.



## ARTICLES

**RANKL and VEGF in autograft healing**

To assess the requirements of RANKL and VEGF signaling during autograft healing, we performed *in vivo* blockade experiments using systemic and local approaches. First, the autografted mice received control IgG, a soluble RANK decoy receptor (RANK:Fc) or neutralizing antibodies specific for VEGF (Fig. 3a–d). We also assessed the effects of blocking RANKL and VEGF locally by transducing the autografts *ex vivo* before implantation with AAV- $\beta$ -gal, AAV-osteoprotegerin (OPG), AAV-sFlt1 (soluble Flt1, the receptor for VEGF) or a combination of AAV-OPG and AAV-sFlt1 (Fig. 3e–g). Radiographic and histologic analyses of the autograft healing showed that disruption of either RANKL or VEGF signaling, systemically or locally, significantly ( $P < 0.05$ ) inhibited new bone formation on the cortical surface of the grafts. Notably, dual blockade did not induce additional inhibitory effects, indicating that these factors act in series to recruit and differentiate osteoclast progenitors to the cortical surface.

**Transduction efficiency of freeze-dried rAAV**

With the hypothesis that addition of crucial signals to the cortical surface of allografts will lead to autograft-like healing, we attempted to develop an approach to efficiently transfer these signals. Previously, a gene-activated matrix was developed for this purpose, in which naked plasmid DNA is immobilized onto osteoinductive materials<sup>16</sup>. Unfortunately, others and we have been unable to achieve effective transduction efficiencies in our models using gene-activated matrices. Based on the empirical advantages of rAAV vectors for orthopedic gene therapy<sup>17</sup>, and the clinical potential of this vector<sup>18</sup>, we evaluated the effects of freeze-drying and storage at  $-80^{\circ}\text{C}$  on rAAV transduction efficiency. Resuspension of rAAV in a sorbitol solution facilitates its application to various organic and inorganic implant materials (Fig. 4a,b). Application of the freeze-dried rAAV- $\beta$ -gal to a monolayer of 293 human embryonic kidney cells leads to efficient transduction as indicated by X-gal staining of the culture plates, which showed a mosaic distribution of blue cells throughout the plates (Fig. 4c,d). No staining was detected in control cultures without virus (Fig. 4e). This result suggests that the rAAV rehydrates and freely diffuses in the culture medium before infecting the cells. To assess the effects of freeze-drying and storage on the immobilized rAAV,  $5 \times 10^7$  transducing units of rAAV- $\beta$ -gal were directly placed on a monolayer of 293 cells, as a positive control; or freeze-dried onto pins and stored at  $-80^{\circ}\text{C}$  for various times before addition to the monolayer (Fig. 4f). Notably, we were able to recover  $\sim 100\%$  of the  $\beta$ -galactosidase activity in all of the samples. Thus, this coating process does not affect the infection capacity of the virus.

To assess the transduction efficiency of freeze-dried rAAV- $\beta$ -gal *in vivo*, we performed a dose-response experiment in which we coated femoral allografts with various doses of virus and transplanted them into mice. X-gal staining of histological sections showed that fibroblasts in the inflammatory tissue between the bone and muscle were readily transduced (Fig. 4g,h). The number of blue cells per section peaked at a dose of  $5 \times 10^7$  particles/allograft. Thus, we used this as our effective dose in our gain-of-function studies.

**Revitalization of rAAV-RANKL and rAAV-VEGF coated allografts**

To evaluate the effect of exogenous RANKL and VEGF on processed cortical bone healing, allografts were coated with freeze-dried rAAV- $\beta$ -gal, rAAV-RANKL, rAAV-VEGF or a combination of rAAV-RANKL and rAAV-VEGF. First, we confirmed the *in vivo* target gene expression following transplantation by determining serum levels of RANKL and VEGF over time (Fig. 5a). By day 4 a substantial increase in VEGF was detected, which peaked at day 8 before returning to baseline levels at 3 weeks. Analysis of RANKL did not detect levels above the detection limit ( $\sim 30$  pg/ml) in any of our samples.

Next, we histologically analyzed the treatment effects on allograft healing. Although there were no obvious effects of the first three treatments based on the appearances of the allografts, we observed a marked amount of live new bone on the periosteal surfaces, and focally on the endosteal surfaces of the rAAV-VEGF + rAAV-RANKL-coated allografts that was never observed in uncoated allografts in this model (Fig. 5b–d). The presence of the new bone on the outer surfaces of these allografts outside irregular reversal lines suggested that it had been laid down at sites of previous resorption of the allograft periosteal bone (Fig. 5b), showing that regions of the allografts have been partially resorbed and replaced by new bone, whereas others were still being resorbed at the time of killing of the mice as a result of the combined therapy. They include: (i) resorption of up to 50% of the thickness the allograft cortical bone, predominantly from the periosteal surface, and replacement of the resorbed dead bone with viable new bone (Fig. 5c and Fig. 6e,f), which in some cases extended the entire length of the allograft; (ii) reversal lines that clearly delineate the depth of dead allograft resorption and the sites of new bone formation (Fig. 6e,f), and indicate the location of a new bony union between the live host bone and the allograft surfaces; (iii) continuing active resorption of the dead cortical bone (Fig. 6b,d,g) with new bone formation

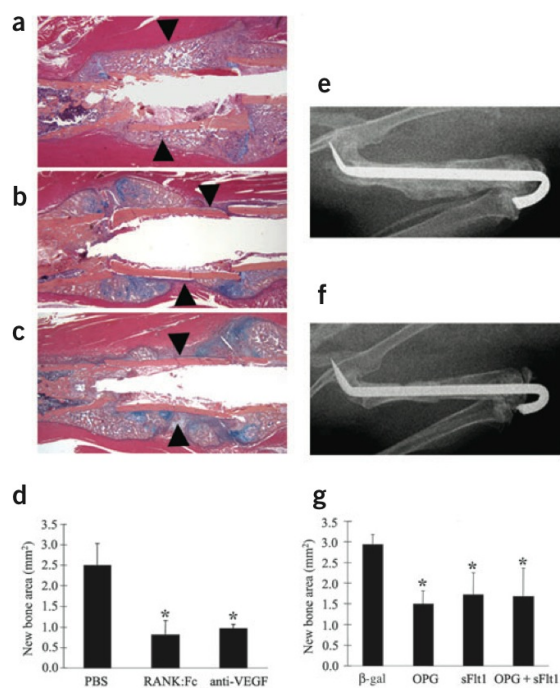


**Figure 3** Systemic and local loss of either RANKL or VEGF results in defective autograft healing. Mice received untreated autografts followed by injections of control IgG (a), RANK:Fc (b), or anti-VEGF (c) therapy, and were killed four weeks later. Representative hematoxylin and eosin-stained sections from these mice show a reduction in the amount of new bone formation around the autografts (arrow heads) and persistence of cartilage (blue in b,c). Representative radiographs from mice that received autografts transduced with rAAV- $\beta$ -gal (e) or a combination of rAAV-OPG and rAAV-sFlt1 (f), 2 weeks after fracture are shown. Histomorphometry of the area of new bone formation on the autografts (d,g). \* $P < 0.05$  compared to the IgG or rAAV- $\beta$ -gal controls.

## ARTICLES

(Fig. 6c,d,g) representative of tunneling remodeling, which does not occur physiologically in mouse cortical bone; (iv) neovascularization of the marrow cavity along the length of the allograft (Fig. 6e,f), in contrast to the necrotic marrow seen in samples from the other 3 groups (Fig. 6h); and (v) the complete absence of the fibrotic tissue reaction that typically surrounds allografts (Fig. 1g, Fig. 4g,h and Fig. 6h) as evidenced by the thin periosteal layer between the muscle and cortical bone (Fig. 6a,f).

Considering that none of these observations was made in any of the other groups of grafted mice we have studied ( $n > 300$ ), our findings provide evidence that the combination of exogenous RANKL and VEGF can induce vascularization and remodeling of processed structural allografts. This impression was supported by histomorphometry, which showed that the mean cortical thickness in the rAAV-VEGF + rAAV-RANKL-coated allografts was similar to that of the allografts that did not receive the RANKL-VEGF combination (Fig. 5b), suggesting

that this new bone must have followed the removal of up to ~100  $\mu\text{m}$  of cortical bone. Consistent with the idea that RANKL and VEGF function in series during cortical graft healing, we did not observe any substantial effects of transferring either one of these factors alone. Although the resorption and new bone formation was observed in all of the mice given rAAV-VEGF + rAAV-RANKL-coated allografts, the amount and extent of resorption and new bone formation were variable, as evidenced by the observation that parts of some of the grafts were being resorbed for the first time at the time of killing, 4 weeks after surgery.

## DISCUSSION

Although major progress has been made in many aspects of musculoskeletal repair procedures<sup>19,20</sup>, including the use of bone morphogenetic proteins as adjuvants for spinal fusion and fracture union<sup>21,22</sup>, processed structural allografts and nonremodeling bone substitutes remain the materials of choice for reconstructive orthopedic surgery. Although bone morphogenetic proteins represent a great advance for these indications, it has long been recognized that they are not useful for large critical defects because of their short half-life. As an alternative, many groups have been working on gene therapy approaches for skeletal healing<sup>23–27</sup>. Although gene therapy offers the potential of local, sustained gene expression, the development of a safe and effective delivery vector remains elusive<sup>28</sup>.

Over the last two decades, much work has been done to understand the critical differences between the efficacy of live autografts and processed allografts during bone healing<sup>5,29,30</sup>. Although these studies show that there is a host-acquired immune response to the allograft, it is clear that the most notable difference between the two grafts is the presence of live cells in the autograft, which directly contribute to angiogenesis and subsequent remodeling. We have addressed two central questions to advance our understanding of these differences: what prominent signals are present in autografts and absent in allografts that induce revascularization and remodeling and can introduction of these signals onto the cortical surface of structural allografts induce revascularization and remodeling? The first notable finding with the mouse femoral graft model was that bone morphogenetic protein expression is not substantially different between autografts and allografts. This result is somewhat contrary to the current thinking that introducing osteogenic signals to an osteoinductive and osteoconductive biomaterial is the best approach to improve bone healing. In contrast, our findings led us to explore an alternative hypothesis that stimulation of resorption of the graft through angiogenesis and osteoclast formation and activation leading to new bone formation on the cortical surface of allografts is a superior method to improve graft incorporation. In support of this hypothesis, we show that disruption of RANKL and VEGF signaling results in a decrease in new bone formation on the autograft cortical surface (Fig. 3).

To evaluate gain of RANKL and VEGF function in our model, we developed a technique in which rAAV can be immobilized to the cortical surface by freeze-drying (Fig. 4). There are many potential methods by which rAAV could be immobilized onto the allografts, including simple electrostatic interactions and more sophisticated bonding. Here we chose virus freeze-drying because of its ease and practicality. Although this method does not alter the infectivity of the virus and allows for effective transduction, the overall *in vivo* transduction efficiency is modest (1–5% of cells in immediate proximity to the allograft). It is likely that this low efficiency combined with transduction of cells that are rapidly turning over resulted in undetectable levels of RANKL and transient elevation of VEGF concentrations in the blood of the mice (Fig. 5a). The kinetics of the exogenous VEGF expression are also interesting from the standpoint that the rAAV-delivered VEGF compensates for the allograft VEGF deficiency at this crucial time point compared to autografts

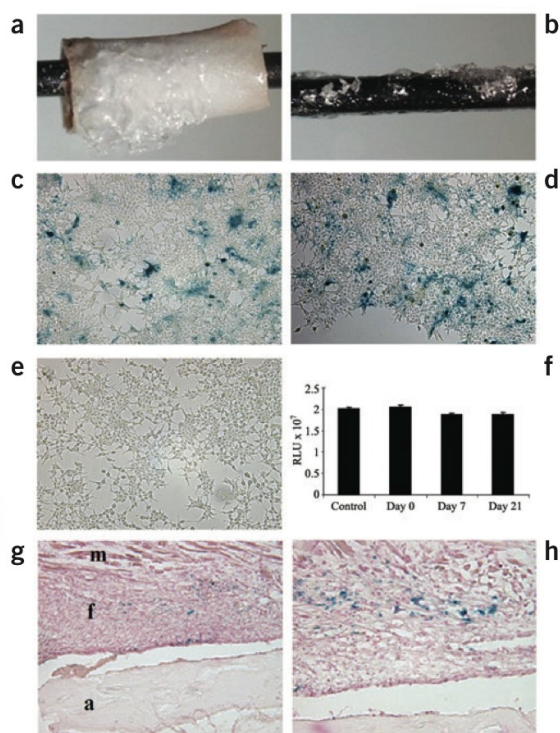


**Figure 4** Transduction efficiency of rAAV- $\beta$ -gal following freeze-drying onto allografts and implants *in vitro* and *in vivo*.  $5 \times 10^7$  transducing units of rAAV- $\beta$ -gal was lyophilized onto mouse femoral allografts (a) or stainless steel pins (b). The transduction efficiency was determined *in vitro* by incubating the coated pins on top of a monolayer of confluent 293 human embryonic kidney cells for 72 h. Photographs of the X-gal-stained cells distal (c) and proximal (d) to the coated pin, as well as an uncoated control pin (e) are shown. The transduction efficiency of the coated pins was also quantified after the indicated storage time at  $-80^\circ\text{C}$ . RLU, relative light units. (f). As a control,  $5 \times 10^7$  transducing units of rAAV- $\beta$ -gal in 50  $\mu\text{l}$  PBS was directly placed on a monolayer of 293 cells. The  $\beta$ -galactosidase activity in the cultures was determined using the Galacto-Light system. No significant differences were observed. The efficiency of *in vivo* transduction 14 d after transplantation is shown at  $\times 10$  (g) and  $\times 40$  (h) magnification, where the blue staining indicates transduction of the fibroblasts (f) between the allograft (a) and the muscle (m).

## ARTICLES

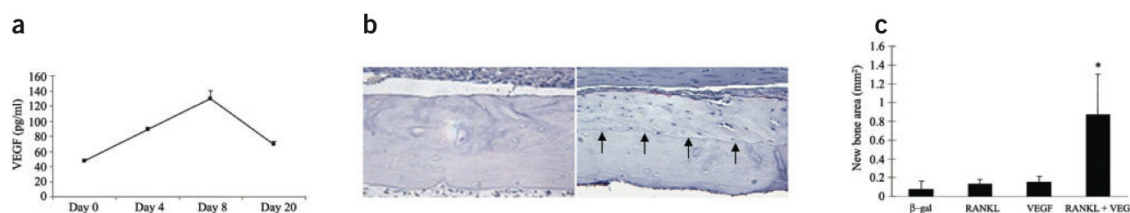


**Figure 5** Revitalization of processed allografts via rAAV mediated-RANKL and VEGF gene transfer. Allografts containing  $5 \times 10^7$  particles of rAAV- $\beta$ -gal, rAAV-RANKL, rAAV-VEGF or a combination of rAAV-RANKL and rAAV-VEGF were transplanted into mice and evaluated 28 d after surgery. *In vivo* VEGF expression was analyzed in sera taken from the combined coated allografts at the indicated time after surgery (a). VEGF levels in uncoated allografts were consistently  $>50$  pg/ml throughout the time course. Representative histology from the medial segment of the lateral cortex of a rAAV- $\beta$ -gal (b) and rAAV-RANKL + rAAV-VEGF (c) coated allograft on day 28. Of note is the considerable amount of new bone on the rAAV-RANKL + rAAV-VEGF-coated allograft highlighted by a reversal line (arrows) and its similarity in cortical thickness to the rAAV- $\beta$ -gal coated allograft. The new bone that formed on the allografts was quantified by histomorphometry (d) and the data are presented as the area of new bone formation on the graft  $\pm$  s.d. (\* $P < 0.05$  versus  $\beta$ -gal control).

(Fig. 2). Despite this modest transduction, the effects of combination gene transfer were evident and significant (Figs. 5 and 6;  $P < 0.05$ ). In so doing, we show that RANKL and VEGF are sufficient signals to markedly alter allograft healing to generate a live, vascularized, remodeling, bony union.

In retrospect, the identification of VEGF and RANKL as critical regulators of autograft healing in our microarray screen is not notable. In addition to its role in angiogenesis, a VEGF gradient produced by hypertrophic chondrocytes is needed for directional growth and invasion of cartilage by blood vessels in endochondral ossification during development<sup>11</sup> and in fracture healing<sup>9</sup>. Because remodeling of bone requires osteoclastic resorption, and RANKL is the final effector molecule that differentiates mononuclear precursors into osteoclasts<sup>12</sup>, a crucial role of RANKL is obvious. Furthermore, it is believed that the induction of RANKL in stromal cells in response to hypocalcemia or microfracture is the most proximal event that triggers *de novo* bone remodeling<sup>12</sup>. Our microarray screen also identified many other putative players that could similarly affect allograft healing including transcription factors, signaling molecules, receptors and other cytokines, but further studies will be required to determine if they can increase the efficacy of our current approach.

Here we show a new method of freeze-drying rAAV onto a surgically implantable surface, which is a safe and effective approach that could potentially be used in other conditions in which local delivery of gene products may be indicated. The resorption and subsequent formation of new bone did not occur uniformly on the allograft surfaces with parts of some allografts only being resorbed for the first time at killing, 4 weeks after surgery. This variable response probably reflects variation in the levels and temporal expression of the target genes, and in local tissue damage and subsequent infection of cells around the grafts. To show the clinical utility of our coated allografts we have committed to the development of a large animal model of structural allografting in which functional *in vivo* radiology can formally prove complete vascular invasion. Biomechanical testing in this model will also be necessary to show the advantage of remodeling versus nonremodeling allografts.

## METHODS

**Mouse segmental femoral graft model.** All animal studies were conducted in accordance with principles and procedures approved by the University of Rochester Committee for Animal Resources. We used 8-week-old C57BL/6 mice for femoral grafting as we have previously described<sup>13</sup>. We cleaned allografts from ICR mice with 70% ethanol, rinsed them three times in saline to remove residual ethanol, and then froze them at  $-80$  °C for at least 24 h before use. This procedure is based on the methods used by the Musculoskeletal Transplant Foundation to prepare clinical allografts. Graft healing was followed radiographically using a Faxitron X-ray system as described previously<sup>15</sup>.

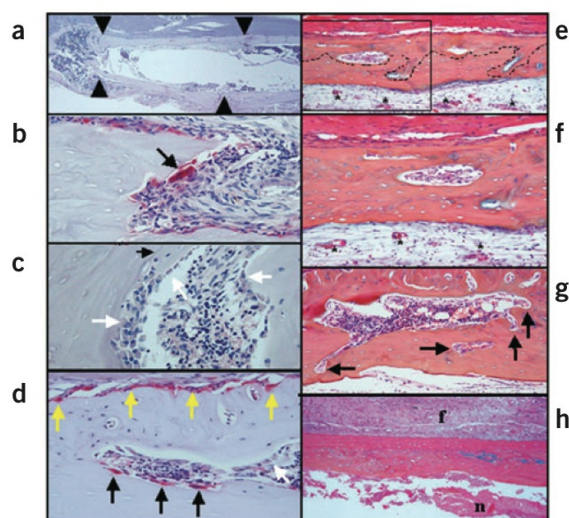


**Figure 6** rAAV-mediated gene transfer of RANKL and VEGF induces cortical bone resorption, vascularization and remodeling in processed allografts *in vivo*. Representative TRAP-stained histologic sections from mice in the combination group (a–d). An example of a rAAV-VEGF + rAAV-RANKL-coated allograft in which remodeled bone extends the entire length of the graft (arrow heads) is shown (a). The novel histologic features of the combination group were characterized by osteoclastic resorption of the necrotic bone (black arrows in b,d,g), osteoblastic new bone formation in the resorption lacunae (white arrows in c,d) and osteoclastic remodeling of the new woven bone (yellow arrows in d). Hematoxylin and eosin-stained sections of allografts from the combination group revealed asymmetric reversal lines (dashed line in e and shown at higher magnification without the lines in g, and black arrow in c) between dead bone and newly formed live bone, new blood vessel formation inside the marrow cavities (\* in e,f), and active tunneling resorption (arrows in f) in the necrotic bone. In contrast, none of the other groups showed these features and were all characterized by a fibrotic tissue (f) that covered the periosteal surface and necrotic tissue (n) that filled the marrow cavity (h).

## ARTICLES

**In vivo treatments.** For loss-of-function studies with biologics, we administered antibodies against VEGF (R&D Systems, Inc.), RANK:Fc fusion protein (a gift from Immunex, Inc.), or goat IgG (Sigma) in phosphate-buffered saline (PBS) by intraperitoneal injection every 3 d until mice were killed, as described previously<sup>31</sup>. *Ex vivo* gene transfer to live autografts were performed by harvesting the specimen, incubating it in 20  $\mu$ l of sterile PBS containing  $5 \times 10^7$  transducing units of rAAV for 10 min at room temperature and rapidly placing it back in the original donor. We performed *in vivo* gene transfers to processed allografts by pipetting  $5 \times 10^7$  particles of rAAV in 50  $\mu$ l of a 1% sorbitol-PBS solution onto the cortical surface of the grafts. The allografts were then frozen at  $-80^\circ\text{C}$ , lyophilized and stored at  $-80^\circ\text{C}$  until they were transplanted. We used at least six mice in each treatment group.

**Histological and histomorphometric analysis.** Following killing of mice, the grafted femurs were processed and stained with hematoxylin, eosin, Orange G and alcian blue (H&E), or for tartrate-resistant acid phosphatase (TRAP) activity and counterstained with hematoxylin as we have described previously<sup>31,32</sup>. We performed X-gal (Sigma) staining on sections counterstained with eosin as we have described previously<sup>32</sup>. Histomorphometric analysis was carried out using Osteometrics software as we have described previously<sup>13</sup>.

**Real-time quantitative RT-PCR assays and microarrays.** We harvested autografts and allografts from killed mice, immediately froze them in liquid nitrogen, minced them using a 6750 Freezer/Mill (SPEX CertiPrep, Inc.), and extracted total RNA using TRIzol (Invitrogen Corp.). We made single-stranded cDNA using a reverse transcription kit (Invitrogen) and used it as template for real-time PCR with SYBR Green PCR Master Mix (Applied Biosystems) and gene-specific primers in a Rotor-Gene 2000 (Corbett Research) as previously described<sup>15</sup>. The mean cycle threshold (Ct) values from quadruplicate measurements were used to calculate the gene expression, with normalization to  $\beta$ -actin as an internal control. The primer sequences for *Tnfsf11* are: forward, 5'-TCTCATAACCTGATGAAAGG-3'; reverse 5'-GCATCTTGATCCGGATCCAG-3'. The primer sequences for *Vegfa* are: forward, 5'-GATGTGAATGCAGACCAAAG-3'; reverse, 5'-CACATCTGCAAGTACGTTCG-3'. The Functional Genomics Core Facility performed the microarray experiments, under the direction of A. Brooks. The experiments were performed by pooling the RNA extracted from six independent samples per group (autografts or allografts) in duplicate. Total RNA from day 10 samples were biotinylated and amplified using the T7 linear amplification approach previously described<sup>33</sup>. Affymetrix m430\_2.0 arrays, which represent approximately 45,000 mouse probe sets, were run following the manufacturer's protocol. Signal values were calculated using a probe level analysis normalization tool (Robust Multichip Analysis, RMA) before making pair-wise comparisons between allograft and autograft samples.

**Preparation of rAAV vectors.** The rAAV- $\beta$ -gal<sup>34</sup> and rAAV-OPG<sup>35</sup> vectors have been described previously. Plasmids containing cDNA for *Vegfa*<sup>36</sup>, *Tnfsf11* (ref. 37) and *Fli1* (ref. 38) were used for subcloning into the pAAV-BGHA transfer vector using oligonucleotide primers containing restriction sites for *NotI* and *EcoRI* at the 5' and 3' end, respectively. After ligation and transformation, positive clones grown in *E. coli* were confirmed by restriction digests and DNA sequencing. The resulting plasmids were used to produce the rAAVs through a helper-virus-free method, which were titered by dot blot<sup>39</sup>. The function of each rAAV vector was verified by assessing protein production in vitro by enzyme-linked immunosorbent assay (ELISA; R&S systems) as described<sup>35</sup>. The functional activities of the rAAV-RANKL and rAAV-VEGF vectors were also confirmed by *in vitro* osteoclastogenesis<sup>35</sup> and angiogenesis<sup>40</sup> assays, respectively. *In vivo* expression of VEGF and RANKL was assessed by serum ELISA as we have described previously<sup>35</sup>. The transduction efficiency of rAAV- $\beta$ -gal was determined in vitro by X-gal staining and by assaying for  $\beta$ -galactosidase activity using the Galacto-Light system (Tropix Inc.) as described previously<sup>34</sup>.

**Statistical analysis.** An observer blinded to the treatment performed the histomorphometry. Data were calculated as the mean  $\pm$  s.d., and the groups were compared using two-tailed analysis of variance (ANOVA). Statistical significance was set at  $P < 0.05$ .

**Accession numbers.** The GEO accession numbers for the primary data files are GSM37204 and GSM37205.

## ACKNOWLEDGMENTS

We thank: H. Burchardt (Musculoskeletal Transplant Foundation) for advice with this research. J. Huard (University of Pittsburgh) for providing us with the sFlt-1 cDNA, W. Min (Yale University) for providing us with the *Vegfa* cDNA, Amgen Inc. for providing us with the OPG and *Tnfsf11* cDNA and the RANK:Fc. We also thank C. Hock and D. Reynolds for assistance with the serum ELISA studies, B. Fan, L. Gehan and B. Stroyer for assistance with the histology, H. Awad for assistance with manuscript preparation, and R. Guldborg and A. Lin for  $\mu$ CT analyses. This work was supported by research grants from the Orthopedic Research and Education Foundation, the Musculoskeletal Transplant Foundation, US National Institutes of Health grants AR51469, AR48149, AR48681, AR43510, ES011854 and HL066973, and unrestricted research grants from DePuy, J&J Inc.

## COMPETING INTERESTS STATEMENT

The authors declare competing financial interests (see the *Nature Medicine* website for details).

Received 12 April; accepted 14 December 2004

Published online at <http://www.nature.com/naturemedicine/>

- Garbus, D.S., Masri, B.A. & Czitrom, A.A. Biology of allografting. *Orthop. Clin. North. Am.* **29**, 199–204 (1998).
- Goldberg, V.M. & Stevenson, S. The biology of bone grafts. *Semin. Arthroplasty* **4**, 58–63 (1993).
- Einhorn, T.A. The cell and molecular biology of fracture healing. *Clin. Orthop.* **S7–S21** (1998).
- Burchardt, H. Biology of bone transplantation. *Orthop. Clin. North. Am.* **18**, 187–196 (1987).
- Gould, S.E., Rhee, J.M., Tay, B.-B., Otsuka, N.Y. & Bradford, D.S. Cellular contribution of bone graft to fusion. *J. Orthop. Res.* **18**, 920–927 (2000).
- Enneking, W.F. & Campanacci, D.A. Retrieved human allografts: a clinicopathological study. *J. Bone Joint Surg. Am.* **83-A**, 971–986 (2001).
- Lord, C.F., Gebhardt, M.C., Tomford, W.W. & Mankin, H.J. Infection in bone allografts. Incidence, nature, and treatment. *J. Bone Joint Surg. Am.* **70**, 369–376 (1988).
- Berrey, B.H., Jr., Lord, C.F., Gebhardt, M.C. & Mankin, H.J. Fractures of allografts. Frequency, treatment, and end-results. *J. Bone Joint Surg. Am.* **72**, 825–833 (1990).
- Colnot, C., Thompson, Z., Miclau, T., Werb, Z. & Helms, J.A. Altered fracture repair in the absence of MMP9. *Development* **130**, 4123–4133 (2003).
- Kon, T. *et al.* Expression of osteoprotegerin, receptor activator of NF- $\kappa$ B ligand (osteoprotegerin ligand) and related proinflammatory cytokines during fracture healing. *J. Bone Miner. Res.* **16**, 1004–1014. (2001).
- Ferrara, N., Gerber, H.P. & Lecouter, J. The biology of VEGF and its receptors. *Nat. Med.* **9**, 669–676 (2003).
- Boyle, W.J., Simonet, W.S. & Lacey, D.L. Osteoclast differentiation and activation. *Nature* **423**, 337–342. (2003).
- Tyapatanaputi, P. *et al.* A novel murine segmental femoral graft model. *J. Orthop Res* **22**, 1254–1260 (2004).
- Hadjjiargyrou, M. *et al.* Transcriptional profiling of bone regeneration. Insight into the molecular complexity of wound repair. *J. Biol. Chem.* **277**, 30177–30182 (2002).
- Zhang, X. *et al.* Cyclooxygenase-2 regulates mesenchymal cell differentiation into the osteoblast lineage and is critically involved in bone repair. *J. Clin. Invest.* **109**, 1405–1415 (2002).
- Bonadio, J., Smiley, E., Patil, P. & Goldstein, S. Localized, direct plasmid gene delivery *in vivo*: prolonged therapy results in reproducible tissue regeneration. *Nat. Med.* **5**, 753–759 (1999).
- Schwarz, E.M. The adeno-associated virus vector for orthopaedic gene therapy. *Clin. Ortho. & Rel. Res.* **379S**, S31–S39 (2000).
- Rabinowitz, J.E. & Samulski, R.J. Building a better vector: the manipulation of AAV virions. *Virology* **278**, 301–308 (2000).
- Wu, D., Razzano, P. & Grande, D.A. Gene therapy and tissue engineering in repair of the musculoskeletal system. *J. Cell. Biochem.* **88**, 467–481 (2003).
- Gamradt, S.C. & Lieberman, J.R. Genetic modification of stem cells to enhance bone repair. *Ann. Biomed. Eng.* **32**, 136–147 (2004).
- Boden, S.D., Kang, J., Sandhu, H. & Heller, J.G. Use of recombinant human bone morphogenetic protein-2 to achieve posterolateral lumbar spine fusion in humans: a prospective, randomized clinical pilot trial: 2002 Volvo Award in clinical studies. *Spine* **27**, 2662–2273 (2002).
- Friedlaender, G.E. OP-1 clinical studies. *J. Bone Joint Surg. Am.* **83-A** Suppl 1, S160–S161 (2001).
- Lieberman, J.R., Ghivizzani, S.C. & Evans, C.H. Gene transfer approaches to the healing of bone and cartilage. *Mol. Ther.* **6**, 141–147 (2002).
- Baltzer, A.W. & Lieberman, J.R. Regional gene therapy to enhance bone repair. *Gene Ther.* **11**, 344–350 (2004).
- Sandhu, H.S., Boden, S.D., An, H., Kang, J. & Weinstein, J. BMPs and gene therapy for spinal fusion: summary statement. *Spine* **28**, S85 (2003).
- Musgrave, D.S. *et al.* *Ex vivo* gene therapy to produce bone using different cell types. *Clin. Orthop.* **378**, 290–305 (2000).
- Hidaka, C. *et al.* Acceleration of cartilage repair by genetically modified chondrocytes over expressing bone morphogenetic protein-7. *J. Orthop. Res.* **21**, 573–583 (2003).
- Verma, I.M. & Somia, N. Gene therapy -- promises, problems and prospects. *Nature* **389**, 239–242 (1997).

## ARTICLES

29. Bos, G.D., Goldberg, V.M., Powell, A.E., Heiple, K.G. & Zika, J.M. The effect of histocompatibility matching on canine frozen bone allografts. *J. Bone Joint Surg. Am.* **65**, 89–96 (1983).
30. Stevenson, S., Li, X.Q., Davy, D.T., Klein, L. & Goldberg, V.M. Critical biological determinants of incorporation of non-vascularized cortical bone grafts. Quantification of a complex process and structure. *J. Bone Joint Surg. Am.* **79**, 1–16 (1997).
31. Childs, L.M. *et al.* *In vivo* RANK signaling blockade using the receptor activator of NF- $\kappa$ B:Fc effectively prevents and ameliorates wear debris-induced osteolysis via osteoclast depletion without inhibiting osteogenesis. *J. Bone Miner Res.* **17**, 192–199 (2002).
32. Childs, L.M., Goater, J.J., O'Keefe, R.J. & Schwarz, E.M. Effect of anti-tumor necrosis factor- $\alpha$  gene therapy on wear debris-induced osteolysis. *J. Bone Joint Surg. Am.* **83-A**, 1789–1797. (2001).
33. Musatov, S. *et al.* Inhibition of neuronal phenotype by PTEN in PC12 cells. *Proc. Natl. Acad. Sci. USA* **101**, 3627–3631 (2004).
34. Goater, J. *et al.* Empirical advantages of adeno associated viral vectors *in vivo* gene therapy for arthritis. *J. Rheumatol.* **27**, 983–989 (2000).
35. Ulrich-Vinther, M. *et al.* Recombinant adeno-associated virus-mediated osteoprotegerin gene therapy inhibits wear debris-induced osteolysis. *J. Bone Joint Surg. Am.* **84-A**, 1405–1412 (2002).
36. Zhang, R. *et al.* Etk/Bmx transactivates vascular endothelial growth factor 2 and recruits phosphatidylinositol 3-kinase to mediate the tumor necrosis factor-induced angiogenic pathway. *J. Biol. Chem.* **278**, 51267–51276 (2003).
37. Lacey, D.L. *et al.* Osteoprotegerin ligand is a cytokine that regulates osteoclast differentiation and activation. *Cell* **93**, 165–176 (1998).
38. Peng, H. *et al.* Synergistic enhancement of bone formation and healing by stem cell-expressed VEGF and bone morphogenetic protein-4. *J. Clin. Invest.* **110**, 751–759 (2002).
39. Xiao, X., Li, J. & Samulski, R.J. Production of high-titer recombinant adeno-associated virus vectors in the absence of helper adenovirus. *J. Virol.* **72**, 2224–2232 (1998).
40. Deckers, M. *et al.* Effect of angiogenic and antiangiogenic compounds on the outgrowth of capillary structures from fetal mouse bone explants. *Lab. Invest.* **81**, 5–15 (2001).



**PAPER II**

**Biological Effects of rAAV-caAlk2 Coating on Structural Allograft Healing**

Koefoed M. et al. *Mol Ther.* 2005 Aug;12(2):212-8.

## Biological Effects of rAAV-caAlk2 Coating on Structural Allograft Healing

Mette Koefoed,<sup>1</sup> Hiromu Ito,<sup>1</sup> Kirill Gromov,<sup>1</sup> David G. Reynolds,<sup>1</sup> Hani A. Awad,<sup>1</sup> Paul T. Rubery,<sup>1</sup> Michael Ulrich-Vinther,<sup>2</sup> Kjeld Soballe,<sup>2</sup> Robert E. Guldberg,<sup>3</sup> Angela S.P. Lin,<sup>3</sup> Regis J. O'Keefe,<sup>1</sup> Xinping Zhang,<sup>1</sup> and Edward M. Schwarz<sup>1,\*</sup>

<sup>1</sup>The Center for Musculoskeletal Research, University of Rochester, Rochester, NY 14642, USA

<sup>2</sup>The Department of Orthopedics, Aarhus University Hospital, Aarhus, Denmark

<sup>3</sup>Institute for Bioengineering and Bioscience, Georgia Institute of Technology, Atlanta, GA, USA

\*To whom correspondence and reprint requests should be addressed at The Center for Musculoskeletal Research, University of Rochester Medical Center, 601 Elmwood Avenue, Box 665, Rochester, NY 14642, USA.  
Fax: +1 585 756 4727. E-mail: Edward.Schwarz@URMC.Rochester.edu.

Available online 20 April 2005

Structural bone allografts often fracture due to their lack of osteogenic and remodeling potential. To overcome these limitations, we utilized allografts coated with recombinant adeno-associated virus (rAAV) that mediate *in vivo* gene transfer. Using  $\beta$ -galactosidase as a reporter gene, we show that 4-mm murine femoral allografts coated with rAAV-LacZ are capable of transducing adjacent inflammatory cells and osteoblasts in the fracture callus following transplantation. While this LacZ vector had no effect on allograft healing, bone morphogenetic protein signals delivered via rAAV-caAlk2 coating induced endochondral bone formation directly on the cortical surface of the allograft by day 14. By day 28 there was evidence of remodeling of the new woven bone and massive osteoclastic resorption of the cortical surface of the rAAV-caAlk2-coated allografts only. Micro-CT analysis of rAAV-LacZ- vs rAAV-caAlk2-coated allografts after 42 days of healing demonstrated a significant increase in new bone formation ( $0.67 \pm 0.21$  vs  $2.49 \pm 0.40$  mm<sup>3</sup>;  $P < 0.005$ ). Furthermore, the 3D micro-CT images of femurs grafted with rAAV-Alk2-coated allografts provided the first evidence that complete bridging of bone around a cortical allograft is possible. These results indicate that cell-free, rAAV-coated allografts have the potential to revitalize *in vivo* following transplantation.

**Key Words:** allograft, recombinant adeno-associated virus, bone morphogenetic protein

### INTRODUCTION

Bone grafting is commonly used in orthopedic reconstruction surgeries such as spinal fusion, revision of failed total joint arthroplasty, or repair of skeletal defects following trauma or the removal of tumor. Over 1 million such cases are performed per year [1]. Both experimental and clinical studies have shown that fresh autogenous grafts are vastly superior to allograft bone in graft repair and remodeling [2,3]. However, due to the size limitations of autogenous bone grafts, problems with chronic pain at the donor site [4], and also complications of the procedures [5,6], processed allograft remains an attractive substitute for bone grafting. Extensive research has shown that the critical difference between autograft and allograft healing is the participation of the grafted cells [7,8]. To show this formally *in vivo*, we recently demonstrated that there are no significant differences between the healing of an allograft and a processed isograft from a

genetically identical animal, using a murine model of femoral graft healing [9].

The repair and incorporation of bone graft is a regulated process that is very similar to fracture healing. The initial phase is characterized by inflammation and vascular invasion from the host bed, which facilitates recruitment of mesenchymal stem cells (MSC) that will differentiate into the bone-forming cells [10]. In the case of autografts, both graft and host bones contribute these osteogenic cells [11]. In contrast, since allograft does not contain any live cells, healing relies upon invasion of the graft by host cells and tissues. While the later phases of graft healing are characterized by remodeling, allografts remodel very slowly, and in the case of large structural allografts, remodeling along the allograft is very limited. The limited bone forming and remodeling of structural allografts is associated directly with the 25 to 35% failure rate due to nonunion and fracture [12,13]. These fractures

typically occur 1 to 2 years after implantation and are related to the propagation of microfractures within the dead cortical bone. Thus, a major challenge to the field of bone grafting is to elucidate the central factors that govern autograft healing and devise a method to transfer them to processed allograft such that it will have similar healing properties.

There are two conceivable approaches by which osteoinductive and remodeling properties can be conferred onto processed allograft. The first is to engraft MSC that will act as an artificial periosteum to promote bone formation from the graft and subsequent vascular ingrowth and remodeling. While several groups have demonstrated the efficacy of this approach [14,15], many issues remain regarding its clinical potential, including the source of the cells, reproducible engraftment of cells onto the graft, and added cost and complexity. The other approach is to introduce the critical factor(s) onto the allograft directly. In the case of cancellous grafts and bone graft substitutes, this approach has come to fruition in the form of FDA-approved bone morphogenetic protein (BMP) [16]. Unfortunately, high required dose and short protein half-life limit this strategy for large structural grafts. We believe gene therapy offers a cost-effective solution to these problems and it is the focus of the present study.

Transient transduction of bone marrow stromal cells with adenoviral constructs containing BMP has demonstrated efficacy for the enhancement of bone regeneration in a number of animal models [17,18]. More recently, recombinant adeno-associated viruses (rAAV) expressing BMP have been utilized in combination with cultured MSC for *ex vivo* and *in vivo* models of bone healing [19–21]. However, an effective *in vivo* gene therapy approach to heal a large bone defect without the addition of exogenous cells has yet to be demonstrated.

Since BMP gene therapy requires a high level of gene expression for efficacy, our laboratory has focused on the activin receptor-like kinase-2 (ALK2). The specificity of ALK2 to BMP signaling was illustrated in early *Xenopus* embryos in which the constitutively active form of the ALK2 receptor (caAlk2) generated signals similar to BMP but not activin signals [22]. Recently, we have shown that caAlk2 can potently induce mesenchymal cell differentiation *in vitro* and *in vivo* and that injection of a caAlk2-expressing retrovirus into chick limbs dramatically induced chondrogenesis and endochondral bone formation [23]. Based on these findings we have developed a functional rAAV-caAlk2 vector. We have also established a method to immobilize rAAV onto the cortical surface of allografts via freeze-drying [24]. Here we demonstrate the remarkable osteogenic and remodeling properties of rAAV-caAlk2-coated allografts in our murine femur model, in terms of their osteogenic and remodeling potential.

## RESULTS AND DISCUSSION

### rAAV Freeze-Dried onto the Allograft Cortical Surface Mediates Efficient Transduction *in Vivo*

With the hypothesis that addition of critical signals to the cortical surface of allografts will lead to autograft-like healing, our challenge was to develop an approach to transfer these signals efficiently. To this end we evaluated the effects of freeze-drying and storage at  $-80^{\circ}\text{C}$  on rAAV transduction efficiency. Previously, we demonstrated that freeze-drying rAAV in a sorbitol solution onto various implant materials does not affect the infectious titer *in vitro* [24]. To assess the transduction efficiency of freeze-dried rAAV-LacZ *in vivo*, we performed a dose-response experiment in which various amounts of virus were coated onto femoral allografts and transplanted into mice. Two weeks after implantation, the allografts were harvested for X-gal staining. Macroscopic comparison of the uncoated and coated allografts demonstrated  $\beta$ -gal activity throughout the repair tissue surrounding the coated allografts only (Figs. 1A and 1B). Similarly,

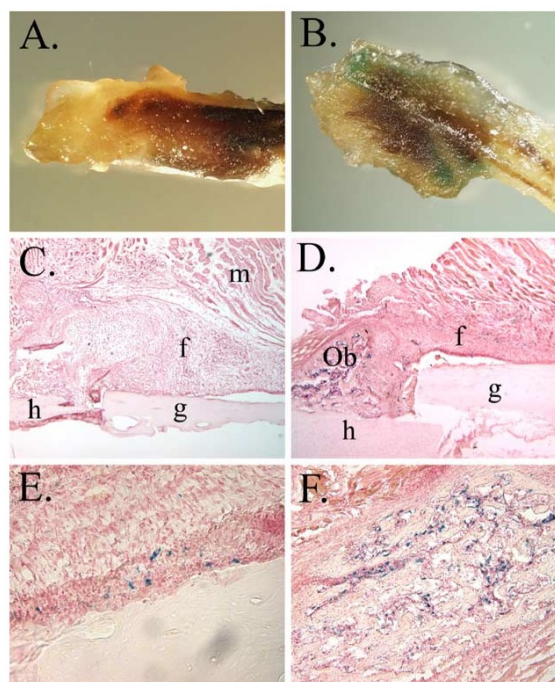


**FIG. 1.** *In vivo* transduction efficiency of rAAV-LacZ-coated allografts. (A and C) Uncoated allografts or (B, D, E, and F) allografts coated with  $5 \times 10^7$  transducing units of rAAV-LacZ were transplanted into mice. The efficiency of *in vivo* transduction 14 days after transplantation was evaluated on whole tissue (A and B) or microscopy (C–F) after X-gal staining. Representative histology is shown at  $10\times$  (C and D) and  $40\times$  (E and F) original magnification, in which the blue staining indicates transduction of the fibroblasts (f) and osteoblasts (Ob) between the allograft (g) or host (h) bone and the muscle (m).

## ARTICLE

doi:10.1016/j.jymthe.2005.02.026

analysis of histological sections from these tissues revealed that fibroblasts in the inflammatory tissue between the bone and the muscle (Fig. 1E) and osteoblasts in the creeping callus (Fig. 1F) were readily transduced. The percentage of blue cells per section peaked at a dose of  $5 \times 10^7$  particles/allograft, at a value of ~5%. Thus, we used  $5 \times 10^7$  particles/allograft as our effective dose in our subsequent gain-of-function studies.

#### Revitalization of Processed Structural Allografts via rAAV-caAlk2 Gene Transfer

To evaluate formally the efficacy of transferring BMP signals to the cortical surface of processed allografts we coated femoral allografts with rAAV-LacZ (control) or rAAV-caAlk2 (experimental) and evaluated healing responses in our mouse allograft model at 2, 4, and 6-weeks. Fig. 2 demonstrates several remarkable features of rAAV-caAlk2-coated allograft healing including: (i) the absence of a foreign body reaction that normally encases the allograft in inflammatory tissue, (ii) endochondral bone formation directly on the allograft sur-

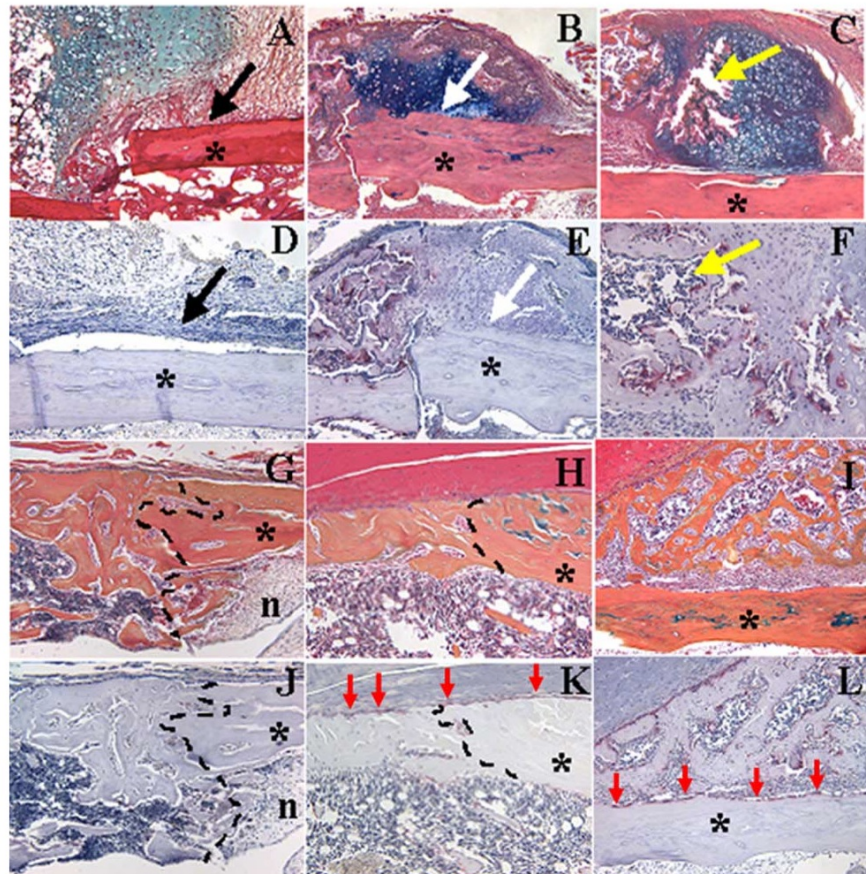
face, (iii) vascularization of the cartilage over the graft, (iv) a new bone collar that extends the entire length of the allograft, (v) live bone marrow within the allograft, and (vi) osteoclastic resorption of the allograft. Historically, these features have never been seen with structural allografts, and we have not observed them in >500 uncoated allografts in our murine femur model.

To quantify these features, we performed histomorphometry to assess new bone formation after 6 weeks of healing, as we have previously described [9]. This revealed an obvious trend demonstrating that rAAV-caAlk2-coated allografts have an increase in new bone formation ( $0.87 \pm 0.65$  vs  $1.66 \pm 0.45$  mm<sup>2</sup>). However, the variability within the groups was very large, and consequently the results failed to reach statistical significance ( $P > 0.09$ ).

#### Micro-CT Analysis of Femoral Graft Healing

While histomorphometry is a widely used quantitative method, it is a two-dimensional outcome measure of a three-dimensional (3D) structure. Thus, its limitations based on chosen fields of view and high intragroup

**FIG. 2.** Histological evidence of the osteogenic, angiogenic, and remodeling potential of rAAV-caAlk2-coated allografts. Murine femoral allografts (\*) were coated with  $5 \times 10^7$  (A, D, G, J) rAAV-LacZ or (B, C, E, F, H, I, K, L) rAAV-caAlk2 and transplanted into mice as described under Materials and Methods. Tissues were obtained after 2 (A–F) or 4 weeks (G–L), and sections were prepared and stained with H&E/orange G/Alcian blue (A–C, G–I) or for tartrate-resistant acid phosphatase to visualize osteoclasts (D–F, J–L). Consistent with uncoated allografts, rAAV-LacZ-coated allografts induce a foreign body reaction that encases the graft in a fibrous tissue (black arrows in A and D) that inhibits healing. In contrast, rAAV-caAlk2-coated allografts show cartilage forming directly on the cortical bone surface (white arrows in B and E), vascular ingrowth (yellow arrows in C and F), and endochondral ossification by 28 days yielding a new bone collar (I and L). At this time, large numbers of osteoclasts (red arrows in K and L) can be found only on the cortical surface of rAAV-caAlk2-coated allografts. Although the rAAV-LacZ-coated allografts achieve cortical union between the graft and the host (dashed lines in G and J) at day 28, the marrow space inside the allograft remains necrotic (n). In contrast, there is contiguous live bone marrow at the graft–host junction of rAAV-caAlk2-coated allografts at day 28 (H and K).



doi:10.1016/j.ymthe.2005.02.026

ARTICLE

variability are well known, particularly for spatially heterogeneous tissue structures. To overcome these limitations several labs have established 3D radiological outcome measurements to quantify bone healing [25]. To establish micro-CT methods for our murine femur model, we first analyzed 6-week autografts and allografts (Fig. 3). These data are consistent with our previous X-ray and histology data [9] and confirm our conclusions regarding the differences between autograft and allograft healing as stated above. Most notable is the uniform new bone cortex that forms completely around the autograft and the extensive remodeling that occurs, which makes it difficult to identify the ends of the original graft. Equally impressive are the absence of new bone around the

allograft and the lack of remodeling of the original graft bone.

Since allografts are not remodeled over the first 6 weeks, we used this time point to establish a region of interest (ROI) to quantify new bone formation in our model. Fig. 4 shows how we used the ends of the allografts to define the boundaries of the ROI of the reconstructed micro-CT images, which were further spatially segmented to identify new bone formation by subtracting the implanted allograft. Using this method to quantify the new bone in the same samples analyzed by histomorphometry, we were able to show a significant difference between rAAV-LacZ- and rAAV-caAlk2-coated allografts ( $0.67 \pm 0.21$  vs  $2.49 \pm 0.40$  mm<sup>3</sup>;  $P < 0.005$ ). Visualization of 3D images provides the explanation for the apparent discrepancy between the histomorphometry and the micro-CT results (Fig. 5). In contrast to autograft healing, the new bone that forms around rAAV-caAlk2-coated allografts is nonuniform and has a highly variable form, making it impossible to measure accurately by 2D histomorphometry. The lack of new bone formation around the rAAV-LacZ-coated allografts was the same as that seen in the uncoated allografts, indicating the innocuous effects of the vector.

The lack of an effective treatment to repair large structural defects remains a major orthopedic problem. While the commercial development of BMP as an adjuvant for spinal fusion and fracture healing has formally demonstrated its clinical utility, the high doses (milligrams) that must be used to observe efficacy and the short half-life (hours) limit its utility for large structural grafts. Although gene therapy offers a potential solution to these obstacles, a safe, effective, practical method to deliver the therapeutic gene and allograft during surgery remains elusive.

The first attempt to combine an osteoconductive bone substitute with *in vivo* gene therapy was performed by Bonadio *et al.*, who developed the gene-activated matrix (GAM) [26]. In this approach the investigators evaluated the potency of plasmid gene delivery from genes physically entrapped in a polymer matrix using bone regeneration in a canine critical defect as the endpoint. While this study demonstrated target gene expression for 6 weeks, and the induction of centimeters of normal new bone in a stable, reproducible, dose- and time-dependent manner, GAM *in vivo* transduction efficiency has never been reported. Unfortunately, others and we have been unable to achieve effective transduction efficiencies in our models using GAMs and have turned to viral-mediated gene transfer approaches. Based on the empirical advantages of rAAV vectors for orthopedic gene therapy [27], and the clinical potential of this vector [28], we evaluated the effects of freeze-drying and storage at  $-80^{\circ}\text{C}$  on rAAV transduction efficiency [24]. These studies revealed that rAAV vectors are remarkably durable, as we routinely recover  $\sim 100\%$  of the transducing

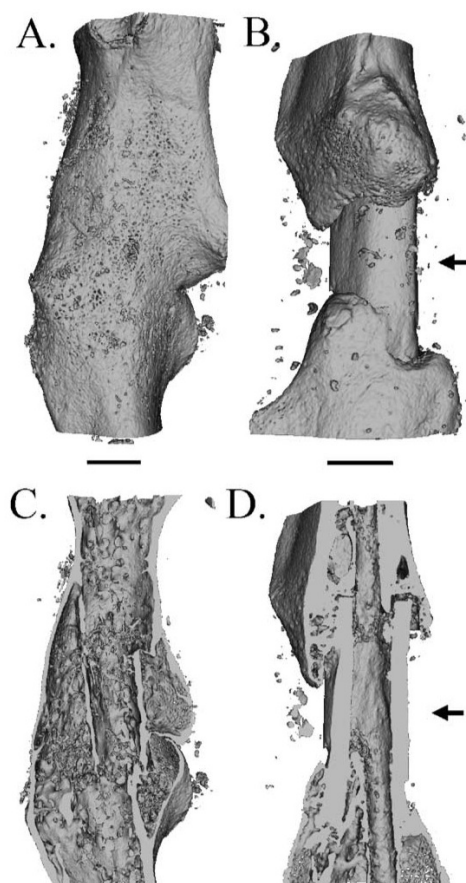
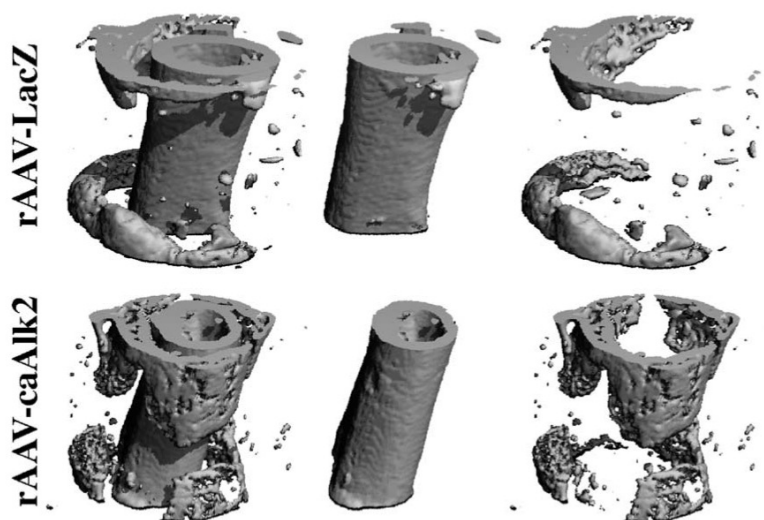


**FIG. 3.** Micro-CT analysis of allograft and autograft healing at 6 weeks. (A and C) Autografts and (B and D) allografts were harvested from the mice after 6 weeks and scanned in a micro-CT scanner. Three-dimensional volumetric reconstructions of the outer surface of the femurs (A and B) and medial cross sections through the reconstructed volumes (C and D) were generated. Representative examples are shown ( $n = 5$ ). Of note are the absence of new bone around the allograft and the lack of remodeling (arrows), compared to the autograft. Scale bars represent 1 mm.

## ARTICLE

doi:10.1016/j.jymthe.2005.02.026

**FIG. 4.** Volumetric quantitation of new bone formation by micro-CT. Femurs were scanned and imaged by micro-CT as described under Materials and Methods. To quantify new bone formation surrounding the allografts a region of interest was defined extending from the proximal to the distal end of the defect region. For each image, total bone volume was calculated, including both the implanted allograft and the surrounding new bone formation (left). Following manual segmentation, a second evaluation was performed to calculate bone volume of the allograft alone (center). The difference between the two volumes defined the volume of new bone formation surrounding the allograft (right).



units after freeze-drying and storage. Here we show that this method can lead to the transduction of up to 5% of cells at the surgical site (Fig. 1). From a practical standpoint, this rAAV-coating process can be easily adaptable to standard operating procedures used by tissue banks to prepare clinical allografts.

In their work that demonstrated an effective *in vivo* stem cell-based gene therapy approach to heal large bone defects, Gazit and colleagues formally proposed a paradigm to explain the autocrine and paracrine effects of genetically engineered MSC and how they function in regenerative medicine [29–31]. This theory posits that while the autocrine BMP is important for exogenous MSC differentiation, its greater effect is on endogenous MSC as

a paracrine factor. Thus, our choice to use a constitutively active BMP receptor as the target gene, instead of the cytokine, is based on the low level of *in vivo* expression required to induce significant endochondral bone formation [23] and the fact that caAlk2 signals cannot be blocked by the endogenous BMP antagonists noggin and chordin.

Based on the results in our study we find that the efficacy of the rAAV-caAlk2 coating is derived from four effects that are never observed in uncoated or rAAV-LacZ-coated allografts: osteogenesis, inhibition of the foreign-body reaction, angiogenesis, and osteoclastic resorption of the allograft. While the induction of orthotopic bone formation on the cortical surface is readily explained by

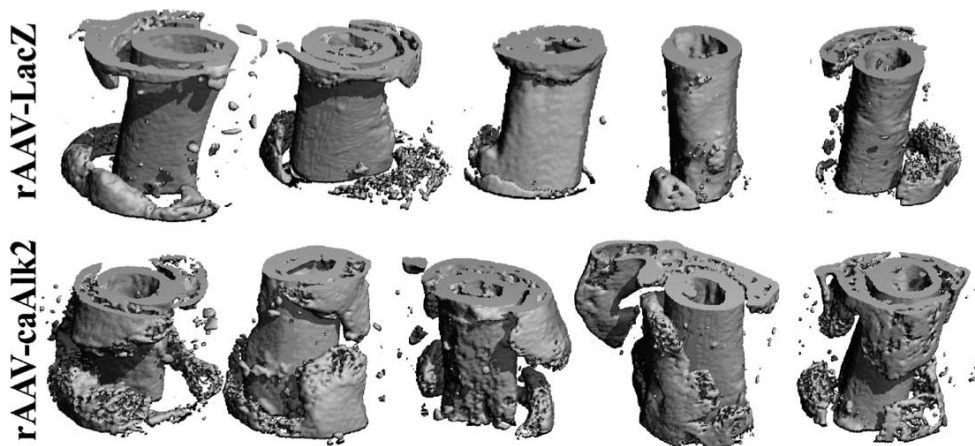


**FIG. 5.** rAAV-caAlk2-coated allografts produce a new bone collar *in vivo*. The rAAV-coated allografts like those analyzed by histomorphometry were analyzed by micro-CT to quantify the new bone formation at 6 weeks as described for Fig. 4. Reconstructed images of the allografts demonstrate the lack of new bone around the rAAV-LacZ-coated allografts and reflects the variability in size and distribution of the new bone that forms around the rAAV-caAlk2-coated allografts.

the caAlk2 transduction of MSC, the molecular mechanism by which this gene therapy prevents the formation of fibrotic tissue around the allograft, promotes blood vessel ingrowth, and stimulates osteoclastogenesis remains to be formally proven. Based on our previous results with caAlk2 gene transfer in the chicken limb bud [23], it is likely that the osteogenic effects result from the induction of Indian hedgehog and parathyroid hormone receptor signaling pathways. Additionally, the caAlk2-transduced MSC could trigger a cascade of events that involves other mesenchymal and hematopoietic cells, to establish a milieu that strongly favors healing and inhibits fibrosis, such as observed with MSC transduced with BMP-2 [29]. The angiogenic effects of caAlk2 could be due to the induction of vascular endothelial growth factor in osteoblasts, which stimulates vascular ingrowth during bone formation [32]. It could also be that caAlk2 transduction of inflammatory cells alters the innate immune response to the allograft such that the necrotic bone is perceived to be the host rather than a foreign body. Alteration of these events immediately following transplantation allows for later healing events, such as vascular ingrowth and osteoclastic remodeling of the allograft, even after the target gene expression is lost due to cell division and/or turnover.

Over the past few years there have been efforts to establish more robust quantitative three-dimensional imaging techniques that can overcome the limitations of two-dimensional histomorphometry. Our data provide an excellent example of such limitations. While histomorphometry of tissue sections is a reliable outcome measure to assess uniform healing, such as that which occurs on the surface of autografts (Fig. 3), it fails to quantify accurately the highly irregular bone formation that occurs around rAAV-caAlk2-coated allografts (Fig. 5). These observations emphasize the advantages of quantitative 3D micro-CT as a tool to monitor structural bone repair better. Future studies should attempt to correlate the quantitative features captured by micro-CT with the biomechanical properties of the repairing bone as the most important functional outcome.

Although our results demonstrate the potential of rAAV coating as a method to revitalize structural allografts, there are three additional advances that are needed to further this technology for human use. The first is to improve the connectivity of the new bone that forms around the host bone and the allograft, as a junction-to-junction union of new cortical bone is the primary goal. This could be done by using corrugated allografts or a bone graft substitute that allows a uniform distribution of the rAAV before freeze-drying. Another necessary advance is the establishment of technology and protocols for *in vivo* 3D imaging of new bone formation and vascular ingrowth of allografts with metal screws and plates for large-animal preclinical and clinical trials. Recently there has been new technology developed in

this area that may serve this purpose [33,34]. Finally, since the primary function of structural bone is to support *in vivo* loads, the biomechanical properties of rAAV-coated allografts must be determined and correlated with volumetric and morphometric parameters determined by micro-CT in auto- and allografts after various healing periods. Success in these areas will be necessary to demonstrate the efficacy of rAAV-caAlk2 coating therapy, which may result in the first remodeling allograft for large bone defects.

## MATERIALS AND METHODS

**Murine segmental femoral graft model.** All animal studies were conducted in accordance with principles and procedures approved by the University of Rochester Committee for Animal Resources. Auto- and allograft transplant surgeries were performed as we have previously described [9]. Briefly, 8-week-old C57BL/6 mice were anesthetized, and a 7- to 8-mm-long incision was made on the right leg and the femur was exposed by blunt dissection. A 4-mm middiaphyseal segment was removed by osteotomizing the bone using an electric saw. A 4-mm segment of bone graft was obtained either from the same femoral shaft of the animal (autograft) or from that of a different strain of mouse: ICR mouse (allograft). This allograft was cleaned with 70% ethanol, rinsed three times in saline to remove residual ethanol, and then frozen at  $-80^{\circ}\text{C}$  for at least 24 h before use. After the segment was placed into the midshaft of the femur, the bone graft was secured with a 22-gauge steel pin through the marrow cavity. The incision was closed with absorbable sutures, and each animal was given 0.5 mg/kg Burprenorphine subcutaneously every 12 h for the next 3 days for pain management. The mice were allowed to move freely after recovery from anesthesia.

**Preparation of rAAV-LacZ and rAAV-caAlk2.** The rAAV-LacZ vector, which was obtained directly from the Gene Core Facility of the University of North Carolina, contains the gene for LacZ under the transcriptional control of the CMV promoter. To generate the pAAV-caAlk2 transfer plasmid the rat cDNA was removed from a pcDNA3 plasmid [23] at the BamHI sites of both ends and subcloned into pSL301 and then excised by the NotI site at the 5' end and the EcoRI site at the 3' end. This fragment was then ligated into pAAV-BGHA, and positive clones were confirmed via restriction digests and DNA sequencing. Purified transfer vector (0.5 mg; Qiagen, Inc.) was sent to the Gene Core Facility, University of North Carolina (Chapel Hill, NC, USA), which prepared the purified rAAVs via a helper-virus-free method [35]. The resulting rAAVs were titered by dot blot to determine the concentration of virus particles. The transduction efficiency of rAAV-LacZ was determined *in vitro* by X-gal staining and by assaying for  $\beta$ -galactosidase activity using the Galacto-Light system (Tropix, Inc., Bedford, MA, USA) as described previously [36]. The transduction efficiency of the rAAV-caAlk2 vector was determined using primary chicken upper sternal chondrocytes transfected with a BMP-inducible reporter plasmid as described previously [23].

**In vivo treatments.** *In vivo* gene transfers to processed allografts were performed by pipetting  $5 \times 10^7$  particles of rAAV in 50  $\mu\text{l}$  of a 1% sorbitol-PBS solution onto the cortical surface of the grafts. The allografts were then frozen at  $-80^{\circ}\text{C}$ , lyophilized, and stored at  $-80^{\circ}\text{C}$  until they were transplanted. At least five mice were used in each treatment group.

**Volumetric quantitation of new bone formation by micro-CT.** After sacrifice and tissue harvest, the grafted femurs were positioned vertically and scanned individually on a microcomputed tomography system (VivaCT 40; Scanco, Inc., Bassersdorf, Switzerland) to quantify new bone formation surrounding the allografts as we have described previously for other long bones [25]. Briefly, the allografted regions were scanned at 21- $\mu\text{m}$  voxel resolution using an integration time of 200 ms, energy of 55 kVp, and intensity of 109  $\mu\text{A}$ . A volume of interest for quantitative analysis was defined, extending from the proximal to the distal end of the

defect region. The transition regions between host bone and allograft bone were evident upon careful slice-by-slice examination of the gray-scale 2D slice images. The volume of interest was selected to include only slices in which the cross section of allograft bone was visible, and contours were drawn to exclude any host bone. These 2D slices were thresholded based on X-ray attenuation and stacked to create a binarized 3D image of this volume of interest. For each 3D image, total bone volume was calculated, including both the implanted allograft and the surrounding new bone formation. Following manual segmentation, a second evaluation was then performed to calculate bone volume of the allograft alone. Finally, the volume of new bone formation surrounding the allograft was determined by subtracting the allograft volume from the total volume.

**Histological and histomorphometric analysis.** Following micro-CT scanning, the grafted femurs were harvested, fixed in 10% neutral-buffered formalin or 4% paraformaldehyde, and decalcified in 0.5 M EDTA for 21 days, and 3- $\mu$ m paraffin-embedded sections were prepared and stained with hematoxylin and eosin/orange G/Alcian blue or for tartrate-resistant acid phosphatase activity and counterstained with hematoxylin as we have described previously [31,32].

X-gal (Sigma, St. Louis, MO, USA) staining was performed *in situ* on whole femurs or on sections counterstained with eosin as we have described previously [37]. Histomorphometric analysis was carried out using Osteometrics software to determine the area of new bone on top of the bone graft using methods similar to those we have described for fracture callus [38]. Briefly, a hypothetical line was drawn in the middle of the graft–host bone junction to separate bone formation on the host or the graft side. Then the new bone on the cortical surface of the graft was traced and its area was calculated. An observer blinded to the treatment performed the histomorphometric analysis.

**Statistical analysis.** Data reported in this article represent the means  $\pm$  standard deviation. Statistical analysis of the quantitative effects of rAAV coating treatment vs rAAV-LacZ controls was performed using two-tailed *t* test, and statistical significance was set at  $P < 0.05$ .

#### ACKNOWLEDGMENTS

We thank Dr. Hans Burchardt (Musculoskeletal Transplant Foundation) for critical advice with this research. We also thank C. Canary and B. Stroyer for assistance with the histology. This work was supported by research grants from the Danish Rheumatism Association, the Orthopaedic Research and Education Foundation, and the Musculoskeletal Transplant Foundation and NIH Grants AR51469, AR46545, and AR051336; NSF Grants BES-0101239 and EEC-9731643; and unrestricted research grants from DePuy, J&J, Inc. P.T.R., R.J.O., and E.M.S. are founding members of LAGeT, Inc.

RECEIVED FOR PUBLICATION DECEMBER 2, 2004; ACCEPTED FEBRUARY 5, 2005.

#### REFERENCES

1. Yaszemski, M. J., Payne, R. G., Hayes, W. C., Langer, R., and Mikos, A. G. (1996). Evolution of bone transplantation: molecular, cellular and tissue strategies to engineer human bone. *Biomaterials* **17**: 175–185.
2. Garbuz, D. S., Masri, B. A., and Czitrom, A. A. (1998). Biology of allografting. *Orthop. Clin. North Am.* **29**: 199–204.
3. Stevenson, S. (1999). Biology of bone grafts. *Orthop. Clin. North Am.* **30**: 543–552.
4. Deluca, J. V., Cianelli, C., and Friedlaender, G. E. (1987). A comparative histomorphometric study of bone remodeling in human paired cancellous autografts and allografts. *Trans. Orthop. Res. Soc.* **11**: 376.
5. Younger, E. M., and Chapman, M. W. (1989). Morbidity at bone graft donor sites. *J. Orthop. Trauma* **3**: 192–195.
6. Summers, B. N., and Eisenstein, S. M. (1989). Donor site pain from the ilium: a complication of lumbar spine fusion. *J. Bone Joint Surg. (Br.)* **71**: 677–680.
7. Stevenson, S., Shaffer, J. W., and Goldberg, V. M. (1996). The humoral response to vascular and nonvascular allografts of bone. *Clin. Orthop.* **86**–95.
8. Stevenson, S., Li, X. Q., Davy, D. T., Klein, L., and Goldberg, V. M. (1997). Critical biological determinants of incorporation of non-vascularized cortical bone grafts: quantification of a complex process and structure. *J. Bone Joint Surg. Am.* **79**: 1–16.
9. Tiyyapanaputi, P., Rubery, P. T., Carmouche, J., Schwarz, E. M., O'Keefe, R. J., and Zhang, X. (2004). A novel murine segmental femoral graft model. *J. Orthop. Res.* **22**: 1254–1260.
10. Einhorn, T. A. (1998). The cell and molecular biology of fracture healing. *Clin. Orthop.* **57**–521.
11. Burchardt, H. (1987). Biology of bone transplantation. *Orthop. Clin. North Am.* **18**: 187–196.
12. Lord, C. F., Gebhardt, M. C., Tomford, W. W., and Mankin, H. J. (1988). Infection in bone allografts: incidence, nature, and treatment. *J. Bone Joint Surg. Am.* **70**: 369–376.
13. Berrey, B. H. Jr., Lord, C. F., Gebhardt, M. C., and Mankin, H. J. (1990). Fractures of allografts: frequency, treatment, and end-results. *J. Bone Joint Surg. Am.* **72**: 825–833.
14. Lieberman, J. R., Daluiski, A., and Einhorn, T. A. (2002). The role of growth factors in the repair of bone: biology and clinical applications. *J. Bone Joint Surg. Am.* **84-A**: 1032–1044.
15. Gafni, Y., Turgeman, G., Liebergal, M., Pelled, G., Gazit, Z., and Gazit, D. (2004). Stem cells as vehicles for orthopedic gene therapy. *Gene Ther.* **11**: 417–426.
16. Einhorn, T. A. (2003). Clinical applications of recombinant human BMPs: early experience and future development. *J. Bone Joint Surg. Am.* **85-A**(Suppl. 3): 82–88.
17. Lieberman, J. R., Ghivizzani, S. C., and Evans, C. H. (2002). Gene transfer approaches to the healing of bone and cartilage. *Mol. Ther.* **6**: 141–147.
18. Baltzer, A. W., and Lieberman, J. R. (2004). Regional gene therapy to enhance bone repair. *Gene Ther.* **11**: 344–350.
19. Chen, Y., et al. (2003). Gene therapy for new bone formation using adeno-associated viral bone morphogenetic protein-2 vectors. *Gene Ther.* **10**: 1345–1353.
20. Luk, K. D., Chen, Y., Cheung, K. M., Kung, H. F., Lu, W. W., and Leong, J. C. (2003). Adeno-associated virus-mediated bone morphogenetic protein-4 gene therapy for *in vivo* bone formation. *Biochem. Biophys. Res. Commun.* **308**: 636–645.
21. Gafni, Y., et al. (2004). Gene therapy platform for bone regeneration using an exogenously regulated, AAV-2-based gene expression system. *Mol. Ther.* **9**: 587–595.
22. Chen, Y., Bhushan, A., and Vale, W. (1997). Smad8 mediates the signaling of the ALK-2 [corrected] receptor serine kinase. *Proc. Natl. Acad. Sci. USA* **94**: 12938–12943.
23. Zhang, D., Schwarz, E. M., Rosier, R. N., Zuscik, M. J., Puzas, J. E., and O'Keefe, R. J. (2003). ALK2 functions as a BMP type I receptor and induces Indian hedgehog in chondrocytes during skeletal development. *J. Bone Miner. Res.* **18**: 1593–1604.
24. Ito, H. (2005). Remodeling of cortical bone allografts mediated by adherent rAAV-RANKL and VEGF gene therapy. *Nat. Med.* **11**: 291–297.
25. Guldberg, R. E., et al. (2003). Analyzing bone, blood vessels, and biomaterials with microcomputed tomography. *IEEE Eng. Med. Biol. Magn.* **22**: 77–83.
26. Bonadio, J., Smiley, E., Patil, P., and Goldstein, S. (1999). Localized, direct plasmid gene delivery *in vivo*: prolonged therapy results in reproducible tissue regeneration. *Nat. Med.* **5**: 753–759.
27. Schwarz, E. M. (2000). The adeno-associated virus vector for orthopaedic gene therapy. *Clin. Orthop. Relat. Res.* **379S**: S31–S39.
28. Rabinowitz, J. E., and Samulski, R. J. (2000). Building a better vector: the manipulation of AAV virions. *Virology* **278**: 301–308.
29. Gazit, D., et al. (1999). Engineered pluripotent mesenchymal cells integrate and differentiate in regenerating bone: a novel cell-mediated gene therapy. *J. Gene Med.* **1**: 121–133.
30. Moutsatsos, I. K., et al. (2001). Exogenously regulated stem cell-mediated gene therapy for bone regeneration. *Mol. Ther.* **3**: 449–461.
31. Turgeman, G., et al. (2001). Engineered human mesenchymal stem cells: a novel platform for skeletal cell mediated gene therapy. *J. Gene Med.* **3**: 240–251.
32. Gerber, H. P., Vu, T. H., Ryan, A. M., Kowalski, J., Werb, Z., and Ferrara, N. (1999). VEGF couples hypertrophic cartilage remodeling, ossification and angiogenesis during endochondral bone formation. *Nat. Med.* **5**: 623–628.
33. Guldberg, R. E., Lin, A. S., Coleman, R., Robertson, G., and Duvall, C. (2004). Microcomputed tomography imaging of skeletal development and growth. *Birth Defects Res. C Embryo Today* **72**: 250–259.
34. Duvall, C. L., Robert Taylor, W., Weiss, D., and Guldberg, R. E. (2004). Quantitative microcomputed tomography analysis of collateral vessel development after ischemic injury. *Am. J. Physiol. Heart Circ. Physiol.* **287**: H302–H310.
35. Xiao, X., Li, J., and Samulski, R. J. (1998). Production of high-titer recombinant adeno-associated virus vectors in the absence of helper adenovirus. *J. Virol.* **72**: 2224–2232.
36. Goater, J., et al. (2000). Empirical advantages of adeno associated viral vectors *in vivo* gene therapy for arthritis. *J. Rheumatol.* **27**: 983–989.
37. Childs, L. M., Goater, J. J., O'Keefe, R. J., and Schwarz, E. M. (2001). Effect of anti-tumor necrosis factor-alpha gene therapy on wear debris-induced osteolysis. *J. Bone Joint Surg. Am.* **83-A**: 1789–1797.
38. Zhang, X., Schwarz, E. M., Young, D. A., Puzas, J. E., Rosier, R. N., and O'Keefe, R. J. (2002). Cyclooxygenase-2 regulates mesenchymal cell differentiation into the osteoblast lineage and is critically involved in bone repair. *J. Clin. Invest.* **109**: 1405–1415.

**PAPER III**

**AAV2 mediated VEGF gene transfer leads to increased bone formation and remodeling of bone allografts**

**Koefoed M. et al. Manuscript ready for submission.**

## **AAV2 mediated VEGF gene transfer leads to increased bone formation and remodeling of bone allografts**

Koefoed M.<sup>1,2</sup>, Pedersen A.G.<sup>1</sup>, Foldager C.B.<sup>2</sup>, Hansen K.<sup>3</sup>, Pedersen M.<sup>3</sup>, Cucchiarini M.<sup>4</sup>, Schwarz E.M.<sup>5</sup>, Soballe K.<sup>2</sup>, Jensen T.G.<sup>1\*</sup>, Ulrich-Vinther M.<sup>2</sup>.

<sup>1</sup>Department of Human Genetics, Aarhus University, Aarhus, Denmark.

<sup>2</sup> Orthopaedic Research Laboratory, Aarhus University Hospital, Aarhus, Denmark.

<sup>3</sup>MR Research Center, Aarhus University Hospital, Aarhus, Denmark.

<sup>4</sup>Experimental Orthopaedics and Osteoarthritis Research, Saarland University, Homburg, Germany

<sup>5</sup>The Center for Musculoskeletal Research, University of Rochester, Rochester, NY 14642, USA.

\*Correspondence: Thomas G. Jensen, Department of Human Genetics, Wilhelm Meyers Allé, build. 1242, 8000 Aarhus C, Denmark. E-mail: thomas@humgen.au.dk

### **Abstract**

Bone allografts are used to repair bone fractures although they often fail to heal properly due to a limited formation of new bone and blood vessels. This study investigated whether coordinating vessel and bone formation is achieved using Vascular Endothelial Growth Factor (VEGF) and Fibroblast Growth Factor-2 (FGF2) gene transfer mediated by immobilized recombinant adeno-associated viral vectors (rAAV). Nonvital allografts were coated with rAAV and studied in a mouse femoral allograft model. Luciferase was used as reporter to evaluate the gene expression kinetics. Localized gene expression appeared between day 4 and 9 and continued for more than 6 months. VEGF coated allografts led to an almost two fold increase in new bone volume compared to controls (VEGF:  $31.7 \pm 11.6 \text{ mm}^3$ , GFP:  $16.4 \pm 8.6 \text{ mm}^3$ ,  $p < 0.05$ ). Histology and 3D reconstructions using micro-CT revealed new bone covering the entire surface of the VEGF-treated grafts.

Furthermore, clear signs of remodeling were identified at the ends and along the surface of the grafts. In conclusion, allografts coated with immobilized AAV have the potential to improve the repair of large bone defects.

## **INTRODUCTION**

Structural bone allografts are used to reconstruct large skeletal defects following trauma or removal of tumor. Both experimental and clinical studies have shown that fresh autogenous grafts are superior to allograft bone for graft repair and remodeling [1, 2]. In the case of autografts, both graft and host bone contributes to the osteogenesis. Living cells contained in the autografts can produce early new bone, growth factors and bone inducing substances. Following bone union autografts continue to remodel, and these processes are sustained through normal bone homeostasis. In contrast, as frozen allografts does not contain living cells, healing relies upon invasion of the graft by host cells [3]. Consequently, a large segment at the mid part of the graft is prone to lack of revascularization and loss of strength, causing a 20-25% failure rate due to nonunion and fracture [4].

Allografts heal by endochondral bone formation only [5]. Several growth factors are expressed in a distinct pattern during this healing response playing a role in bone repair [6]. The most promising of these are the Bone Morphogenic Proteins (BMPs), which have been used in clinical trials with varying effect, and in best case being capable to promote fracture healing following use of very high doses [7]. Furthermore, recent reports have shown adverse effects after treatment with recombinant human BMP (rhBMP) including soft tissue swelling and heterotopic ossification [8, 9].

Besides BMPs, other pathways are involved in bone formation. For example, angiogenesis is important since inhibition of Vascular Endothelial Growth Factor (VEGF) can disturb BMP induced osteogenesis [10]. During endochondral ossification the inhibition of VEGF leads to decreased bone formation at the growth plate secondary to suppression of vessel formation and impairment of cartilage resorption [5, 11].

Fibroblast growth factor-2 (FGF2) is another regulator of neoangiogenesis, and the mitogenic effect of FGF2 on endothelial cells, chondrocytes, fibroblasts and osteoblasts and has been demonstrated essential to the osteogenesis of mesenchymal stem cells [12, 13]. Both VEGF and FGF2 can promote bone formation in vivo [11, 14, 15]. Furthermore, the combination of VEGF and FGF2 has been shown to induce faster bone formation together with an increased formation of blood vessels in a model of vascular bone graft healing in mice [16]. Recently, an increased angiogenesis and blood vessel maturation was demonstrated in an acellular collagen scaffold loaded with both VEGF and FGF2 [17].

As the lack of formation of novel blood vessels is one of the major problems associated with allograft healing we used allografts coated with immobilized adeno-associated viral vectors [18-20] to obtain local and sustained expression of VEGF and FGF2, and we assessed new bone formation by histology and micro-CT analysis. We hypothesized that bone healing would be enhanced when coordinating vessel and bone formation using a combined treatment of VEGF and FGF2.

## RESULTS

### **Freeze-dried adeno-associated viral vectors are released from the bone graft surface within the first minute**

Murine femoral allografts coated with adeno-associated viral vectors are capable of transducing adjacent cells in the fracture callus following implantation [18, 19]. In order to measure the release of the viral coating from the bone surface coated allografts were placed onto confluent layers of 293 cells. Each minute the grafts were moved to new wells, and 48 h later the number of GFP positive cells was measured by flow cytometry. As seen in fig. 1, most of the AAV vectors (88%) in the coating were released from the graft surface within the first minute. Only 2.4% of the total transduction capacity was measured between 3-15 min.

### **Luciferase expression measured by bioluminescence is localized to the graft insertion in the right femur and continues for more than 6 months**

Based on the release profile demonstrated in vitro, we examined the kinetics of the viral coating in vivo using a murine femoral allograft model as done previously [18, 19]. Each allograft was coated with  $1 \times 10^9$  particles of rAAV-luciferase and inserted in the femur of the mice as described in the materials and methods section. As seen in fig. 2A, gene expression was localized to the site of insertion of the graft in the right femur of the mouse. Significant transgene expression was detected at day 9, reached a steady level around day 50 and could still be detected at day 178 (fig. 2B). 3D scans were performed to confirm the localization at the right site of the animal close to the surface, matching the site of insertion (fig. 2C). No expression at ectopic tissues was observed indicating that shedding of the viral vectors to tissues outside this region did not take place.

### **Muscle and fibrous tissue are the main targets of allograft coated AAV transduction**

In order to further define the location of the transgene expression we divided the right femur into different tissue groups by dissection: (1) skin, (2) the femur and (3) muscle and fibrous tissue surrounding the femur. As seen in fig. 3, bioluminescence imaging clearly defined the muscle and fibrous tissue surrounding the graft as the main location of luciferase expression. The bone did not show gene expression above control levels. It

has previously been shown that cells within the newly woven bone are transduced with AAV using LacZ as marker gene, but most likely we were not able to detect any light signal from these cells due to shielding of the signal by the overlying calcified bone. Finally, the skin showed low levels of gene expression localized to the area just above the site, where the muscle has been split. This may generate a potential route for escape of the viral vectors, emphasising the importance of sealing of the allograft within the muscle. There was no sign of transduction of the surrounding skin (data not shown).

### **rAAV-VEGF coated allografts lead to increased bone formation**

AAV2 mediated gene expression of VEGF<sub>165</sub> and FGF2 was used to study the effect of stimulation of both neovascularisation and bone formation. Mice (n=48) were divided in 4 groups receiving either VEGF, FGF2, a combination of the two and a GFP-control group. Micro-CT scans were performed after 10 weeks (fig. 4). Bone volume analysis of acquired micro-CT imaging data allowed calculation of total bone volume, graft volume and new bone volume. Interestingly, VEGF treated allografts led to an almost 2-fold increase in formation of new bone compared to GFP-controls ( $31.7 \pm 11.6 \text{ mm}^3$  vs.  $16.4 \pm 8.6 \text{ mm}^3$ ,  $p < 0.05$ ). 3D reconstructions of the micro-CT data showed formation of new bone along the entire length of the VEGF treated allografts in 5 of 8 samples (fig. 5). In contrast, animals in the control were dependent on bone bridging at the host-graft boundaries, leaving the mid part of the graft unaffected. Treatment with FGF2 or combination of VEGF and FGF2 had no effect on the amount of new-generated bone.

### **Histological features of AAV-VEGF coated allograft healing**

Histological sections were stained with Goldner Trichrome and tartrate-resistant acid phosphatase to investigate the effect of AAV-VEGF treatment (fig. 6). Histology confirmed formation of a new bone callus along the entire length of the allograft. The new bone was situated directly on the surface of the graft bone and between the host and graft bone, with active resorption of the necrotic graft bone both at the ends of the graft and also along the central part of the graft surface (fig. 7). The surface of the graft was irregular and invaded by new bone marrow in the remodeling callus. Finally, calcified cartilage and osteoid were present at the mid part of the graft in some animals, indicating that bone formation continued after 10 weeks.

**AAV-FGF2 leads to increased remodeling of processed allografts**

Even though there was no significant increase in new bone formed in the FGF2 treated group, histological evaluation revealed an irregular surface of the allograft with numerous osteoclasts in areas covered with new bone. Furthermore, micro-CT revealed a significantly decreased graft bone volume in the FGF2 group compared to the control (0.009 vs. 0.012 cm<sup>3</sup>, p<0.05), indicating active remodeling in the FGF2 treated animals (fig. 8).

## DISCUSSION

This experimental study in mice showed that AAV-VEGF gene transfer improved bone formation and remodeling during devitalized allograft healing. The effect is explained by the formation of a new bone collar that surrounds the entire graft and numerous active osteoclasts on the graft surface not normally seen in allograft healing..

Processed bone allografts are often problematic to use clinically due to a lack of revascularization and loss of mechanical strength. These grafts lack the biological osteoinductive activity to induce bone formation in their surroundings and have decreased ability to participate in osteogenesis [1]. Nonetheless, they are widely used because of the problems associated with autografts: limited size, availability and donor site morbidity [21]. Several approaches based on gene transfer have been investigated to improve allograft healing, including the transfer of factors expressing growth factors released from artificial scaffolds and cell based approaches with engineered mesenchymal stem cells expressing transgenes important for osteogenesis [14, 22, 23]. Recently, the delivery of immobilized self-complementary AAV (scAAV) mediated transfer of BMP2 has been shown to induce bone formation and remodeling of processed allografts [20]. The same method of immobilized AAV mediated gene transfer was in this study used to demonstrate the appearance of luciferase gene expression between day 4 and day 9 (fig. 2). We found this optimal considering that VEGF is normally expressed by hypertrophic chondrocytes on day 10 after fracture [24]. Gene expression was localized to the site of insertion with no indication of shedding of the viral vector to other organs, confirming previous findings with AAV coated allografts inserted in the quadriceps muscle in mice [25]. However, we observed low levels of gene expression in the skin in close proximity to the dissection of the muscle during insertion (fig. 3). Considering the fast release of the viral vector coating measured in vitro, this observation suggests that care must be taken to avoid disruption of the coating during insertion.

The sustained luciferase enzyme expression for more than 6 months may be explained by the transduction of muscle cells with a long life cycle. Others have shown that luciferase expression declined 3-4 weeks following insertion of coated allografts into muscle [25]. This difference could be explained by differences in animal models as the

insertion into muscle is less traumatic and less likely to elicit a regenerative response, which may induce AAV second strand synthesis necessary for gene expression. Nevertheless, for safety reasons the expression profile has to be carefully evaluated.

For successful integration of the grafted bone tissue coordinated action of progenitor cells, kinetics of growth factors and revascularization is essential. We attempt to recapitulate aspects of the bone regenerative environment by using dual growth factor stimulation coated onto the surface of processed bone allografts to repair a critical sized defect in vivo. In a similar model, combination of VEGF and receptor activator of nuclear factor  $\kappa$ B ligand (RANKL) improved bone allograft healing through angiogenesis and osteoclast activation, leading to new bone formation [18]. However, the treatment led to inferior biomechanics of the bone due to extensive resorption of the grafts. The reported synergistic effects between angiogenic and osteogenic factors on bone formation [26, 27] suggest that stimulation of both angiogenesis and bone formation in combination will lead to an improved healing response of processed bone allografts.

In contrast to what has previously been shown using this animal model [18], we found that VEGF treatment alone was sufficient for induction of increased bone formation (fig. 4). This effect may be due to the use of a higher amount of viral vectors ( $1 \times 10^9$  vs.  $5 \times 10^7$  viral particles) as VEGF has been sufficient for induction of new bone formation previously [11, 14]. This response emphasizes the importance of performing dose-response studies when evaluating the effect of growth factors. To extend the understanding of the VEGF effect biomechanics of the allograft healing has to be evaluated to ensure proper performance of the reconstructed bone. Furthermore, evaluating the induced neovascularization in an in vivo animal model may also provide additional information about the role of VEGF.

We surprisingly found that the combination of VEGF and FGF2 did not lead to increased formation of new bone, contrary to a model of vascularized bone allotransplants, where these factors both increased the amount of new vessels formed and bone volume [16]. Furthermore, we found no significant effect of FGF2 gene transfer on bone formation. In the 3D reconstructions of the healing allografts (fig. 5) we clearly demonstrated a new bone collar encapsulating the entire graft in newly formed bone in contrast to the lack of

bone formation at the mid part of the graft in the controls. This observation was confirmed by the histology (fig. 6 and fig. 7). FGF2 alone had no effect on new bone formation but caused induction of remodeling and increased resorption of the allograft compared to control (fig. 8). This is in agreement with the effect of FGF2 on osteoclast differentiation through the upregulation of Receptor activator of nuclear factor  $\kappa$ B ligand (RANKL) [28].

In summary, we showed that expression of VEGF mediated by immobilized AAV is beneficial for improved healing of devitalized allograft. The VEGF treatment of the bone defects lead to the formation of new bone, covering the entire graft, lack of fibrous tissue surrounding the graft and evidence of remodeling of the graft surface. These features are normally associated with the healing of vital autografts. Thus our findings suggest that immobilized AAV-VEGF could be used to overcome the lack of fracture repair in large bone defects associated with decreased blood supply.

## MATERIAL AND METHODS

**rAAV vector preparation.** rAAV-GFP, rAAV-Luc and rAAV-VEGF<sub>165</sub> vectors, all serotype 2/2 were produced at the Gene Therapy Center of the University of North Carolina, Chapel Hill. The cDNA for VEGF<sub>165</sub> were subcloned into the pAAV-BGHA transfer vector prior to viral vector production [18]. The human basic fibroblast growth factor cDNA was inserted into rAAV-LacZ (rAAV-FGF2). The rAAV were packaged, purified and titrated as previously described [29-31].

**Murine segmental femoral graft model.** All animal studies were conducted in accordance with procedures approved by the Danish Animal Experiments Inspectorate. Male C57Bl/6 mice 8 weeks old were used for the femoral grafting procedure as described previously [32]. Briefly, the mice were anesthetized using ketamine/xylazine. A 10 mm incision was made in the right femur and the bone exposed by blunt dissection. A 4 mm segment of bone was removed using an electrical saw, and a piece of allograft bone was inserted in the gap and fixed with a 0.6 mm titanium pin through the marrow canal. The incision in the skin was closed using absorbable sutures. The animals received an injection of Buprenorphine (0.1 mg/kg) immediately after surgery followed by three days of oral Buprenorphine (0.7-1.4 mg/kg) for pain management. The mice were allowed to move freely after recovery from the anesthesia.

**Bone allograft processing.** Bone allografts were harvested from BalbC mice, cleaned and rinsed in 70% ethanol, rinsed three times in steril saline to remove residual ethanol, and then frozen for at least 24 h before use. In order to coat the graft with rAAV vectors, the vector was suspended in a total of 50  $\mu$ L of a 1% sorbitol-PBS solution, and the solution pipetted on to the graft surface while the graft was on dry ice followed by freeze-drying [18].

**Release of AAV vectors from murine bone allograft in vitro.** Allografts were coated with  $1 \times 10^8$  particles of rAAV-GFP. The time for release, transduction and gene expression was determined by placing allografts on a confluent layer of HEK 293 cells. The grafts were moved to a new well each minute. The number of GFP-positive cells was determined by flow cytometry after 48 h (n=3).

**Bioluminescence imaging.** All bioluminescence imaging data was obtained using the IVIS Spectrum imaging system (Caliper Life Sciences, Hopkinton, Massachusetts). In order to demonstrate gene expression over time, allografts coated with  $1 \times 10^9$  particles of rAAV-luciferase were inserted in the right femur of the mice, and the animals were scanned at different time points. At each time point each mouse was injected with the substrate D-luciferin potassium salt using a concentration of 15 mg/mL/10 g body weight (Synchem OHG, Felsberg-Altenburg, Germany). A standardized region of interest was defined and the radiance efficiency was measured (photons/cm<sup>2</sup>/sec/sr). 3D bioluminescence imaging followed manufacturer's protocol for diffuse light imaging tomography with the following settings: emission filter range of 560-660 nm (6 in total), exposure time 1, medium binning, and f-stop 1. Following acquisition, surface topography and bioluminescence source reconstruction was performed and the total flux was measured. To determine the location of the cells transduced with the luciferase enzyme, the skin was removed from the right side of the lower back, the femur was harvested and the muscle and fibrous tissue surrounding it was isolated. The skin, the muscle and fibrous tissue and the femoral bone were analyzed individually and the radiance efficiency from the entire tissue segments was measured.

**Quantification of new bone formation using  $\mu$ CT analysis.** Following sacrifice of the mice, the grafted femurs were harvested and fixed in 70% ethanol for 5 days. The tissue blocks were dehydrated gradually in ethanol (70%–100%) at 4 °C and embedded in methylmethacrylate at -20 °C. The grafted femurs were positioned vertically and positioned in a micro-CT system (VivaCT 40, Scanco, Bassersdorf, Switzerland) to quantify the volume of newly formed bone surrounding the allograft [19]. The allograft region was scanned with a 16  $\mu$ m isotropic voxel resolution. The imaging software OsiriX ([www.osirix-viewer.com](http://www.osirix-viewer.com)) was used for data processing. Initially, the two ends of the graft were precisely identified to standardise a fixed examination-volume, bounded by the graft itself plus the addition of exactly 15 slices to each end of the graft. A blinded observer determined an appropriate threshold-value for the bone voxels, and this threshold-value was kept constant throughout the analyses for each femur. The threshold value then served as the basis for a semiautomatic creation of regions of

interest that was finally propagated throughout the dataset in order to measure bone volume.

To exclude the allograft in the evaluation of bone healing, a second region of interest was limited to the graft itself. The volume of newly bone formed was calculated by subtracting the graft volume from the entire examination-volume. The volume rendering application in OsiriX was used to create indicative 3D representations, with intensity and colour settings referring to subjective preferences.

**Histology.** The femurs were embedded in extra MMA, cut in 7  $\mu\text{m}$  sections and stained with Goldners Trichrome, Hematoxyline and Eosine or tartrate-resistant acid phosphatase (TRAP) activity for qualitative analyses [33].

**Statistical analysis.** Analyses of the micro-CT data were performed blinded. The data were tested for normal distribution and homogeneity of variance. When these conditions were fulfilled the groups were compared using parametric analyses (Student's t-test) and the data are presented as mean  $\pm$ SD or mean  $\pm$ SEM. The level of statistical significance was  $p < 0.05$ .

## ACKNOWLEDGMENTS

We thank The Interdisciplinary Nanoscience Center at Aarhus University for the use of the IVIS Spectrum imaging system (Caliper Life Sciences, Hopkinton, Massachusetts). We thank J. Pauli for assistance with the histology. The study was supported by research grants from the Faculty of Health Sciences, Aarhus University, Denmark

## REFERENCES

1. Stevenson, S., et al., *Critical biological determinants of incorporation of non-vascularized cortical bone grafts. Quantification of a complex process and structure.* J Bone Joint Surg Am, 1997. **79**(1): p. 1-16.
2. Stevenson, S., *Biology of bone grafts.* Orthop Clin North Am, 1999. **30**(4): p. 543-52.
3. Enneking, W.F. and D.A. Campanacci, *Retrieved human allografts : a clinicopathological study.* J Bone Joint Surg Am, 2001. **83-A**(7): p. 971-86.
4. Eward, W.C., et al., *Free vascularized fibular graft reconstruction of large skeletal defects after tumor resection.* Clin Orthop Relat Res, 2010. **468**(2): p. 590-8.
5. Gerber, H.P., et al., *VEGF couples hypertrophic cartilage remodeling, ossification and angiogenesis during endochondral bone formation.* Nat Med, 1999. **5**(6): p. 623-8.
6. Huang, Z., et al., *The sequential expression profiles of growth factors from osteoprogenitors [correction of osteroprogenitors] to osteoblasts in vitro.* Tissue Eng, 2007. **13**(9): p. 2311-20.
7. Garrison, K.R., et al., *Bone morphogenetic protein (BMP) for fracture healing in adults.* Cochrane Database of Systematic Reviews, 2010(6): p. -.
8. Mannion, R.J., A.M. Nowitzke, and M.J. Wood, *Promoting fusion in minimally invasive lumbar interbody stabilization with low-dose bone morphogenetic protein-2-but what is the cost?* Spine J, 2010.
9. Yaremchuk, K., M. Toma, and M. Somers, *Acute Airway Obstruction Associated with the Use of Bone-Morphogenetic Protein in Cervical Spinal Fusion.* Laryngoscope, 2010. **120**(S4): p. S140.
10. Mori, S., et al., *Antiangiogenic agent (TNP-470) inhibition of ectopic bone formation induced by bone morphogenetic protein-2.* Bone, 1998. **22**(2): p. 99-105.
11. Street, J., et al., *Vascular endothelial growth factor stimulates bone repair by promoting angiogenesis and bone turnover.* Proc Natl Acad Sci U S A, 2002. **99**(15): p. 9656-61.
12. Nakamae, A., et al., *Acceleration of surgical angiogenesis in necrotic bone with a single injection of fibroblast growth factor-2 (FGF-2).* J Orthop Res, 2004. **22**(3): p. 509-13.
13. Huang, Z., et al., *Modulating osteogenesis of mesenchymal stem cells by modifying growth factor availability.* Cytokine, 2010. **51**(3): p. 305-10.
14. Geiger, F., et al., *Vascular endothelial growth factor gene-activated matrix (VEGF165-GAM) enhances osteogenesis and angiogenesis in large segmental bone defects.* J Bone Miner Res, 2005. **20**(11): p. 2028-35.
15. Keiichi, K., et al., *Induction of new bone by basic FGF-loaded porous carbonate apatite implants in femur defects in rats.* Clin Oral Implants Res, 2009. **20**(6): p. 560-5.
16. Larsen, M., et al., *Augmentation of surgical angiogenesis in vascularized bone allotransplants with host-derived a/v bundle implantation, fibroblast growth factor-2, and vascular endothelial growth factor administration.* J Orthop Res, 2010. **28**(8): p. 1015-21.
17. Nillesen, S.T., et al., *Increased angiogenesis and blood vessel maturation in acellular collagen-heparin scaffolds containing both FGF2 and VEGF.* Biomaterials, 2007. **28**(6): p. 1123-31.

18. Ito, H., et al., *Remodeling of cortical bone allografts mediated by adherent rAAV-RANKL and VEGF gene therapy*. Nat Med, 2005. **11**(3): p. 291-7.
19. Koefoed, M., et al., *Biological effects of rAAV-caAlk2 coating on structural allograft healing*. Mol Ther, 2005. **12**(2): p. 212-8.
20. Yazici, C., et al., *Self-complementary AAV2.5-BMP2-coated Femoral Allografts Mediated Superior Bone Healing Versus Live Autografts in Mice With Equivalent Biomechanics to Unfractured Femur*. Mol Ther, 2011.
21. Younger, E.M. and M.W. Chapman, *Morbidity at bone graft donor sites*. J Orthop Trauma, 1989. **3**(3): p. 192-5.
22. Zhang, X., et al., *Periosteal progenitor cell fate in segmental cortical bone graft transplantations: implications for functional tissue engineering*. J Bone Miner Res, 2005. **20**(12): p. 2124-37.
23. Xie, C., et al., *Structural bone allograft combined with genetically engineered mesenchymal stem cells as a novel platform for bone tissue engineering*. Tissue Eng, 2007. **13**(3): p. 435-45.
24. Ferguson, C., et al., *Does adult fracture repair recapitulate embryonic skeletal formation?* Mech Dev, 1999. **87**(1-2): p. 57-66.
25. Yazici, C., et al., *The effect of surface demineralization of cortical bone allograft on the properties of recombinant adeno-associated virus coatings*. Biomaterials, 2008. **29**(28): p. 3882-7.
26. Peng, H., et al., *Synergistic enhancement of bone formation and healing by stem cell-expressed VEGF and bone morphogenetic protein-4*. J Clin Invest, 2002. **110**(6): p. 751-9.
27. Wang, X., et al., *Combined VEGF and LMP-1 delivery enhances osteoprogenitor cell differentiation and ectopic bone formation*. Growth Factors, 2011. **29**(1): p. 36-48.
28. Chikazu, D., et al., *Regulation of osteoclast differentiation by fibroblast growth factor 2: stimulation of receptor activator of nuclear factor kappaB ligand/osteoclast differentiation factor expression in osteoblasts and inhibition of macrophage colony-stimulating factor function in osteoclast precursors*. J Bone Miner Res, 2001. **16**(11): p. 2074-81.
29. Cucchiaroni, M., et al., *Improved tissue repair in articular cartilage defects in vivo by rAAV-mediated overexpression of human fibroblast growth factor 2*. Mol Ther, 2005. **12**(2): p. 229-38.
30. Cucchiaroni, M., et al., *Selective gene expression in brain microglia mediated via adeno-associated virus type 2 and type 5 vectors*. Gene Ther, 2003. **10**(8): p. 657-67.
31. Cucchiaroni, M., et al., *Restoration of the extracellular matrix in human osteoarthritic articular cartilage by overexpression of the transcription factor SOX9*. Arthritis Rheum, 2007. **56**(1): p. 158-67.
32. Tiyapatanaputi, P., et al., *A novel murine segmental femoral graft model*. J Orthop Res, 2004. **22**(6): p. 1254-60.
33. Childs, L.M., et al., *Effect of anti-tumor necrosis factor-alpha gene therapy on wear debris-induced osteolysis*. J Bone Joint Surg Am, 2001. **83-A**(12): p. 1789-97.

**Figure 1** In vitro release of AAV vectors coated onto the surface of bone allografts. The release of AAV-GFP vectors was determined by placing coated allografts on a confluent layer of HEK 293 cells. Every minute the grafts were moved to a new well. The number of GFP positive cells was determined by flow cytometry.

**Figure 2** Continuous and localized gene expression mediated by recombinant adeno-associated viral vectors through the use of bone allografts. **(A)** Bioluminescence images of mice grafted with rAAV-luciferase coated bone allografts show the light signal specifically localized to the site of the bone graft in the right femur of the mice. **(B)** The light signal was detected at day 9 and reached a steady level, which could still be visualized at day 178. This is based on the bioluminescence light signal intensity computed from a standardized region of interest (mean +/- SEM, n ≥ 4).

**Figure 2C** Localized expression of luciferase activity after insertion of bone graft coated with rAAV-luc. 3D reconstruction of bioluminescence intensity using the IVIS Spectrum Imaging System. The luciferase activity is solely expressed at the site of insertion of the coated graft in the right femur of the mouse. There is no visible shedding of the viral vector to the rest of the body.

**Figure 3** Cells within muscle and fibrous tissue are the main targets when using rAAV-mediated gene transfer from coated allografts. The radiance efficiency measured from the whole mouse equals the light signal measured from the muscle and fibrous tissue after dissection indicating these are the main focus of gene transfer. We found very little light emission from the back of the skin and from the femur. There may be transduced cells within the callus which we are not able to detect because the light signal are blocked by the overlying calcified bone. Data is presented as mean  $\pm$  SEM, n = 5.

**Figure 4** Increased new bone formation in allograft healing using rAAV-mediated VEGF gene transfer. Using a murine femoral allograft model 4 groups of mice were treated with rAAV expressing either VEGF, bFGF2, a combination of the two and a GFP-control group. New bone formation was evaluated after 10 weeks using microCT. VEGF treated allografts led to an almost two fold increase in new bone volume compared to GFP-controls ( \*p< 0.05, mean +/- SEM, n  $\geq$  7).

**Figure 5** Representative 3D reconstructions of rAAV-VEGF treated graft and a GFP-control graft. The rAAV-VEGF treated graft has developed a uniform new bone formation covering the entire allograft making it indistinguishable from a healing autograft. In contrast the control lack bone formation at the entire mid part of the graft as expected. This is demonstrated by 3D reconstructions of microCT data obtained after 10 weeks.

**Figure 6** Increased bone formation and induction of resorption of processed allografts by rAAV-mediated gene transfer of VEGF. Representative Goldner Trichrome stained histological sections from mice in the control group (**A**) and the group treated with VEGF (**B-F**). Graft is marked by asterisk. An example of a VEGF-coated allograft completely encaged in newly formed bone (**B**). In contrast the control are entirely dependent on creeping callus from the host bone (**A**). The VEGF treated group is characterized by new bone laid down directly on the surface of the graft (**C**) and at the time of killing of the mice after 10 weeks, there is still calcified cartilage (light blue), and osteoid (red) at the mid part of the graft indicating bone formation is still ongoing (**E, F**, the marked area in E at a higher magnification). There is a new bony union between the host and the graft with active tunneling resorption within the necrotic graft bone and the surface of the graft bone is irregular and invaded by new bone marrow within the remodeling callus(**D**, black arrows). In contrast the control group showed none of these features. (A, B: 1.25 x. C, D, E: 10 x. F: 20 x magnification).

**Figure 7** Resorption of the processed allograft induced by rAAV-mediated gene transfer of VEGF. Representative TRAP-stained histological sections. The graft bone is being actively resorped mostly from the periosteal surface represented by resorption lacunae both at the ends of the graft (**A**) and in a higher magnification in (**C**) and also localized to the central part of the graft surface (**B**). In contrast in the control group there are several osteoclasts located in the remodeling creeping callus but the graft bone shows no sign of resorption (**D**).

**Figure 8** AAV-FGF2 gene transfer leads to increased remodeling of coated allografts. TRAP stained histological section demonstrating several active osteoclasts (red) on the irregular surface of the allograft in close proximity to the newly formed bone. The graft bone is marked by asterisk (**A**). The microCT data demonstrate a significant decrease in allograft bone in the FGF2 group after 10 weeks (\* $p < 0.05$ ) (**B**).

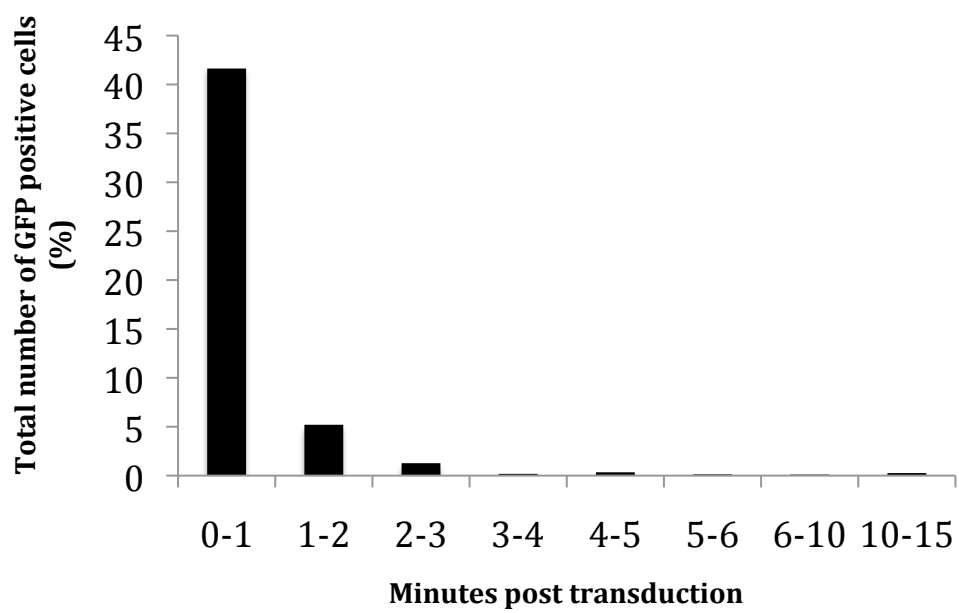


**Figure 1.**

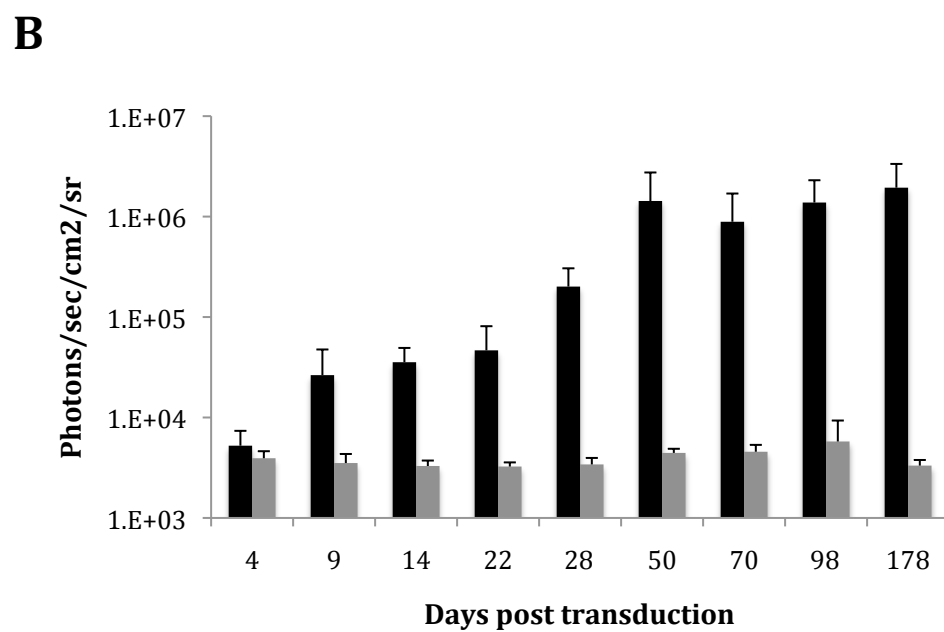
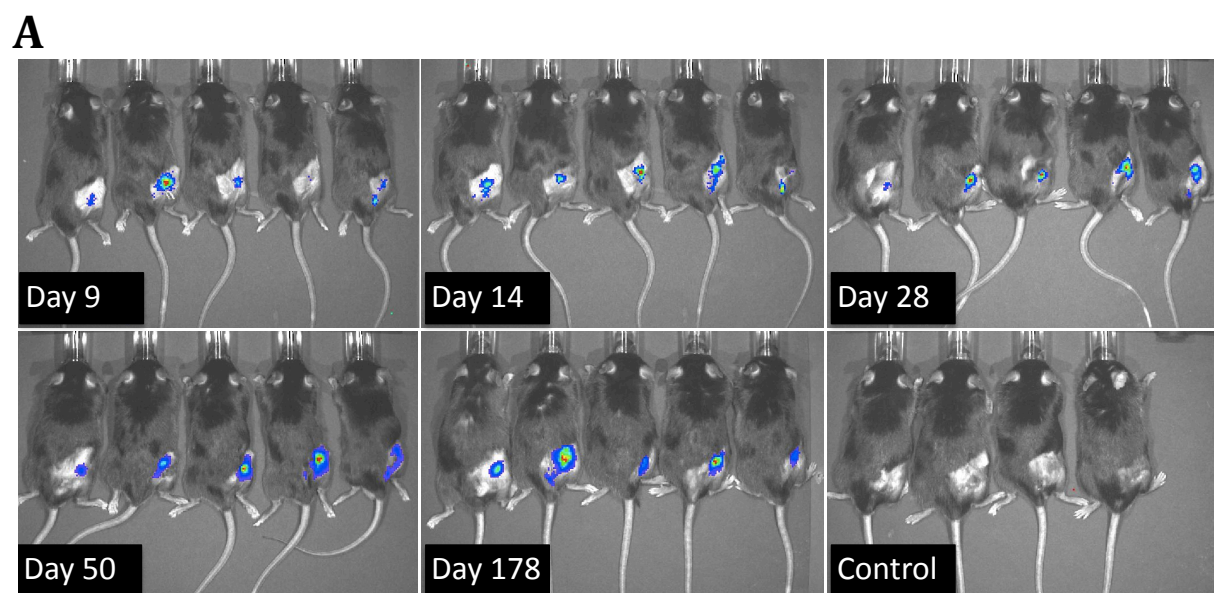


**Figure 2.**

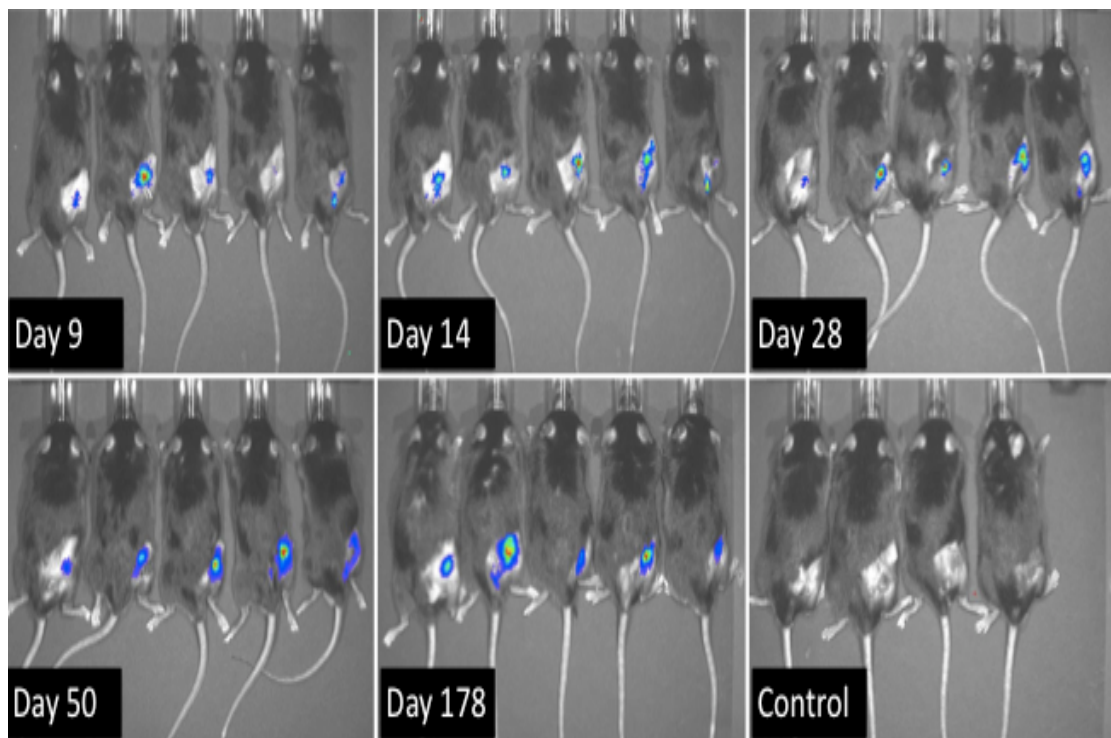


**Figure 2c.**

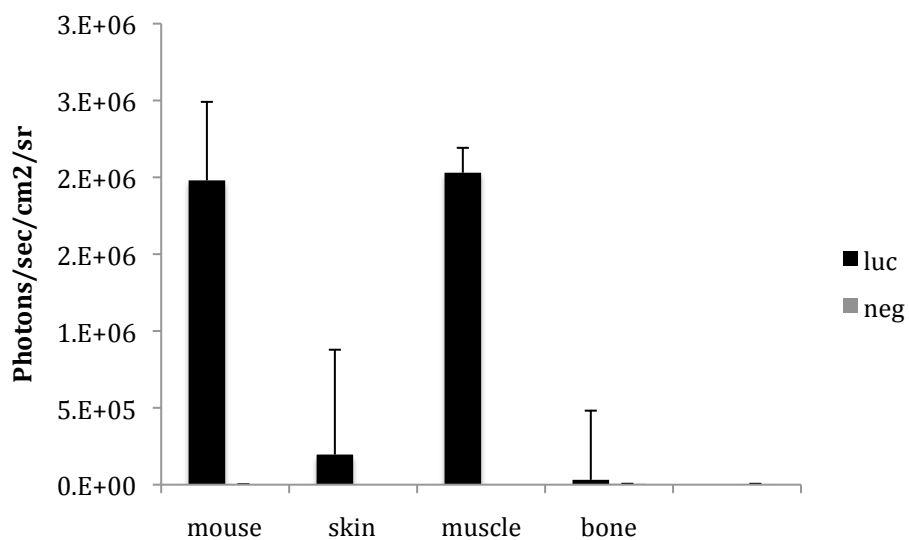
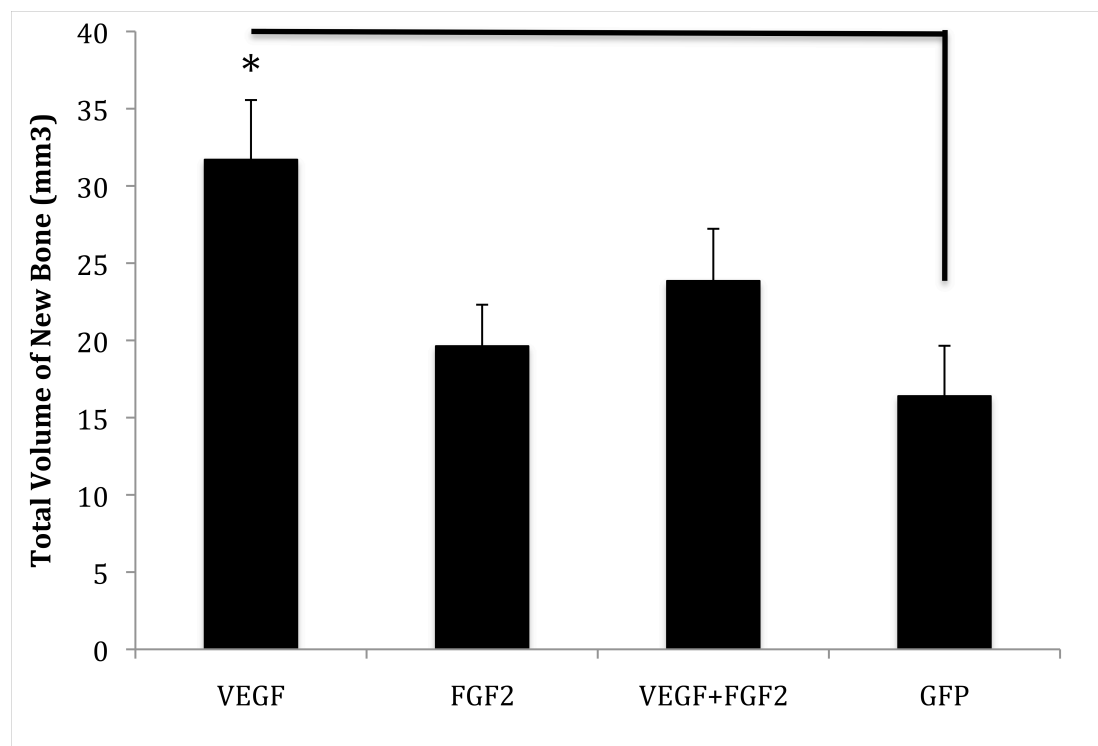
**Figure 3.****Figure 4.**



Figure 5.

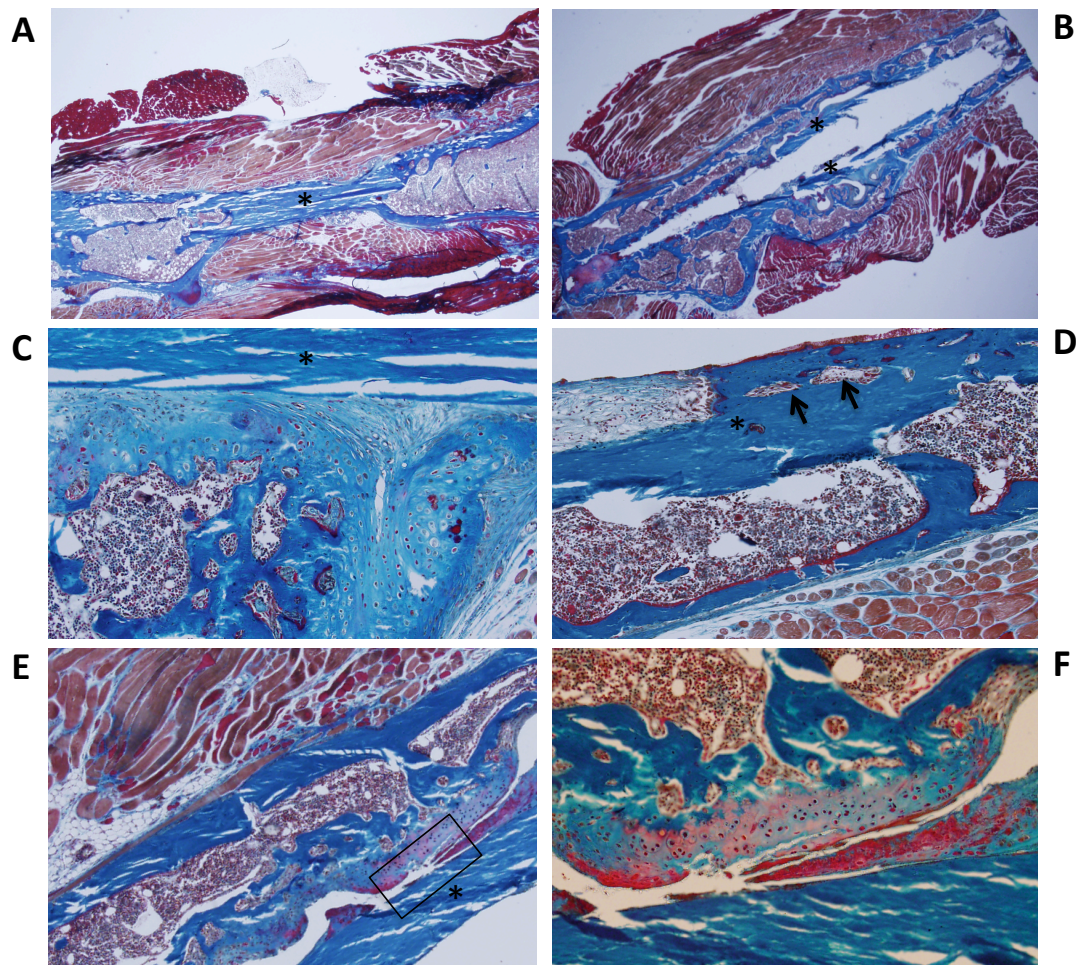
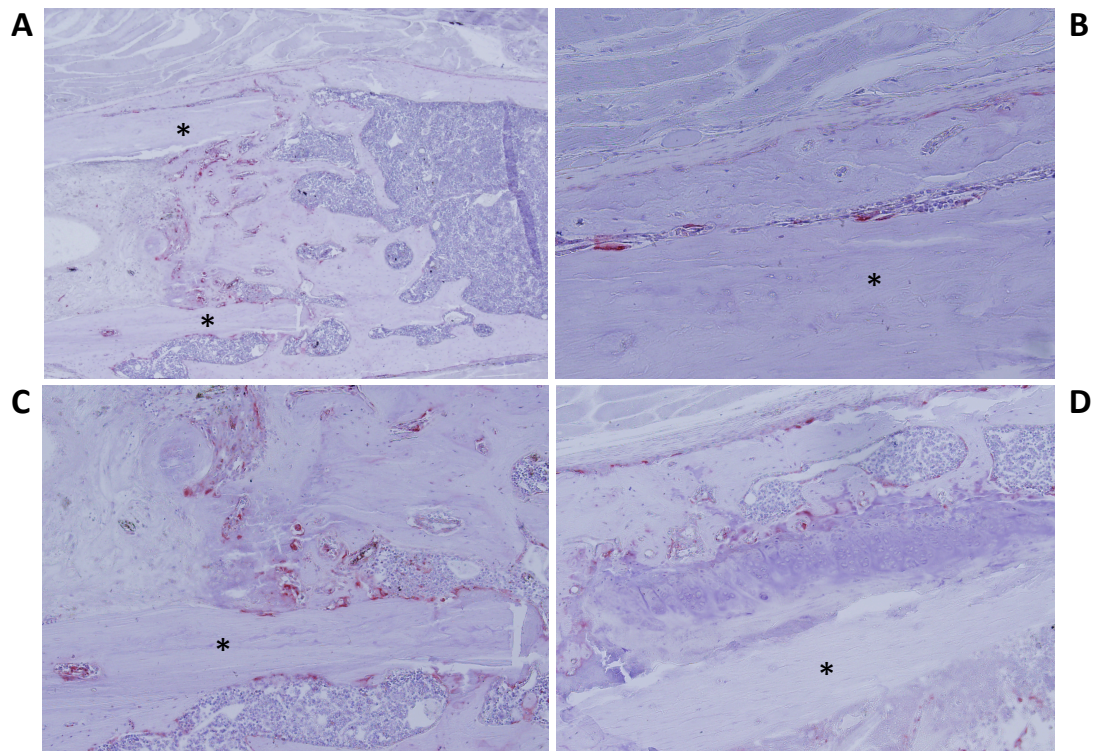
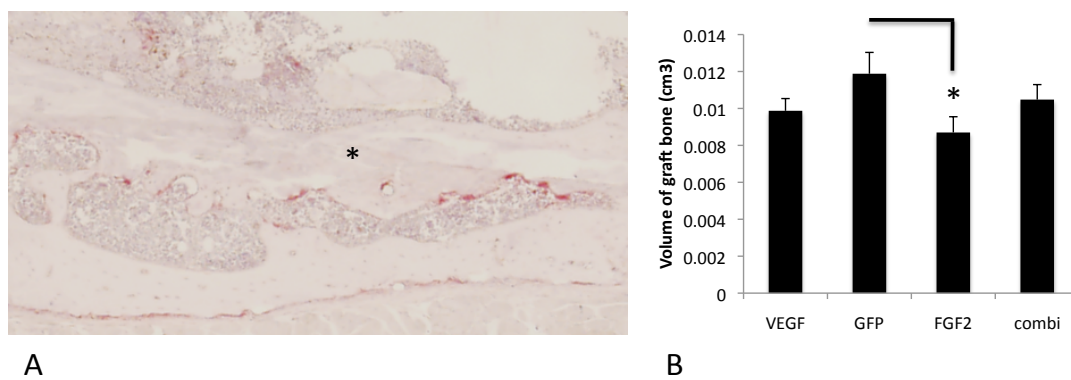


Figure 6.



**Figure 7.**



**Figure 8.**